WDPCP AFFECTS SKELETOGENESIS VIA THE HEDGEHOG PATHWAY

by

Mark T. Langhans

B.S., University of Notre Dame, 2009

Submitted to the Graduate Faculty of

University of Pittsburgh School of Medicine in partial fulfillment

of the requirements for the degree of

Doctor of Philosophy

University of Pittsburgh

2015

UNIVERSITY OF PITTSBURGH

SCHOOL OF MEDICINE

This dissertation was presented

by

Mark T. Langhans

It was defended on

April 14, 2015

and approved by

Michael W. Tsang, Ph.D.
Committee Chair
Associate Professor, Department of Developmental Biology

Lance A. Davidson, Ph.D.
Associate Professor, Department of Bioengineering and Developmental Biology

Adam V. Kwiatkowski, Ph.D.
Assistant Professor, Department of Cell Biology

Cecilia W. Lo, Ph.D.
Professor and Chair, Department of Developmental Biology

Rocky S. Tuan, Ph.D.
Major Advisor
Professor, Department of Bioengineering and Orthopaedic Surgery

WDPCP AFFECTS SKELETOGENESIS VIA THE HEDGEHOG PATHWAY

Mark T. Langhans, Ph.D.

University of Pittsburgh, 2015

A forward genetics screen in mice identified a mutation in the gene *Wdpcp* that leads to severe skeletal dysmorphogenesis with disrupted formation of the primary cilium. The primary cilium is a transiently formed organelle that facilitates the processing of hedgehog transcription factors Gli2 and Gli3. Conditional deletion of *Wdpcp* in the limb bud mesenchyme recapitulates the appendicular skeletal phenotype of the constitutive *Wdpcp* loss of function mutant. Loss of *Wdpcp* disrupts formation of the repressor form of Gli3, leading to hyper activation of hedgehog pathway. This hyper activation delays chondrogenesis via increased expression of bone morphogenetic protein (BMP) inhibitor *Grem1*, suppressing activation of BMP pathway necessary for chondrogenesis. Suppression of hedgehog signaling and *Grem1* expression and concomitant rescue of chondrogenesis is demonstrated with treatment of in vitro limb bud micromass cultures with direct hedgehog transcription factor Gli inhibitor GANT61, but not hedgehog signal transducer Smoothened inhibitor. This indicates that *Wdpcp* functions below Smoothened in the hedgehog pathway and directly implicates hedgehog signaling in the observed chondrogenic delay. In order to determine the effects of *Wdpcp* loss independent of this observed chondrogenic delay, we generated chondrocyte specific deletion mouse model of *Wdpcp*. Loss of *Wdpcp* and formation of the primary cilium in chondrocytes disrupts formation of trabecular bone, and mouse embryonic fibroblasts (MEFs) lacking *Wdpcp* have diminished in vitro osteogenesis. Activation of hedgehog pathway in MEFs lacking *Wdpcp* is rescued with lentiviral infection with a form of Gli2 mimicking amino terminal phosphorylation. We also

demonstrate that overactivation of PKA in MEFs can restore disrupted formation of the repressor form of Gli3. These findings define an important role for *Wdpcp* and primary cilia in skeletal development and in coordinating the post-translational modification of Gli transcription factors necessary for normal hedgehog signaling.

TABLE OF CONTENTS

PREFACE ..... **XIV**

1.0 INTRODUCTION **1**

1.1 DEGENERATIVE DISEASES OF THE SKELETON AND SKELETAL DEVELOPMENT **1**

1.2 SKELETAL DEVELOPMENT **4**

1.2.1 Model organisms for study of the skeletal development **4**

1.2.2 Origins of the vertebrate skeleton **5**

1.2.3 Appendicular skeletal development **6**

1.3 IMPORTANT SIGNALING PATHWAYS IN SKELETAL DEVELOPMENT **9**

1.3.1 Hedgehog signaling **9**

1.3.1.1 Hedgehog receptors and ligands **9**

1.3.1.2 Gli transcription factors **10**

1.3.1.3 Post-translational modifications of Gli **11**

1.3.2 BMP signaling **15**

1.3.2.1 BMP ligands and antagonists **15**

1.3.2.2 BMP receptors and signal transduction **15**

1.4 CHONDROGENESIS **17**

1.4.1 Shh and Gli in the limb bud 17

1.4.2 BMP and Grem1 in the limb bud 18

1.4.3 Coordinated signaling in chondrogenesis 20

1.5 OSTEOGENESIS 23

1.6 PRIMARY CILIA 25

1.6.1 Primary cilia structure and function 25

1.6.2 Role in hedgehog signaling 27

1.6.3 Primary cilia in skeletal development 29

1.6.4 Primary cilia and planar cell polarity (PCP) effector proteins 31

1.7 WDPCP 32

1.8 SUMMARY 34

2.0 LOSS OF WDPCP DISRUPTS SKELETOGENESIS AT MULTIPLE POINTS IN DEVELOPMENT 37

2.1 INTRODUCTION 37

2.2 METHODS 38

2.2.1 Mouse strains 38

2.2.2 Genotyping and injections for *Cre* induction 39

2.2.3 Timed matings 41

2.2.4 Alizarin red and Alcian blue whole mount staining 41

2.2.5 Histology 42

2.2.6 RNA isolation and quantitative real-time polymerase chain reaction (qPCR) 42

2.2.7 Western Blotting 43

2.2.8 Statistical analysis 44

2.3 RESULTS 44

2.3.1 The *Cys40* mutant mouse displays gross skeletal defects 44

2.3.2 *Prx1-Cre;Wdpcp*$^{Cys40/Flox}$ recapitulates appendicular skeletal phenotype of *Cys40* mutant 46

2.3.3 Disruption of limb bud exit to chondrogenesis with Wdpcp deficiency ... 48

2.3.4 Disruption of limb bud signaling with Wdpcp deficiency 49

2.3.5 Chondrocyte specific deletion of Wdpcp disrupts osteogenesis 51

2.4 DISCUSSION 53

2.5 CONCLUSION 55

3.0 WDPCP IS NECESSARY FOR NORMAL CHONDROGENESIS AND OSTEOGENESIS 57

3.1 INTRODUCTION 57

3.2 METHODS 57

3.2.1 In vitro chondrogenic differentiation: limb bud micromass 57

3.2.2 Generation of mouse embryonic fibroblasts (MEFs) 58

3.2.3 In vitro osteogenic differentiation 59

3.2.4 Histology 60

3.2.4.1 Alcian Blue staining 60

3.2.4.2 Alizarin Red staining 60

3.2.5 RNA isolation and qPCR 60

3.3 RESULTS 61

3.3.1 Micromasses lacking functional Wdpcp do not respond to Smo antagonism with enhanced chondrogenesis 61

3.3.2 Direct Gli antagonism rescues chondrogenic deficit in Wdpcp deficient micromasses 63

3.3.3 *Cys40* mutant MEFs display deficient in vitro hedgehog stimulated osteogenesis 65

3.4 DISCUSSION 66

3.5 CONCLUSION 68

4.0 WDPCP AFFECTS HEDGEHOG SIGNALING AT THE PRIMARY CILIUM BY ALTERING GLI PHOSPHORYLATION 71

4.1 INTRODUCTION 71

4.2 METHODS 71

4.2.1 Generation and culture of MEFs 71

4.2.2 Immunofluorescence of primary cilia 72

4.2.3 Generation of Gli mutant lentiviral constructs 73

4.2.4 Infection and cell culture of MEFs 75

4.2.5 Edu proliferation assay 75

4.2.6 Western Blotting 76

4.2.7 RNA isolation and qPCR 76

4.3 RESULTS 77

4.3.1 MEFs lacking *Wdpcp* are not responsive to Smo agonists 77

4.3.2 Direct inhibition of Gli silence ectopic activation of hedgehog pathway due to *Wdpcp* loss 78

4.3.3 Lentiviral overexpression of Gli3R silences ectopic activation of hedgehog pathway due to *Wdpcp* loss 79

4.3.4 MEFs lacking Wdpcp have impaired ciliogenesis 82

4.3.5 Hedgehog signaling and Gli3 processing are responsive to PKA modulation in MEFs lacking Wdpcp 82

4.3.6 MEFs lacking Wdpcp respond to PKA signaling 84

4.3.7 Gli2 mutants mimicking Gli Pc-g phosphorylation rescue loss of hedgehog activation due to Wdpcp loss 85

4.4 DISCUSSION 87

4.5 CONCLUSION 89

5.0 IMPACT AND FUTURE DIRECTIONS 91

5.1 IMPACT 91

5.1.1 Skeletal Development and Tissue Engineering 91

5.1.2 Osteoarthritis 91

5.1.3 Cancer 92

5.2 FUTURE DIRECTIONS 93

APPENDIX A 96

BIBLIOGRAPHY 98

LIST OF TABLES

Table 1. Genotyping PCR primer sequences (5'-3')..... 40

Table 2. Antibodies 44

LIST OF FIGURES

Figure 1. Developmental origins of the vertebrate skeleton. 6

Figure 2. Development of appendicular skeleton 8

Figure 3. Domain structure and post-translational modification sites of Gli2/3..... 13

Figure 4. Hedgehog signaling pathway. 14

Figure 5. BMP signaling pathway 16

Figure 6. Hedgehog, Gli3 repressor, and BMP in the limb bud 20

Figure 7. Hedgehog modulates BMP activity to control onset of chondrogenesis and exit to proliferation..... 22

Figure 8. BMP signaling controls limb bud chondrogenesis..... 22

Figure 9. Markers of osteogenic differentiation. 25

Figure 10. Primary cilium structure. 27

Figure 11. Wdpcp *Cys40* mutant. 34

Figure 12. Genotyping of mouse strains. 40

Figure 13. *Wdpcp* null mice display gross skeletal defects 45

Figure 14. Skeletal phenotype of E14.5 *Cys40* mutant..... 46

Figure 15. *Wdpcp* functions in the limb bud mesenchyme..... 47

Figure 16. Cys40 embryos have smaller appendicular cartilage anlagen..... 48

Figure 17. Loss of *Wdpcp* results in delayed chondrogenesis in the limb bud 49

Figure 18. Loss of *Wdpcp* disrupts Gli3 repressor formation and BMP signaling in the limb bud 51

Figure 19. Skeletal phenotype of chondrocyte specific deletion of *Wdpcp*. 53

Figure 20. In vitro chondrogenesis of micromass culture of *Wdpcp* null limb bud cells cannot be rescued with Smo antagonism 63

Figure 21. In vitro chondrogenesis in micromass cultures of *Wdpcp* null limb buds can be rescued with Gli antagonist treatment 64

Figure 22. *Cys40* MEFs display decreased osteogenesis 66

Figure 23. Effects of *Wdpcp* loss on chondrogenesis are mediated by hedgehog control of BMP signaling. 70

Figure 24. Verification of lentiviral tropism in MEFs. 75

Figure 25. *Cys40* MEFs display decreased responsiveness to modulation of Smo activity. 77

Figure 26. Direct Gli inhibition suppresses hedgehog pathway and proliferation. 79

Figure 27. Lentiviral overexpression of Gli3R suppresses hedgehog pathway and proliferation in *Cys40* MEFs. 81

Figure 28. *Cys40* MEFs display defective ciliogenesis. 82

Figure 29. PKA signaling affects Gli processing independent of *Wdpcp* 83

Figure 30. PKA signaling affects proliferation independent of *Wdpcp*. 84

Figure 31. Lentiviral overexpression of activated Gli2 increases proliferation and hedgehog activity in *Cys40* MEFs. 86

Figure 32. Wdpcp functions at or above PKA in the hedgehog pathway. 88

Figure 33. Craniofacial skeletal defects in *Cys40* mutant mice. 94

PREFACE

First, I would like to thank Rocky, for giving me the opportunity to pursue this project and supporting me through thick and thin—it quite literally would not have been possible without his willingness to allow me to pursue my scientific interests. His breadth of knowledge consistently amazes me, but more so his excitement for good science. It is truly an inspiration to see how excited you get about an experiment or a newly published finding after having achieved as much as you have. Your love for the scientific endeavor is contagious.

This project would not have been possible without Cecilia Lo generously sharing both her mice and scientific expertise. Bing Wang and Ying Wang were instrumental in all aspects of the virus work, providing the vectors, their expertise, and growing the virus for the experiments. They also helped a great deal with mouse genotyping and husbandry. I would also like to thank the members of my committee for helpful suggestions that have steered the course of this research and for all their support and help troubleshooting and designing experiments. Past and present members of the CCME, especially Thomas Lozito, Veronica Ulici, and Peter Alexander have taught me nearly all of the experimental techniques used in these studies and without their patient guidance and expertise, this project would never have been completed.

I would also like to thank my clinical mentors Dr. James Kang and Dr. Chris Harner, who generously shared their time and insights on how to build a career in academic orthopaedic

surgery, and consistently demonstrate that it is possible to be a great surgeon, scientist, and person.

I have to thank my family and friends for all their support throughout this process. I could not have done it without you. My parents and sisters have supported me every step of the way through this process including being tolerating when I had to miss or slip away from important events to run to the lab or finish an experiment. My grandmother has said countless prayers on my behalf. My fellow MSTPs have provided support through all the years in so many ways.

I would also like to thank Manjit Singh and Richard Steinman for their help and support. They run a truly excellent program and have made the experience of pursuing a dual degree considerably more enjoyable and less confusing than I anticipate it is for many on similar paths. I also have to thank Sanjeev Shroff, who supported me on his T32 cardiovascular bioengineering training grant for two years. The Pittsburgh Foundation provided funds that allowed me to acquire one of the mouse strains and helped to cover some expenses for the in vitro experiments. Support for this project was also received from the Pennsylvania Tobacco Fund.

1.0 INTRODUCTION

1.1 DEGENERATIVE DISEASES OF THE SKELETON AND SKELETAL DEVELOPMENT

Degenerative diseases of the skeletal tissues include osteoporosis and osteoarthritis. Osteoporosis is characterized by microarchitectural deterioration of bone and low bone mass and is a major risk factor for fractures of the hip, vertebrae, and distal forearm. Osteoporosis-related hip fracture is associated with 20% mortality and 50% permanent loss of function within one year of injury (Woolf and Pfleger, 2003). There are more than 2 million osteoporosis-related fractures annually in the United States with total costs for treatment of these fractures exceeding $19 billion (Burge et al., 2007). While there are several available medical therapies for osteoporosis including bisphosphonates (e.g. Alendronate), recombinant parathyroid hormone (e.g. Forteo), strontium ranelate (e.g. Protelos), and antibodies against receptor activator of NF- κβ (RANKL) (e.g. Denosumab), each of these therapies has its own limitations including risk of pathological fractures, increased incidence of bone tumors, association with adverse cardiovascular events, and immune dysfunction, respectively (Khosla, 2009). Conservative estimates are that osteoarthritis affects 21% of adults in the United States (Lawrence et al., 2008). In 2007 over $185 billion was spent in the United States on healthcare for the treatment of osteoarthritis (Kotlarz et al., 2009). With the average age of the population increasing, prevalence of this

disease is only expected to increase (Hootman and Helmick, 2006). Osteoarthritis is characterized clinically by joint pain, tenderness, occasional effusions, progressive deformity and loss of joint function resulting from restricted motion. These symptoms are due to progressive degeneration of the articular cartilage that includes fibrillation, ulceration, and eventual joint space narrowing. Current treatments for osteoarthritis are limited to symptomatic management with non-steroidal anti-inflammatory drugs, cyclooxygenase-2 inhibitors, or intra-articular corticosteroid injections. The only currently available treatment for advanced stage osteoarthritis is joint replacement, or joint arthroplasty (Zhang et al., 2008). While joint arthroplasty can successfully alleviate symptoms, patients undergoing joint replacement are typically unable to match functional abilities of their healthy counterparts following the procedure (Bade et al., 2010). Additionally, implants are susceptible to wear and degradation and typically last only 10-15 years, with revision surgery often required at this point. Of the nearly one million hip and knee replacements performed annually, 17.5% and 8.2%, respectively, will require revision at some point (Kurtz et al., 2007).

The current biological approaches for repair of osteoarthritic cartilage, including microfracture, osteochondral autograft transplantation system (OATS), autologous chondrocyte implantation (ACI), matrix assisted autologous chondrocyte implantation (MACI), and approaches utilizing mesenchymal stem cells (MSCs) and platelet-rich plasma (PRP), have failed thus far to yield consistent significant enhancement of regenerative capacity or sustained clinically significant improvement (Anz et al., 2014). Furthermore, the use of OATS, ACI, and MACI is limited to focal defects, which represent a limited subset of patients with osteoarthritis (Rodriguez-Merchan, 2013). The inconsistency associated with MSC and PRP based approaches may lie in the fact that these represent heterogeneous and highly variable populations of cell

types and growth factors, respectively (Anz et al., 2014). In order to overcome these limitations, significantly more targeted and general approaches that harness a mechanistic understanding of cartilage biology are necessary. Stimulating the innate regenerative capacity of cartilage and/or correcting joint and patient specific imbalances in cartilage homeostasis with targeted therapies to halt or reverse the progression of osteoarthritis represent the holy grail of osteoarthritis treatment (Jiang and Tuan, 2014).

The disease that is classified as osteoarthritis has complex, multifactorial origins and develops over long time scales, making it difficult to study. There are inflammatory, biomechanical, and genetic contributions to pathophysiology of osteoarthritis (Abramson and Attur, 2009). The pathophysiology of osteoporosis is similarly complex, with contributions from hormone regulation (e.g. estrogen levels in post-menopausal women), vitamin D balance, exercise and physiologic loading, mutations in genes important for osteoblast and osteoclast generation and survival, and regulation of metabolism, among many others (Burge et al., 2007). Severe forms of early onset arthritis have been associated with mutations in genes that are associated with the embryonic development of articular cartilage and synovial joints. For example, *Gdf5* is a bone morphogenetic protein (BMP) family gene that was demonstrated to be integral to the development of articular cartilage and synovial joints in mouse studies of skeletal development (Francis-West et al., 1999). Recent genome wide association studies have discovered that mutations in *Gdf5* are associated with severe forms of early onset osteoarthritis in humans (Sandell, 2012). The study of mouse knockout models of receptor activator of nuclear factor κβ ligand (*RANKL)* demonstrated the important role for this gene in regulating osteoclastogenesis (Dougall et al., 1999) and paved the way for the development of the RANKL targeted antibody, Denosumab, for treatment of osteoporosis (Rachner et al., 2011). By studying

mouse models in which skeletal development is disrupted, an understanding of the mechanisms by which cartilage and skeletal elements are formed during development and eventually achieve adult homeostasis can be built. Utilizing this framework, the contribution of individual genetic components to the pathophysiology of degenerative diseases of the skeleton can be systematically studied. With understanding gained from these studies, the significance of patient's genetic contributions and risk factors can be modeled, allowing targeted treatments to be derived for effective personalized medicine.

1.2 SKELETAL DEVELOPMENT

1.2.1 Model organisms for study of the skeletal development

The study of skeletal development is necessarily limited to vertebrates. This rules out the use of some classic model organisms used for genetics research including *D. melanogaster* and *C. elegans*. Many of the early studies of the molecular genetics of vertebrate skeletal development were carried out in chickens due to their accessibility, amenability to in ovo manipulation, and relative similarity to mammals. *D. rerio* is an organism that gained increasing traction in recent years for the study of axial and craniofacial skeletal development due to amenability to genetic knockdown with morpholino technology, and more recently, targeted genetic disruption. However, *D. rerio* are less applicable for the study of appendicular skeleton due to their genetic divergence from mammals (Langhans et al., 2014). Other model organisms such *A. carolinesis* (green anole) and *A. mexicanum* (axolotl) have also been studied (Kragl et al., 2009; Lozito and Tuan, 2015), but more for their differences in skeletal development and regeneration potential

than for their similarities to mammals. With the development of more advanced genetics techniques in mice such as targeted gene deletion and, later, more sophisticated methods such as conditional and inducible gene deletion (Gu et al., 1993), mice have become the organism of choice for the study of development of many tissues, including the skeleton.

In terms of developmental biology, mice have an 18-21 day gestation period depending on strain. Unlike humans, mouse skeletal growth continues throughout life and mice never close their growth plates under normal circumstances. Despite these differences, the genetic similarities that exist make mice an excellent model organism to study mammalian skeletal development. Common, conserved genetic mechanisms have been demonstrated to underlie the specification and maturation of skeletal tissues at multiple stages in development (Langhans et al., 2014).

1.2.2 Origins of the vertebrate skeleton

All cells in the developing vertebrate are descended from one of three germ lineages: endoderm, mesoderm, and ectoderm. The mesoderm is formed during gastrulation when cells migrate through the primitive streak (Acloque et al., 2011). At this stage the mesoderm exists in multiple compartments (Figure 1). The lateral plate mesoderm, with contributions from the paraxial mesoderm derived somites for tendon and ligaments, eventually gives rise to the appendicular skeleton and pelvis (Malashichev et al., 2008). Mesenchymal precursor cells in the limb are marked by expression of *Prx1* (Logan et al., 2002). The axial mesoderm gives rise to the notochord, which contributes towards the formation of the nucleus pulposus (NP) of the intervertebral discs (IVD). The paraxial mesoderm gives rise to the somites that will form the ribs, vertebral bodies, annulus fibrosus of the IVD (Smith et al., 2011), and part of the

craniofacial skeletal tissues. The majority of the craniofacial skeletal tissues are derived from neural crest cells, a population of cells that derives from the ectoderm adjacent to the neural tube (Abzhanov et al., 2007).

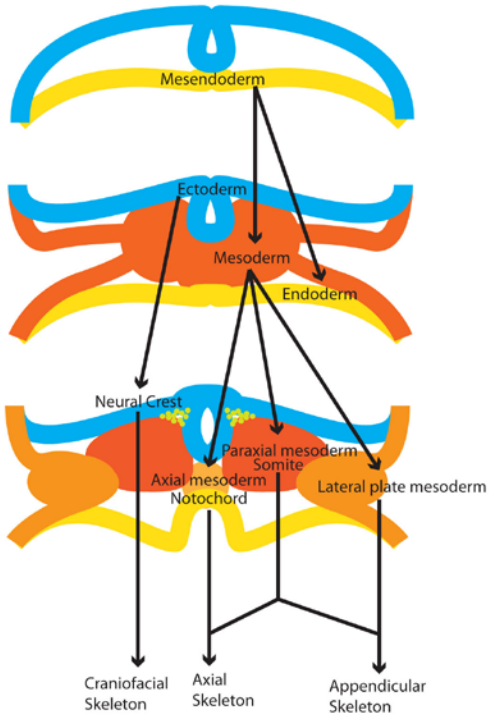

Figure 1. Developmental origins of the vertebrate skeleton.
The three embryonic germ layers, endoderm (yellow), mesoderm (orange), and ectoderm (blue), are formed during the process of gastrulation. The vertebrate skeleton is derived from mesoderm and ectodermal neural crest. The craniofacial skeleton is derived from neural crest, while the axial and appendicular skeletons are derived from mesoderm.

1.2.3 Appendicular skeletal development

The development of the appendicular skeleton begins at embryonic day 9.0 in mice with the formation of the forelimb ridges (Figure 2). The hindlimb ridges lag behind the forelimbs by about 18 hours and form at embryonic day 9.75 due to the rostro-caudal progression of development. The outgrowth of the limb bud is governed by two major signaling centers: the

apical ectodermal ridge (AER) and the zone of polarizing activity (ZPA) (Figure 2). The AER is a specialized ectodermal signaling structure that runs along the dorsoventral edge of the distal edge of the limb bud. The AER arises from the epithelial ectoderm overlying the lateral plate mesoderm and secretes fibroblast growth factors (FGFs) that initiate limb bud outgrowth. The ZPA arises at the posterior aspect of the limb bud at E9.5 and secrets sonic hedgehog protein (Shh). This secreted Shh has effect of both encouraging limb bud outgrowth by sustaining the AER and patterning the anterior/posterior axis of limb by providing a signaling gradient that interacts with and reinforces other pathways controlling this patterning. Interactions between the ZPA, AER, and limb mesenchyme regulate the outgrowth of the limb and the initiation of chondrogenesis at E11.0. At E11.0 mesenchymal condensation takes place to initiate chondrogenesis and chondrocyte differentiation (Pignatti et al., 2014).

Chondrocytes at the center of the cartilage model are the first to hypertrophy and begin secreting signals that set up the structure of the growth plate, a transient developmental structure that eventually closes via endochondral ossification, that takes place during puberty in humans. The growth plate is a highly organized arrangement of chondrocytes that includes a resting zone, a proliferating zone, a pre-hypertrophic zone, and cell polarity a hypertrophic zone. Resting and proliferating chondrocytes are marked by expression of parathyroid hormone related peptide (PTHrP), which is known to inhibit chondrocyte hypertrophy. Proliferating chondrocytes are organized into columns of cells oriented with the long axis towards the hypertrophic region, and this organization is essential for the control of bone shape. The stacking of proliferating chondrocytes is believed to involve elements of planar cell polarity, primary cilium orientation, matrix proteins, and diffusion gradients of growth factors such as BMPs, Indian hedgehog (Ihh), and Wnts and is an area of active investigation (Kuss et al., 2014). Early pre-hypertrophic

chondrocytes are marked by expression of Ihh. As the cells enlarge and enter into hypertrophy (Figure 2), they are marked by expression of the matrix protein, collagen type X (Col10a1). Additionally, they express a number of genes necessary for facilitating the remodeling of the ECM for blood vessel and osteoblast invasion, including matrix metalloproteinases (Mmp9 and Mmp13) and vasculoendothelial growth factor (Vegfa). Hypertrophic chondrocytes are also marked by expression of the early osteoblast transcription factors Runx2 and Osterix (Sp7). More mature hypertrophic chondrocytes also express apoptosis markers, such as Bcl2. Osteogenesis and the process of ossification in the forelimb begins at E14.0 with the differentiation of perichondrial cells adjacent to the hypertrophic chondrocytes into osteoblasts. Together with vascular endothelial cells these precursors invade and remodel the hypertrophic cartilage matrix to mature bone (Kronenberg, 2003).

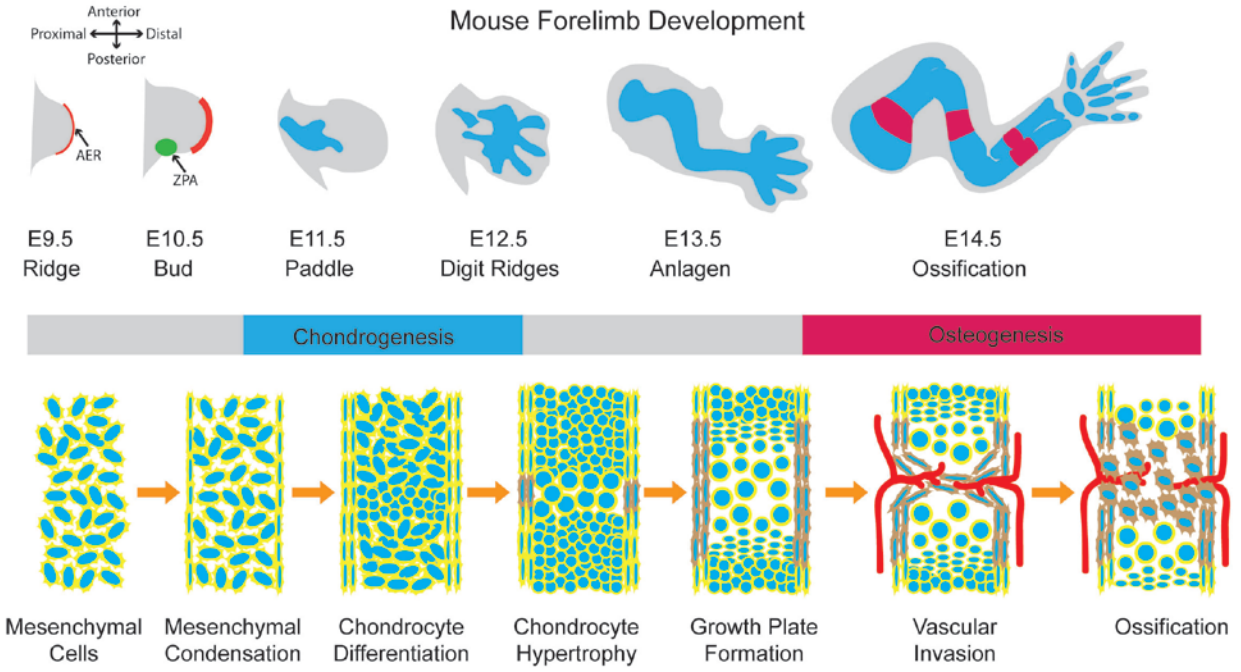

Figure 2. Development of appendicular skeleton

The appendicular skeleton arises at E9.0 with outgrowth of the lateral plate mesoderm (gray) through signaling interactions with the overlying ectoderm (orange) to form the forelimb ridge. By E10.5 the outgrowth has enlarged to form the limb bud. Mesenchymal condensation and the beginning of chondrogenesis occurs at E11.0. Chondrocytes at the center of mesenchymal condensations continue to differentiate and hypertrophy to set up the endochondral growth plate. Vascular invasion and osteogenesis initiates at E14.0.

1.3 IMPORTANT SIGNALING PATHWAYS IN SKELETAL DEVELOPMENT

1.3.1 Hedgehog signaling

1.3.1.1 Hedgehog receptors and ligands

Hedgehog (Hh) was first identified in *D. melanogaster* genetic screens in 1980 by Christiane Nüsslein-Volhard and Eric Weischaus (Nusslein-Volhard and Wieschaus, 1980) in work that would contribute to their 1995 Nobel Prize in Medicine. It was not until 1992 that the *D. melanogaster* Hh gene was independently cloned and molecularly identified as a secreted protein by three laboratories (Lee et al., 1992; Mohler and Vani, 1992; Tabata et al., 1992). Evolutionarily conserved vertebrate homologs sonic hedgehog (*Shh*), indian hedgehog (*Ihh*), and desert hedgehog (*Dhh*) were subsequently identified and their roles in development characterized (Chang et al., 1994; Echelard et al., 1993; Krauss et al., 1993; Riddle et al., 1993; Roelink et al., 1994). The key Hh ligands in skeletal development are *Shh* and *Ihh. Shh* was demonstrated to play a key role in limb development, where it was shown to be capable of reproducing the action of the zone of polarizing activity (ZPA) (Cohn and Tickle, 1996), and in the patterning of neural tube, where it was shown to be capable of reproducing the action of the notochord and floor plate (Jessell, 2000), with grafting and bead experiments. *Ihh* was shown to play a central role in organization of the growth plate and formation of bones via the process of osteogenesis (Kronenberg, 2003).

A number of secreted inhibitors and matrix proteins play important roles in regulating the levels of hedgehog signaling by binding and sequestering hedgehog ligands. *Hhip* is a secreted inhibitor of hedgehog that binds and sequesters hedgehog to prevent its activity within the limb bud (Chuang and McMahon, 1999).

Hedgehog proteins bind to the frizzled domain containing membrane protein receptors *Ptch1* and *Ptch2*. Both *Ptch1* and *Ptch2* interact with all hedgehog proteins with similar affinity. While *Ptch1* is expressed ubiquitously throughout the embryo, high levels of *Ptch2* expression are restricted to the skin and germ cells (Carpenter et al., 1998). *Ptch1* and *Ptch2* both form a complex with another hedgehog pathway component, the membrane receptor *Smo*. When hedgehog ligand is not present and the pathway is inactive, *Ptch* binds to *Smo* and inhibits activation of the Hh pathway by inhibiting *Smo* (Figure 4). When hedgehog ligand is present, Ptch mediated inhibition of Smo is alleviated and the Hh pathway is activated. Animals lacking functional *Ptch1* displayed constitutively active hedgehog pathway activity while animals lacking function *Smo* display constitutively inactive hedgehog pathway activity. *Hhip* and *Ptch1* expression are increased with increased hedgehog activity and serves as a negative feedback control loop to limit hedgehog signaling in vivo (Briscoe and Therond, 2013; Goodrich et al., 1996).

1.3.1.2 Gli transcription factors

The protein cubitus interruptus (*Ci*) was initially identified in *D. melanogaster* as the target of hedgehog signaling. *Ci* is post-translationally processed to either a labile transcriptional activator when the hedgehog pathway is activated or a truncated repressor with the C-terminal activation domain removed when the hedgehog pathway is quiescent (Ohlmeyer and Kalderon, 1998).

In mammals, the *Gli* transcription factors (*Gli1-3*) were shown to be homologs of the *D. melanogaste*r hedgehog target transcription factor *Ci*. Gli1 is not processed, and contains only the activation domain (Dai et al., 1999; Sasaki et al., 1999). *Gli1* has been shown to function primarily as a molecular rheostat for the hedgehog pathway, serving as a positive feedback loop. Activation of the hedgehog pathway corresponds with increased expression of *Gli1* (Dai et al.,

1999).

Gli2 and *Gli3* share the most homology to *Ci* and have the more severe knockout phenotypes compared to *Gli1* (Park et al., 2000). Unlike Gli1, both Gli2 and Gli3 are proteolytically processed to repressor forms when the hedgehog pathway is quiescent (Pan et al., 2006). Gli2 and Gli3 contain N-terminal transcriptional repressor domains and zinc-finger DNA binding domains and C-terminal transcriptional activation domains. Proteolytic cleavage removes the C-terminal activation domain generating an N-terminal repressor that competes with the full-length activator for binding at Gli target sites (Tsanev et al., 2009). The activity of the hedgehog pathway is thus dictated by the balance of Gli repressor and activator bound to Gli target sites in the DNA. Because Gli3 is more readily proteolytically processed than Gli2, Gli3 serves as the primary repressor form while Gli2 serves as the primary activator form in mammals (Sasaki et al., 1999).

1.3.1.3 Post-translational modifications of Gli

The output of the hedgehog pathway is modified by a number of pathways that affect the post-translational modification of the Gli transcription factors. Identified post-translational modifications of Gli proteins include phosphorylation, ubiquitinylation, and sumoylation (Cox et al., 2010; Niewiadomski et al., 2014; Zhang et al., 2013) (Figure 3).

Phosphorylation was one of the first identified post-translational modifications of Gli. Knockout studies in *D. melanogaster* demonstrated that *PKA* and *GSK3* were negative regulators of the hedgehog pathway. It was noted that mutants bearing mutations in *PKA* and/or *GSK3* displayed ectopic activation of the Hh pathway. *GSK3*$^{-/-}$ flies exhibited accumulation of full-length Ci and ectopic Hedgehog target gene expression. While *Smo*$^{-/-}$ animals displayed decreased full length Ci accumulation due to constitutive processing of Ci and hedgehog path

silencing, *GSK3*$^{-/-}$;*Smo*$^{-/-}$ mutants accumulated high levels of full length Ci and rescued the constitutive silencing of Hh target gene expression in Smo$^{-/-}$ mutants. This indicates that *GSK3* functions downstream of *Smo* in the Hh pathway (Jiang and Struhl, 1996) (Figure 4).

Conversely, overexpression of constitutively activated PKA blocked accumulation of Ci155. Overexpression of constitutively activated PKA with concomitant treatment with GSK3 inhibitor resulted in accumulation of full length Ci, indicating that both PKA and GSK3 are required for full length Ci processing. Studies with mutant forms of Ci demonstrated that GSK3 can phosphorylate Ci only after PKA has phosphorylated Ci (Jia et al., 2002). Analogous findings with mammalian homologs Gli2 and Gli3 have demonstrated the same regulation of Gli processing by PKA and GSK3B (Pan et al., 2006; Wen et al., 2010).

Recently, the effects of phosphorylation on Gli activity have been explored in detail with residue specific mutant forms of Gli2 and Gli3. Transfection of a Gli2 with mutations of C-terminal PKA sites, Cki sites, or GSK3 sites that abolished their ability to be phosphorylated resulted in increased hedgehog activity versus transfection of wild type Gli2, indicating specific sites of phosphorylation that modify Gli activity (Pan et al., 2006). While phosphorylation of C-terminal domain was demonstrated to encourage Gli processing and repress hedgehog activity, a recent study demonstrated that phosphorylation of the N-terminal domain blocks Gli processing and activates hedgehog activity (Niewiadomski et al., 2014). These findings highlight the fact that phosphorylation of Gli is a tightly regulated process that lies at the center of the regulation and output of the hedgehog signaling pathway.

In addition to phosphorylation, Gli transcription factors have also been demonstrated to undergo additional modifications including ubiquitinylation and sumoylation. The ubiquitin E3 ligase *Btrc* interacts directly with phosphorylated Gli to facilitate its degradation via

ubiquitinylation (Pan et al., 2006). *Btrc*$^{-/-}$ animals display ectopic hedgehog signaling and defective processing of Gli to shortened repressor (Jiang and Struhl, 1998). Mutation of lysines in the C-terminal domain having demonstrated that ubiquitinylation is required for normal Gli processing and degradation (Kent et al., 2006). Different patterns of ubiquitylation (K-11 versus K-48 linked) have been demonstrated to control the partial processing versus total degradation of Gli, but the mechanism by which Gli is specified to one fate versus the other has not been fully elucidated (Zhang et al., 2013) (Figure 3). Sumoylation of Gli transcription factors has been demonstrated to regulate activator potential. Furthermore, this regulation of activator potential was identified to occur downstream of PKA (Cox et al., 2010) (Figure 4).

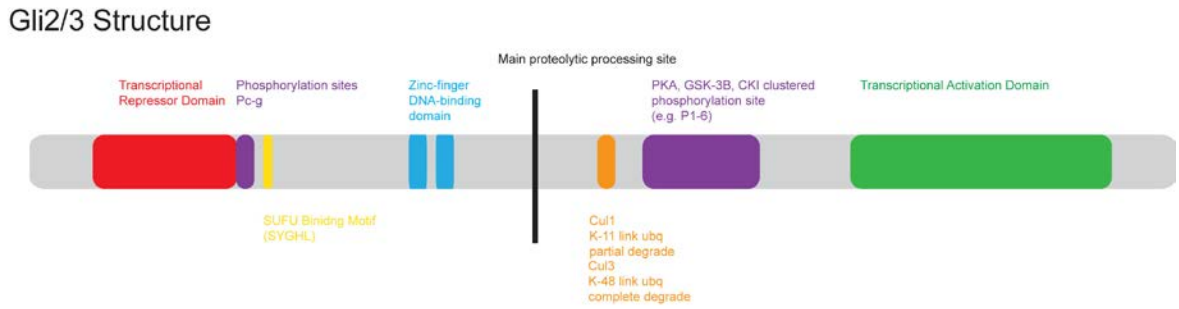

Figure 3. Domain structure and post-translational modification sites of Gli2/3.
Gli2 and Gli3 are post-translationally modified to affect their transcriptional activity. Phosphorylation and ubiquitylation sites have been identified and demonstrated to control maturation of both the activator form of Gli and the processing to the truncated repressor form.

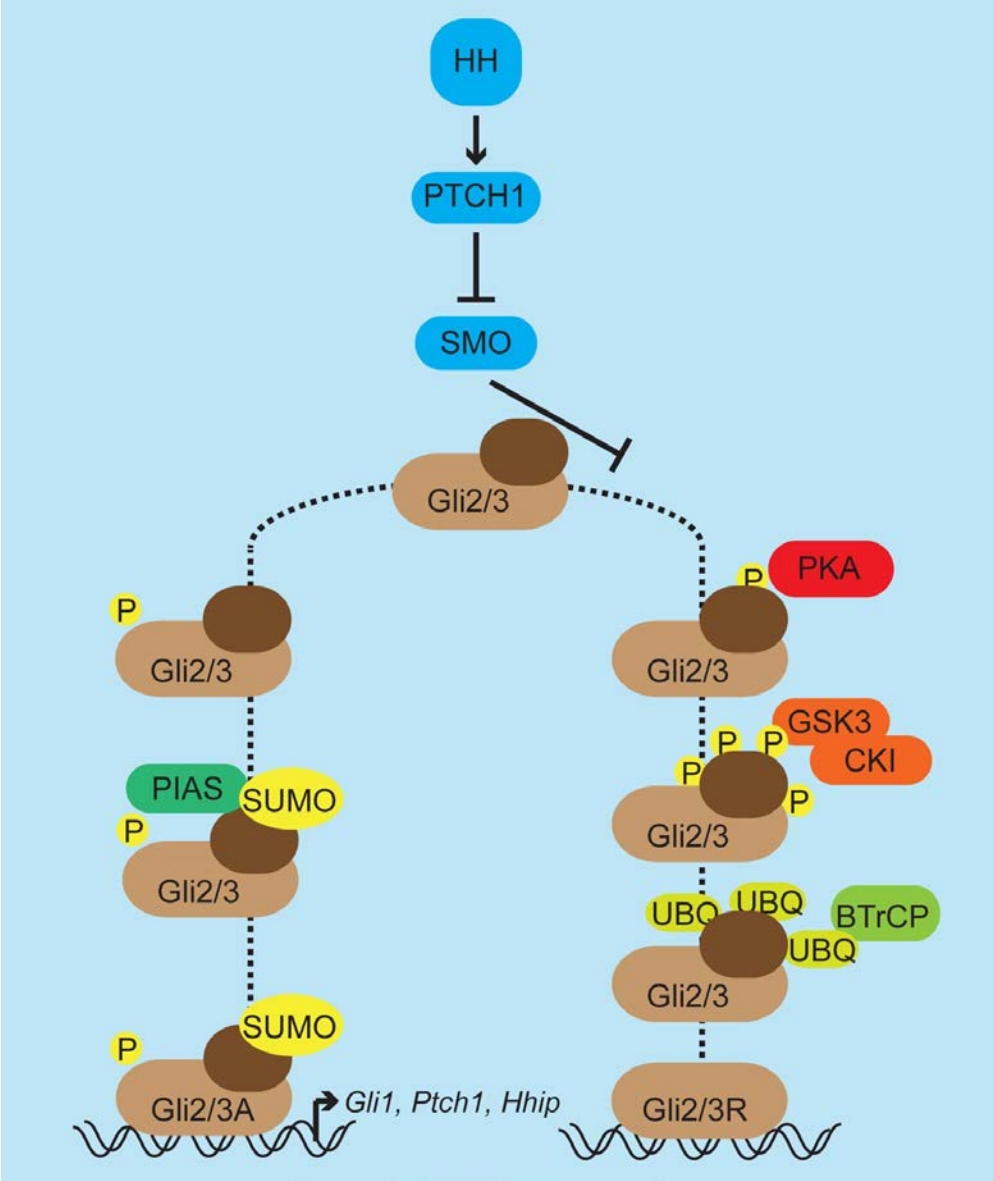

Figure 4. Hedgehog signaling pathway.

Hedgehog signaling output is mediated by the balance of Gli repressor versus Gli activator levels. When quiescent, Ptch inhibits the activity of Smo, allowing Gli3 to be processed to a repressor form and preventing the conversion of Gli2 to activator form. When Hh is present and the pathway is activated, Ptch inhibition of Smo is relieved and Smo inhibits the proteolytic processing of Gli3 while promoting the conversion of Gli2 to activator form.

1.3.2 BMP signaling

1.3.2.1 BMP ligands and antagonists

Bone morphogenetic proteins (BMPs) were first identified by their ability to induce ectopic bone upon subcutaneous application (Urist, 1965). Subsequent studies identified BMP ligands as members of the TGFβ superfamily and identified a number of important functions for them in both embryonic and postnatal development (Hinck, 2012). Twelve BMP ligands have been identified in mammals that can form homo- and heterodimers with different affinities for their receptors. BMP ligands are activated upon secretion by cleavage, at which point they can interact with both receptors and BMP antagonists. Twelve BMP antagonists have been identified in mammals and they have also been shown to play important roles in development. These antagonists function by binding and sequestering BMP ligands to prevent their interaction with receptors (Miyazono et al., 2010; Walsh et al., 2010). BMPs expressed in the developing limb include *Bmp2, Bmp4,* and *Bmp7*. The inhibitor *Noggin* is dynamically regulated during skeletal development and expression occurs after the onset of chondrogenesis (Benazet et al., 2009). The BMP antagonist *Grem1* plays an important in the developing limb bud as a component of the Shh-Grem-AER/FGF signaling feedback loop that controls limb bud outgrowth and chondrogenesis (Pignatti et al., 2014).

1.3.2.2 BMP receptors and signal transduction

BMP receptors are transmembrane glycoproteins with serine-threonine kinase activity. BMP ligand dimers bind to type II BMP receptors (Figure 5) resulting in recruitment and phosphorylation of type I BMP receptors. Phosphorylation of type I BMP receptors triggers phosphorylation of the receptor associated Smads (R-Smads) (*Smad1, Smad5,* and *Smad8/9*).

These phosphorylated R-Smads are capable of translocation to the nucleus with the Smad4 co-receptor where they activate expression of BMP target genes (Pignatti et al., 2014). In the developing limb bud, *Msx2* is a direct target of BMP signaling in the developing limb, and can be used as a reporter for BMP activity (Pizette et al., 2001). *Bmpr1a* and *Bmpr2* are both expressed highly in limb bud. *Smad1*, *Smad5*, *Smad8*, and *Smad4* are expressed uniformly throughout the limb bud (Benazet et al., 2012; Wong et al., 2012).

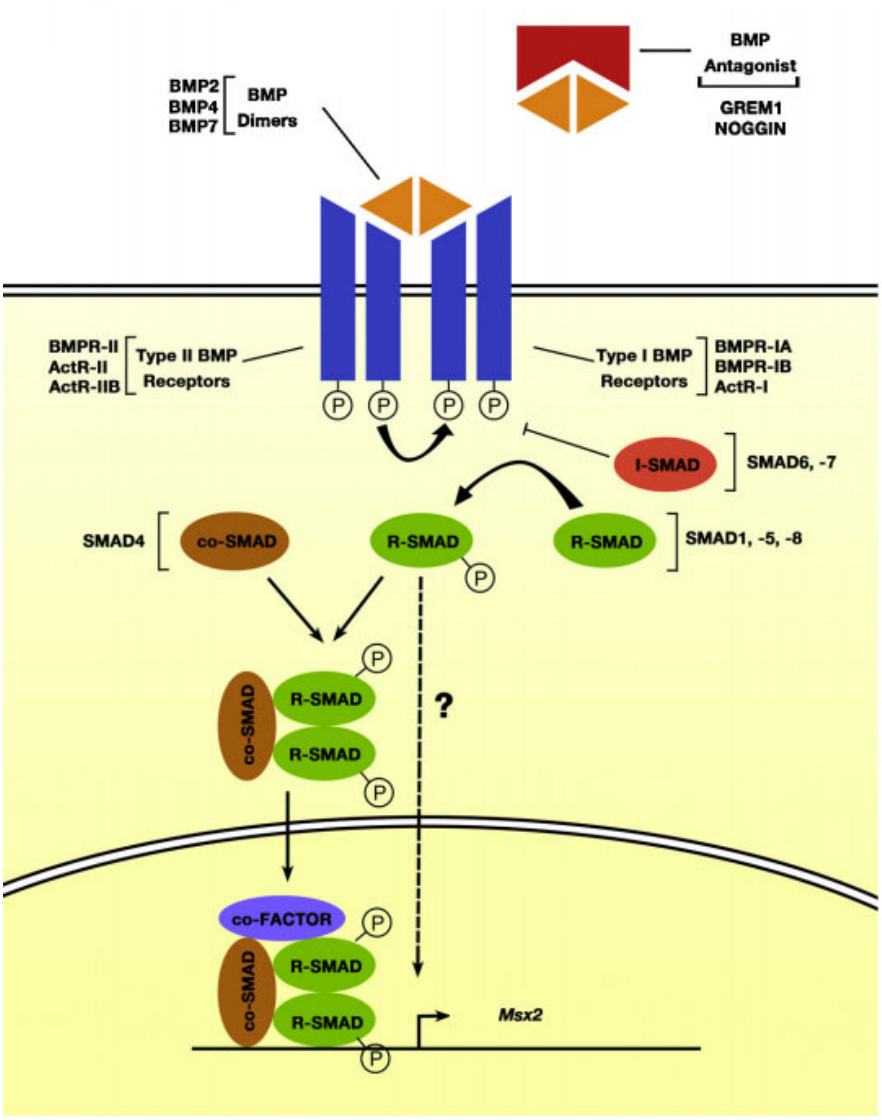

Figure 5. BMP signaling pathway
BMP ligand dimers (BMP2/4/7) act as ligands for type I and type II BMP receptors. Extra-cellular antagonists such as Grem1 and Noggin inhibit BMP pathway activity by binding BMP ligands and preventing their interaction with receptors. BMP receptors are transmembrane glycoproteins with serine-threonine kinase activity. Binding of type II BMP receptors to BMP ligands results in recruitment and phosphorylation of BMP type I receptors. These phosphorylated receptors phosphorylate receptor associated SMADs (R-SMADS) in the cytoplasm. R-SMADs for a complex with co-SMAD and translocate to the nucleus to activate transcription of BMP target gene *Msx2*. (Reproduced with permission from Pignatti et al 2014).

1.4 CHONDROGENESIS

1.4.1 Shh and Gli in the limb bud

The hedgehog signaling pathway plays a central role in multiple processes in the developing limb bud. One of the earliest roles for hedgehog signaling in the limb bud is facilitating limb bud outgrowth. As the AER develops and begins to secrete *Fgf4* and *Fgf8* that stimulate limb bud mesenchyme to proliferate and migrate into the limb bud, it also stimulates the expression of *Shh* in the ZPA. The expression of *Shh*, in turn stimulates expression of *Fgf*s from the AER. This results in a positive feedback loop between Shh-Grem1-AER/Fgfs that promotes limb bud outgrowth (Benazet and Zeller, 2009; Zeller et al., 2009). Both ectopic early activation of hedgehog signaling as well as failure to fully activate hedgehog signaling can disturb this feedback loop resulting in defective limb bud outgrowth (Bastida et al., 2009; Zhu et al., 2008; Zhulyn et al., 2014).

The role of hedgehog and Gli3 in anterior/posterior limb patterning is closely tied to limb bud outgrowth and is one of the most extensively studied areas of limb development (Figure 7). One of the first described skeletal mutant mouse models was the *extra-toes (Xt)* mutant, which carries a null allele of *Gli3* to function as a $Gli3^{-/-}$ mouse. The *Xt* mutant displays severe polydactyly (Johnson, 1967). Further studies revealed that *Gli3* is a key mediator of anterior posterior patterning in the developing limb bud and acts primarily as a repressor in this context. $Prx1Cre;Gli3^{701C}$ mice were engineered to overexpress the repressor form of Gli3 in limb mesenchyme. In contrast to the polydactyly observed in *Xt* mutant, these mice have shortened limbs with single digit oligodactyly. They display significant decreases in expression of hedgehog markers *Gli1* and *Ptch1* (Cao et al., 2013). These mice have a nearly identical

phenotype to the $Shh^{-/-}$ mice, which also display shortened limbs with oligodactyly. Expression patterns of Gli3 and Shh appear to be mutually exclusive in the limb bud. The *Xt* mutant has ectopic expression of Shh in the anterior forelimb bud at E11.0 and E12.0 This ectopic Shh expression is accompanied by ectopic anterior expression of the hedgehog receptor and reporter gene *Ptch1* (Buscher et al., 1997). The $Shh^{-/-}$;$Gli3^{-/-}$ double mutant displays a phenotype identical to the *Xt* mutant, indicating that *Shh* functions above *Gli3* in the determination of digit number and functions independently of *Shh* to determine digit number (te Welscher et al., 2002). Gli3R was later demonstrated to interact with *Hoxd* genes and *Hand2* to regulate digit patterning (Buscher et al., 1997; Chen et al., 2004; Osterwalder et al., 2014; te Welscher et al., 2002).

$Gli2^{-/-}$ mice demonstrate outgrowth defects with shortened humerus, radius, and ulna in the forelimb. However, they do not have overt A/P patterning defects. $Gli2^{-/-};Gli3^{-/-}$ mice display more severe outgrowth defects and long bone shortening than $Gli2^{-/-}$ mice. These findings demonstrate that both *Gli3* repression and *Gli2* activation play important roles in skeletal development (Mo et al., 1997).

1.4.2 BMP and Grem1 in the limb bud

BMP signaling plays a key role in mediating skeletal development in the limb. Formation of the AER is dependent upon *Bmp4* signaling through *Bmpr1a*. *Msx2-Cre;*$Bmpr1a^{flox/flox}$ mice have ectodermal specific deletion of *Bmpr1a* and display failure of the AER maintenance and limb bud outgrowth. *Prx1-Cre;*$Bmpr1a^{flox/flox}$ mice with limb bud mesenchyme deletion of *Bmpr1a* display shortened limbs with decreased cell proliferation that results in complete agenesis of the autopod. Reduced expression of BMP target genes *Msx1* and *Msx2* in these mice coincided with ectopic anterior hedgehog signaling (Ovchinnikov et al., 2006). *Prx1-Cre;*$Bmp4^{flox/flox}$ mice have

limb mesenchyme specific deletion of the main BMP in limb bud development, *Bmp4*, and display polydactyly with delayed induction of the AER and expanded *Shh* expression (Selever et al., 2004).

The *Prx1Cre;Rosa*^{dGrem1} mouse overexpresses *Grem1* within limb mesenchyme and displays significant polydactyly. As expected with overexpression of the BMP inhibitor *Grem1*, limb buds of these mice display decreased expression of BMP target gene *Msx2* and decreased levels of phospho-Smad1/5/8 characteristic of decreased BMP pathway activation. *Shh* expression also showed a significant increase without any ectopic anterior expression. These expression changes coincided with an increase in proliferation and decrease in chondrogenic differentiation as measured by expression of chondrogenic marker gene *Sox9* at E12.5. Additionally, using a mouse model with an early inducible Cre in the limb bud (*Hoxb6-Cre*^{ER}*;Rosa*^{dGrem1}) it was shown that the development of polydactyly depends on overexpression of *Grem1* in a critical window between E10 and E11.5 (Norrie et al., 2014).

The expression of *Grem1* in the limb bud was recently found to be under control of a distant cis-regulatory region (*GRS1*) in the limb bud. Underlying the coordination present between hedgehog and BMP signaling in the limb bud, *GRS1* input on *Grem1* depends on Shh signaling and is modulated by BMP signaling. Chromatin immunoprecipitation revealed that Gli3 binds to core regulatory elements in *GRS1* (Zuniga et al., 2012).

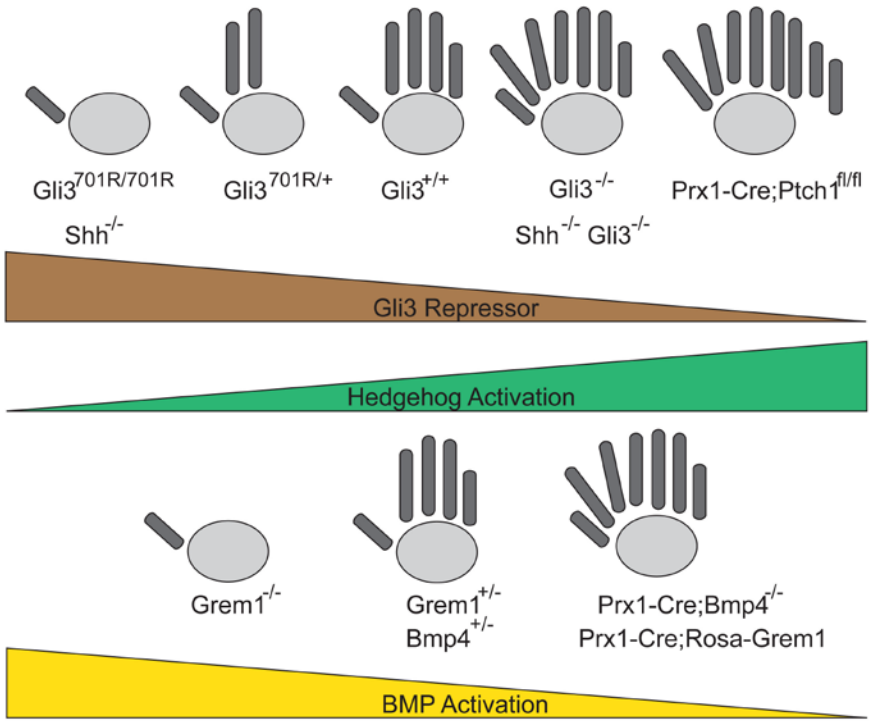

Figure 6. Hedgehog, Gli3 repressor, and BMP in the limb bud

A series of studies that utilize transgenic and targeted knockout mice have revealed that Gli3 repressor levels in the limb are modified by hedgehog signaling activation and serve to control the timing of the exit of proliferating limb bud progenitors to chondrogenesis. Delayed exit results in more digits (polydactyly) while early exit results in fewer digits (oligodactyly). BMP signaling is also able to influence this process with overactivation of BMP signaling resulting in oligodactyly and underactivation resulting in polydactyly.

1.4.3 Coordinated signaling in chondrogenesis

Hedgehog signaling and BMP signaling play significant roles in the initiation of chondrogenesis. Initiation of chondrogenesis in the limb bud is closely coordinated with both outgrowth and anterior/posterior patterning. The polydactyly displayed by *Gli3*$^{-/-}$ mice is closely associated with delayed chondrogenesis in the anterior limb bud. Deletion of *Gli3* leads to increased expression of proliferation markers *Ccnd1* and *Cdk6* concomitant with decreased expression of chondrogenic markers *Col2a1* and *Noggin*. The decrease in expression of chondrogenic markers coincides with decreased expression of BMP target genes *Msx2* and *Id1* along with increased expression of the BMP inhibitor *Grem1*. Furthermore, polydactyly and chondrogenic delay in

Gli3$^{-/-}$ mice is rescued in *Gli3*$^{-/-}$*;Grem1*$^{+/-}$ mice and exacerbated in *Gli3*$^{-/-}$*;Bmp4*$^{+/-}$ mice. These findings demonstrate that Gli3 levels and hedgehog signaling modulate the activity of the BMP signaling pathway to control chondrogenesis (Lopez-Rios et al., 2012).

Concordantly, *Prx1Cre;Ptch1*$^{flox/flox}$ mice with constitutive activation of hedgehog signaling in the limb mesenchyme display polydactyly. Increased hedgehog signaling decreases the level of Gli3R and leads to an increase in *Grem1* expression with corresponding observed decrease in expression of BMP target gene *Msx1* (Butterfield et al., 2009). *Prx1-Cre;Ptch1*$^{flox/flox}$ mice also display delayed onset of chondrogenesis evidenced by Alcian blue staining and expression of chondrogenic marker gene *Col2a1* at E12.5. In vitro micromass demonstrated increased hedgehog signaling was associated with inhibition of chondrogenesis as assayed by Alcian blue staining. For the *Prx1-Cre;Ptch1*$^{flox/flox}$ mice, deficits in chondrogenesis could be rescued by treatment with *Smo* inhibitor cyclopamine. Expression of chondrogenic markers *Sox5, Sox6, Sox9* and *Col2a1* was variable with *Prx1Cre;Ptch1*$^{flox/flox}$ micromasses, with expression compared to controls higher at day 2 but lower at day 4 of culture (Bruce et al., 2010). These findings taken together form a model of limb bud signaling where outgrowth, patterning, and chondrogenesis are controlled by a signaling feed back loop that involves *Shh* control of Gli3R levels modulating BMP signaling to control chondrogenesis (Figure 8).

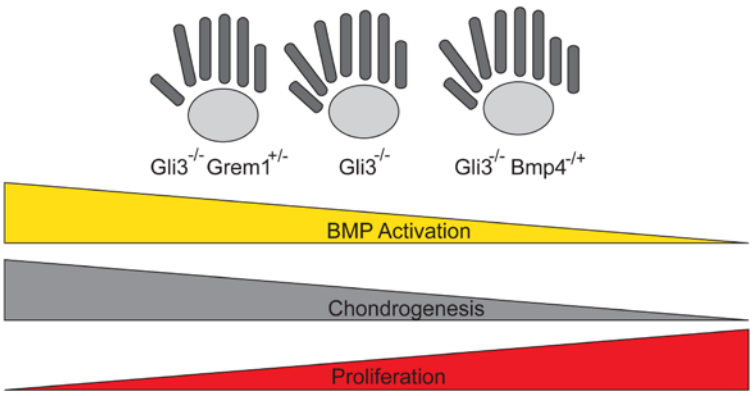

Figure 7. Hedgehog modulates BMP activity to control onset of chondrogenesis and exit to proliferation
The onset of chondrogenesis in the limb bud is closely balanced with continued proliferation to achieve the intended form of the limb. The ability of alterations in BMP signaling level to influence this process in a $Gli3^{-/-}$ background indicates that BMP signaling acts downstream of Gli3 in this process in the limb bud.

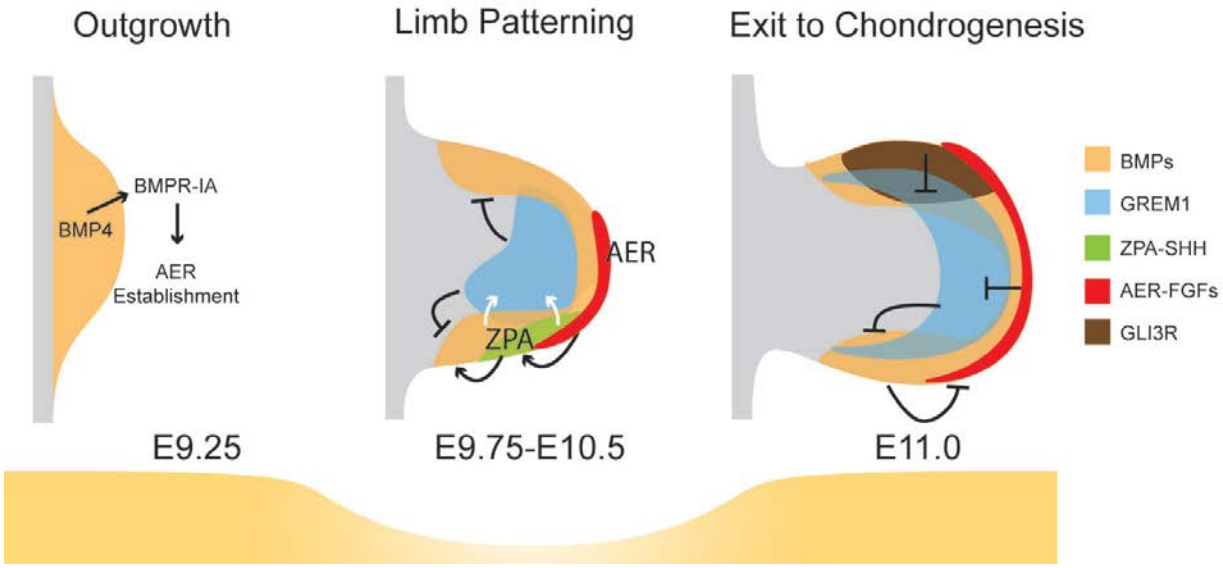

Figure 8. BMP signaling controls limb bud chondrogenesis
The initiation of chondrogenesis within the limb bud is controlled by the action of BMP signaling. A feedback loop between Shh, Grem1, and AER FGFs regulates the levels of Grem1 within the developing limb bud to suppress BMP activity. BMP4 signaling through BMPR1A is necessary to initiate formation of the AER and limb bud outgrowth. Following formation of the AER (red), FGFs from the AER can sustain Shh signaling from the ZPA (green). Shh from the ZPA drives the expression of both limb mesenchyme BMPs and BMP inhibitor Grem1. Grem1 inhibits the action of BMPs to maintain the limb bud in a proliferative state and prevent chondrogenesis. When anterior progenitors have a large enough spatial separation from Shh of the ZPA, hedgehog repressor Gli3R levels rise to suppress Grem1 expression with FGFs, allowing BMP activity to rise and chondrogenesis to initiate. (Adapted from Pignatti et al 2014).

1.5 OSTEOGENESIS

Developmentally, bone is formed by two fundamental processes: endochondral ossification and intramembranous ossification. As described above, endochondral ossification involves the formation of the growth plate, a spatially organized structure within which chondrocytes mature through oriented proliferation, hypertrophy, and eventually either apoptosis or differentiation into osteoblasts; invading osteoblastic progenitor cells then populate the skeletal model, giving rise to a fully formed bone. In contrast, intramembranous ossification involves the direct conversion of mesenchymal progenitors to osteoblasts without the intervening chondrocyte maturation or growth plate structure, and involves the gradual fusion of clusters of osteoblasts known as spicules. The axial and craniofacial skeletons are formed primarily via intramembranous ossification (Abzhanov et al., 2007).

Mature bone is composed of three types of cells: osteoblasts, osteocytes, and osteoclasts. Osteoclasts, responsible for bone resorption, are derived from hematopoietic stem cells. Their regulation and differentiation are tightly linked to osteoblasts and systemic regulators (Asagiri and Takayanagi, 2007). Osteoblasts, responsible for bone synthesis, are derived from $Sox9^{+}$ mesenchymal progenitors that can either continue as chondrocytes or differentiate to preosteoblasts (Akiyama et al., 2005) under the influence of the transcription factors *Runx2*, and later, *Osterix (Sp7*). *Runx2* and *Sp7* are often used as markers of osteoblast differentiation (Figure 9). Mature osteoblasts express the transcription factor activating transcription factor 4 (*Atf4*). *Atf4* is a direct regulator of osteocalcin (*Ocn*) and stimulates expression of Ihh in chondrocytes to encourage maturation and osteoblast differentiation (Long, 2012). Osteoblasts that become embedded within the bony matrix continue to differentiate into osteocytes. Osteocytes, marked by the expression of sclerostin (*Sost*) and dentin matrix protein 1 (*Dmp1*),

compose more than 90% of all mature bone cells and play important roles in signaling to control calcium balance and bone remodeling in response to mechanical and hormonal cues via control of osteoblast and osteoclast differentiation (Bonewald, 2011).

The in vivo hallmark of osteoblastic cells is their ability to lay down a calcified bony matrix. This matrix is composed primarily of type I collagen (*Col1a1*) along with *Ocn*. Calcification requires the expression of alkaline phosphatase (*Alpl*) to provided the necessary phosphate for forming hydroxyapatite along with a host of matrix proteins that support the formation of calcified matrix including osteonectin (*Sparc*), integrin binding sialoprotein (*Ibsp*), and osteopontin (*Spp1*) (Long, 2012).

A number of signaling pathways control the differentiation of osteoblasts. Ihh expression is essential for bone formation—loss of Ihh in mice results in complete failure of bony ossification (St-Jacques et al., 1999). Mutations in the Notch signaling pathway demonstrate that Notch signaling suppresses osteoblast differentiation. Loss of function mutations in the Wnt co-receptor *Lrp5* result in severe osteoporosis, and the canonical Wnt transcription factor β-catenin is required for bone formation in the embryo. A critical threshold of BMP signaling is required for differentiation of mature osteoblasts, but the roles of different receptors and ligands is still an area of active research. FGF signaling plays a role in preosteoblast proliferation and mature osteoblast differentiation, but the precise temporal specificity remains to be investigated (Long, 2012).

The Ihh/PTHrP feedback loop is a major regulator of growth plate chondrocyte hypertrophy and osteogenesis. Ihh secreted by the pre-hypertrophic chondrocytes stimulates hypertrophy of proliferating chondrocytes, but also stimulates expression of *PTHrP*, which inhibits chondrocyte hypertrophy. The interplay of these two signals sets up the orderly

progression of chondrocytes through the growth plate (Vortkamp, 2001; Yeung Tsang et al., 2014). Complete inactivation of hedgehog signaling in osteoblast precursors via deletion of *Smo* from the perichondrium prevents formation of normal bone collar and primary spongiosa. Additionally, chimeric embryos containing $Smo^{-/-}$ cells show no contribution of $Smo^{-/-}$ cells to perichondrium or primary spongiosa (Long et al., 2004). *Gli1*$^{-/-}$ mice display impaired bone formation and perichondrial osteoblast precursors fail to express osteoblast marker genes *Runx*2 or *Osx*. Additionally, in vitro over expression of *Gli1* upregulates early osteogenesis genes *Alp, Bsp, Ocn* in both wild type and $Runx2^{-/-}$ perichondrial cells via direct binding with the 5' regions of these genes. *Gil1*$^{-/-}$ mesenchymal progenitors also display decreased alkaline phosphatase activity in response to *Smo* agonist treatment (Hojo et al., 2012).

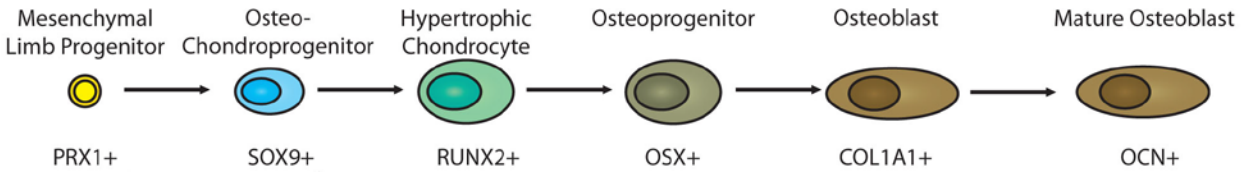

Figure 9. Markers of osteogenic differentiation.
Mesenchymal progenitors express specific osteogenesis related transcription factor and matrix protein genes in a temporally defined manner during osteoblast differentiation. Increases in expression of these markers can be used with in vitro osteogenesis assays to determine osteogenic differentiation.

1.6 PRIMARY CILIA

1.6.1 Primary cilia structure and function

The primary cilium (Figure 10) is a transient organelle that is present on almost all cells in the body at some point. During the G_0 phase of the cell cycle, the primary cilium is formed from one of the centrioles, which serves as the basal body upon which the ciliary microtubule axoneme is

extended. Extension of the ciliary axoneme requires a number of proteins and protein complexes. Intraflagellar (IFT) complex A proteins transport cargo towards the tip of the cilium while IFT complex B proteins transport them from the tip back to basal body. IFT proteins coordinate with dynein and kinesin motors to orchestrate their movement down the microtubule axoneme (Garcia-Gonzalo and Reiter, 2012). At the base of the cilium a number of protein complexes regulate the entry into the ciliary compartment and transition zone between the basal body and axoneme. Identified complexes include the BBsome, which controls IFT assembly and turnaround (Wei et al., 2012), the NPHP module, the MKS/JBTS module, and a number of proteins that span between complexes, as well as a number of whose function is unknown (Ishikawa et al., 2012). The primary cilium and primary cilium membrane are a specialized compartment that is separated from the rest of the cell by a septin diffusion barrier, the assembly of which depends upon the planar cell polarity effector *Wdpcp* (Mostowy and Cossart, 2012).

The primary cilium serves as a signaling hub for a myriad of pathways including hedgehog signaling, Wnt signaling, TGFβ signaling, mechanotransduction, and many others. Disruption of ciliogenesis occurs with disruption of any of the complexes necessary for ciliogenesis and is accompanied by severe phenotypes in both model organisms and humans. Diseases associated with dysfunctional ciliogenesis are characterized as ciliopathies and include polycystic kidney disease, Joubert Syndrome, Meckel-Gruber Syndrome, Alstrom Syndrome, and Bardet-Biedl Syndrome. The phenotypes associated with these ciliopathies affect almost all organ systems and include renal defects, gut malformations, congenital heart defects, deafness, blindness, and skeletal dysmorphogenesis (Goetz and Anderson, 2010).

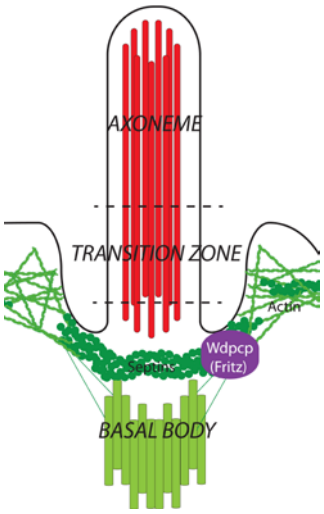

Figure 10. Primary cilium structure.
Primary cilia are a transiently formed organelle present on almost all cells at some point. They are composed of an axoneme which is extended from a basal body. The axoneme (red) composed of 9 microtubules. This structure stains positive for acetylated α-tubilin by immunochemistry. The basal body (green) is formed from one of two centrioles present in all cells and stains positive for γ-tubulin by immunochemistry. Wdpcp localizes to the basal body (light green) and is necessary for the formation of a septin diffusion barrier (dark green) that serves to demarcate the primary cilium compartment.

1.6.2 Role in hedgehog signaling

The primary cilium plays a central role in the hedgehog signaling pathway. Components of the hedgehog pathway are dynamically localized to the primary cilium and rely on the formation of the primary cilium for normal signaling. In *Ptch1*$^{-/-}$ MEFs there is constitutive activation of hedgehog signaling and constitutive localization of Smo to primary cilia. Reintroduction of Ptch1 demonstrates that Ptch1 prevents the accumulation of Smo in cilia in the absence of hedgehog ligand (Rohatgi et al., 2007). Smo is enriched in the primary cilium on hedgehog activation, displacing Ptch1 (Corbit et al., 2005; Wen et al., 2010).

Gli2 and Gli3 also dynamically localize to the primary cilium. Gli2 and Gli3 are present at the cilia tip within 5 minutes of hedgehog activation. PKA stimulation with forskolin inhibits Gli3 accumulation within the cilium as does Smo inhibition with cyclopamine (Wen et al.,

2010). Overexpressed Gli1/Gli2/Gli3 all localize to primary cilia of limb bud cells (Haycraft et al., 2005)

In addition to being necessary for ciliogenesis, intraflagellar transport and kinesin motor proteins have shown to be necessary for hedgehog signaling. IFT proteins are required for formation of both Gli activator forms and repressor forms, indicating that the primary cilium plays a role in both of these processes (Huangfu and Anderson, 2005; Liu et al., 2005). Kif3a$^{-/-}$ mice display a homogenously partially ventralized neural tube with a low level of hedgehog activity that corresponds with expression of *Nkx2.3* and reduced expression Hh signaling markers *Gli1* and *Ptch1*. Additionally, *Kif3a*$^{-/-}$ mouse embryonic fibroblasts (MEFs) are unresponsive to Hh agonists (Huangfu et al., 2003).

PKA localizes to the base of the primary cilium (Tuson et al., 2011). More recent studies have identified negative regulators of PKA activity such as Tulp3, pituitary adenylate cyclase activating polypeptide (PACAP) (Niewiadomski et al., 2013), and Gpr161 that are localized to primary cilia and affect hedgehog signaling. Tulp3 binds to and interacts with IFT complex A, and Gpr161 localizes to the primary cilium in an IFT complex A and Tulp3 dependent manner (Mukhopadhyay et al., 2013).

These studies demonstrate that the primary cilium serves as important scaffold for hedgehog signaling. The specific mechanisms by which post-translational modification of Gli and hedgehog pathway output is controlled by these components will likely prove to intimately involve this organelle.

1.6.3 Primary cilia in skeletal development

Primary cilia have been shown to play essential roles in multiple aspects of skeletal development. Primary cilia are present on both limb ectoderm and limb mesoderm in the E11.5 limb bud. Analysis of the *Ift88Tg*$^{737/Polaris}$ mutant, which carries a mutant allele of the IFT complex B protein Ift88 that disrupts ciliogenesis, shows decreased expression levels of *Gli1* and *Ptch1* in E10.5 posterior limb bud and decreased responsiveness to exogenous Shh conditioned medium. These findings were associated with decreased Gli3 processing as evidenced by inability of exogenous Gli3-GFP to suppress Gli1 expression. It also associated with decreased Gli2 activation as evidenced by the inability of exogenous Gli2-GFP to induce Gli1 expression (Haycraft et al., 2005).

Msx2-Cre;Ift88$^{flox/flox}$ mice display no overt phenotype, indicating that primary cilia function primarily in limb bud mesenchyme during skeletal development. *Prx1-Cre;Ift88*$^{flox/flox}$ mice display polydactyly and shortened limbs with expanded expression of *Grem1* and decreased expression of *Gli*. Growth plates of these animals also displayed decreased expression of *Ptch1* and *Gli1* characteristic of hedgehog pathway dysfunction. Mutants at E18.5 also display shortened limbs with reduced size of growth regions and poorly formed marrow cavity (Haycraft et al., 2007). Dysfunctional growth plate organization was also observed in the *Tg737*^{orpk} mouse which carries a hypomorphic allele of Ift88 (McGlashan et al., 2007). Similarly, *Prx1-Cre;Kif3a*$^{flox/flox}$ mice display shortened limbs with polydactyly, reduced expression of *Gli1* and disrupted Gli3 processing.

Col2a1-Cre;Ift88$^{flox/flox}$ mice display depletion of primary cilia from chondrocytes, disorganized columnar structure and decreased responsiveness to Shh treatment (Chang and Serra, 2013). They also display upregulation of osteoarthritic markers and thickened cartilage

with reduced mechanical properties (Irianto et al., 2014). *Col2a1-Cre;Kif3a*$^{flox/flox}$ mice display post-natal dwarfism due to premature loss of growth plate associated with hedgehog dysfunction (Song et al., 2007).

Deletion of primary cilia within osteoblasts significantly reduces bone formation. *Ocn-Cre;Kif3a*$^{flox/flox}$ mice display reduced primary cilia number and length in osteoblasts. They exhibit a significant reduction in bone mass and develop osteopenia by 6 weeks of age concomitant with reduced hedgehog signaling and impaired osteoblast differentiation (Qiu et al., 2012). *Col1a1-Cre;Kif3a*$^{flox/flox}$ mice display reduction of primary cilia in mature osteoblasts and osteocytes and have decreased formation of bone in response to cyclic loading (Temiyasathit et al., 2012).

Other mutants that affect the formation of the primary cilium display phenotypes similar to knockouts of *Ift88* and *Kif3a. Talpid3*$^{-/-}$ mice display severe polydactyly and shortened long bones. E10.5 limb buds show normal Shh expression with anteriorly expanded *Grem1* expression consistent with and decreased *BMP4, Gli1,* and *Ptch1* expression. Ciliogenesis is disrupted in E10.5 limb bud mesenchyme, but not ectoderm (Bangs et al., 2011). Similarly, *Prx1-Cre;Ofd1*$^{flox/flox}$ mutants display polydactyly with shortened long bones. In these mice, limb bud primary cilia are shortened. They display disrupted hedgehog signaling with normal expression of *Shh*, but decreased *Gli1* and *Ptch1* expression concomitant with increased Gli3 activator to repressor ratio characteristic of disrupted ciliogenesis. At E16.5 in the growth plate there is disrupted hedgehog signaling with normal *Ihh* expression but loss of *Gli1* and *Ptch1* expression along with deficits in proliferation (Bimonte et al., 2011). *Mks1*$^{del64-323}$ mice bear a hypomorphic allele of the cilia basal body protein *Mks1* and display mild polydactyly and defective

ciliogenesis resulting in defective Gli3 processing. In the limb bud there is decreased expression of *Ptch1* and *Gli1* that is accompanied by anterior expansion of *Grem1* (Cui et al., 2011).

These studies point to a common phenotype that results from loss of primary cilia within the limb bud mesenchyme. Mice with disrupted ciliogenesis in the limb bud mesenchyme display shortened limbs with polydactyly. Expression of BMP inhibitor *Grem1* is expanded and expression of hedgehog responsive genes *Ptch1* and *Gli1* is reduced. As detailed in the previous sections this phenotype represents a concomitant disruption of limb bud outgrowth, patterning, and chondrogenesis. Dysfunctional regulation of the growth plates is observed in both limb mesenchyme specific conditional knockout mouse models generated with with *Prx1-Cre* and chondrocyte specific mouse knockout models generated with *Col2a1-Cre*. Analysis of growth plate organization in *Prx1-Cre* and constitutive knockout mouse models is complicated by dysfunction present in the limb bud that leads to delay of chondrogenesis. The reduction in bone formation observed in osteoblast specific mouse knockout models of primary cilia coincides with an observed reduction in hedgehog signaling responsiveness that correlates with the known positive role of hedgehog signaling in osteoblast differentiation.

1.6.4 Primary cilia and planar cell polarity (PCP) effector proteins

Primary cilia and planar cell polarity (PCP) signaling are two closely related pathways. PCP effectors were originally identified in *D. melanogaster* by their ability to disrupt organized, polarized accumulation of F-actin in the imaginal discs characteristic of mutants of the PCP pathway (Wallingford, 2012). The identified PCP effector proteins in *D. melanogaster* include *fritz (Wdpcp)*, *inturned (Intu)*, and *fuzzy (Fuz).* These genes act downstream of the core components of PCP signaling. In addition to their role in PCP, these genes are also essential to

formation of primary cilia. Recently, Wdpcp, Intu, Fuz have been recognized as members of a complex that promotes ciliogenesis (Wallingford, 2012).

The PCP effectors Fuz and Intu have been demonstrated to play important roles in skeletal development. *Fuz*$^{-/-}$ (Heydeck et al., 2009) and *Intu*$^{-/-}$ (Zeng et al., 2010) mice display polydactyly consistent with disrupted Gli3 processing and limb bud mesenchyme displays disrupted ciliogenesis. Additional studies have demonstrated that these proteins play key roles in ciliogenesis via control of IFT complexes (Brooks and Wallingford, 2012; Zeng et al., 2010). The skeletal phenotype of these mice is similar to all mutants with disrupted Gli3 processing and functional loss of Gli3 repressor.

1.7 WDPCP

A mutagenesis screen in mice recovered the *Cys40* (named due to mutation at cysteine 40) mutant, a mouse with severe skeletal defects bearing a null mutation in WD40 domain containing planar cell polarity effector protein (*Wdpcp).* This mutant had a number of hallmarks of altered hedgehog signaling including polydactyly and neural tube defects. Further investigation revealed alterations in ciliogenesis including impaired formation and architecture in multiple tissues (Cui et al., 2013). *Wdpcp* was first characterized in D. melanogaster as the planar cell polarity effector *Fritz*. These genes function cell autonomously downstream of the core planar cell polarity genes to regulate the location and number of wing cell prehair initiation sites via polarized accumulation of F-actin (Collier et al., 2005). A study in *Xenopus* demonstrated a role for the *Wdpcp* homolog *Fritz* in both ciliogenesis and convergent extension via organization of cytoskeletal septins (Kim et al., 2010).

The mouse *Wdpcp* homolog is encoded by 18 exons located at mouse chromosome 11a3.1 and encodes one known protein isoform (a 722 amino protein). The protein sequence of the gene is significantly conserved from flies to humans. In humans *Wdpcp* mutations are associated with ciliopathy syndromes including Bardet-Biedl Syndrome, Alstrom Syndrome, and Meckel Gruber Syndrome (Aliferis et al., 2012; Chen et al., 2011; Kim et al., 2010).

The mouse *Wdpcp*^{Cys40} mutant used in these studies was first described in a 2013 publication that demonstrated a role for *Wdpcp* in many developmental processes. In this mutant, an A to G substitution at nucleotide 224 of the mRNA resulted in a premature stop codon after amino acid 54 (S54X). The conditional *Wdpcp*^{flox} knockout mouse is also described in this study, and is a mouse that bears loxP sites on either side of exon 5. When crossed with a Cre recombinase expressing mouse strain, this results in cleavage and recombination at the loxP sites that leads to deletion of exon 5 in all *Cre* recombinase expressing cells (Figure 11). When crossed with the constitutive expressing Cre strain *CMV-Cre* to generate *CMV-Cre;Wdpcp*$^{flox/flox}$ mice, the homozygous inducible knockout mice bear an identical phenotype to the homozygous *Wdpcp*$^{Cys40/Cys40}$ mice (Cui et al., 2013).

Wdpcp$^{Cys40/Cys40}$ mice display severe polydactyly (7-9 digits) consistent with observed disruption of ciliogenesis and expanded anterior limb bud expression of *Grem1* at E10.5. Consistent with a loss of responsiveness to upstream regulators of hedgehog, *Wdpcp*$^{Cys40/Cys40}$ mutants are able to partially rescue both *Ptch1*$^{-/-}$ and *Smo*$^{-/-}$ embryos (Cui et al., 2013).

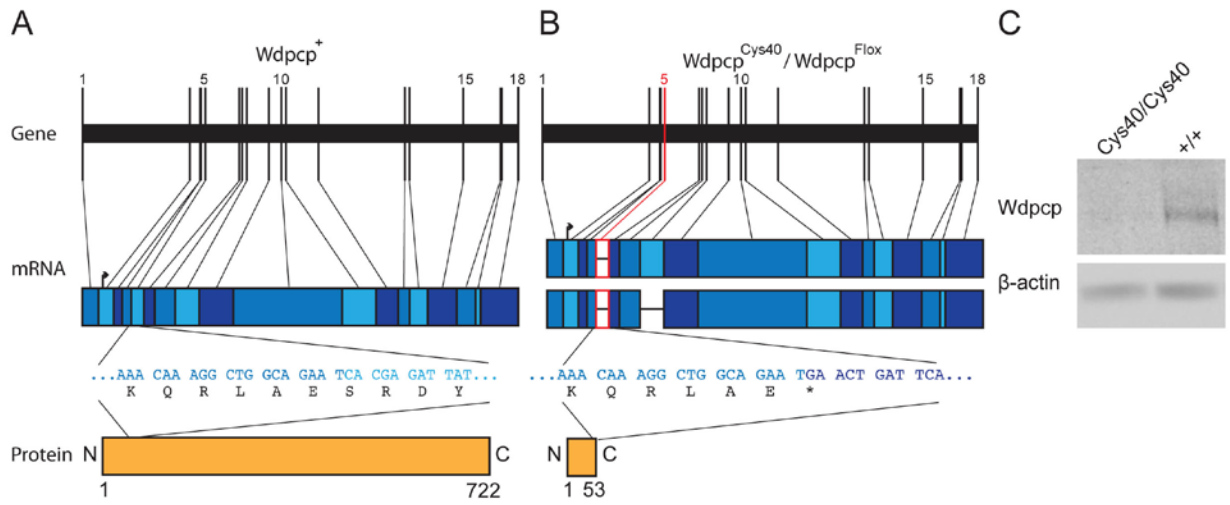

Figure 11. Wdpcp *Cys40* mutant.
Wdpcp (A) is composed of 18 exons located on chromosome 11 in *Mus musculus* that are spliced together to form a mature RNA that encodes a 722 amino acid protein with start codon located within exon 2. $Wdpcp^{Cys40}$ and $Wdpcp^{Flox}$ (B) both encode alleles of Wdpcp that result in a mature RNA lacking exon 5. Exon 4 is spliced directly to exon 6, resulting in a frameshift mutation that leads to an early stop codon, and results in a severely truncated polypeptide 53 amino acids long. Western blot of $Wdpcp^{Cys40/Cys40-}$ forelimb buds reveals absence of Wdpcp protein (C), confirming functional knockout of Wdpcp.

1.8 SUMMARY

Degenerative diseases of the skeletal tissues represent a large and growing burden with limited effective treatments, none of which are fully capable of fully restoring tissue function. The development of highly effective and specific personalized therapies that can exceed the outcomes of current therapies by orders of magnitude will depend upon a deep mechanistic understanding of the processes that govern skeletal tissue development and homeostasis. Study of the development of skeletal tissues in model organisms such as mice has already yielded significant insights into the signaling pathways and mechanisms that govern the formation bone and cartilage that has been exploited for the development of new therapies for degenerative diseases of the skeletal tissues. Forward mutagenesis screens represent a traditional unbiased approach to uncovering genes that regulate specific developmental processes.

Large-scale mutagenesis screens have been conducted in mice to recover animals bearing mutations in genes that affect skeletal development in order dissect the genetic mechanisms governing formation and homeostasis of skeletal tissues. In a screen conducted by our collaborator, Dr. Cecilia Lo, a novel allele of *Wdpcp* (*Cys40)* was identified that when inherited in a homozygous manner led to significant skeletal defects. Further investigations revealed that the *Cys40* allele is a functional deletion of *Wdpcp.* Inheritance of two copies of *Cys40* results in the loss of any function of *Wdpcp* including the absence of transcribed mature *Wdpcp* RNA and Wdpcp protein (Cui et al., 2013). By studying the effects of the loss of *Wdpcp* at specific time points in development and within specific populations of cells that give rise to the skeleton, an understanding of the function of when and where *Wdpcp* functions in skeletal development can be gained. Studies using pharmacologic and genetic activators and inhibitors of specific pathways previously demonstrated to be involved in skeletal development can elucidate how *Wdpcp* mediates its effects in the larger context of skeletal development. Understanding gained from these studies can be exploited to correct pathophysiology associated with *Wdpcp* loss and cell processes that have been demonstrated to be perturbed by *Wdpcp* loss.

The studies described below have the goal of determining the specific function of *Wdpcp* within skeletal development. The first aim involves an extensive characterization of the effects of loss of *Wdpcp* on skeletal development using the *Cys40* constitutive knockout model along with a conditional knockout model. The second aim describes in vitro experiments to study the effects of *Wdpcp* loss and related signaling disruption on the developmental processes of chondrocyte and osteoblast differentiation. The third aim describes studies designed to elucidate the specific mechanistic role of *Wdpcp* in the hedgehog signaling pathway and the regulation of Gli transcription factor signaling. Together these aims will represent the first description of the role

of *Wdpcp* in both skeletal development and hedgehog signaling and pave the way for future studies into the mechanisms of both of these systems.

Specific Aim #1: To characterize the skeletal defects and associated signaling defects present in mice lacking functional *Wdpcp*

Specific Aim #2: To determine the effects and mechanism of *Wdpcp* loss on chondrogenic and osteogenic in vitro differentiation

Specific Aim #3: To determine the mechanism by which hedgehog signaling is disrupted with loss of *Wdpcp*

By completing these aims, a detailed description of the role *Wdpcp* in skeletal development and related signaling will be attained, allowing its role to be placed it in the context of prior and future studies as well as to be potentially exploited for therapeutic benefit. Additionally, insights gained from specific signaling roles in skeletal development may have far reaching implications for other processes that utilize the same signaling pathways such as the development and homeostasis of other tissues as well as dysregulation of these signaling pathways in processes such as cancer and aging. The following chapters detail the results of experiments designed to address each of the above specific aims.

2.0 LOSS OF WDPCP DISRUPTS SKELETOGENESIS AT MULTIPLE POINTS IN DEVELOPMENT

2.1 INTRODUCTION

These studies sought to characterize the skeletal phenotype of the *Cys40* mutant, a functional null mutant of *Wdpcp,* to determine when and where in skeletal development *Wdpcp* functions. Specific investigations into signaling pathways known to regulate chondrogenesis and osteogenesis revealed that loss of *Wdpcp* disrupts hedgehog signaling leading to abnormal regulation of downstream BMP signaling. Characterization included analyses of *Cys40* embryos at different time points in skeletal development to determine potential effects of *Wdpcp* on different processes in skeletal development that occur during known time periods. Following initial characterization of the *Cys40* mutant, the Cre-lox system was used to make tissue and developmental stage specific deletions in the progenitors of the appendicular skeleton to determine the temporal and spatial requirement for *Wdpcp* in skeletal development. These models allowed for examination of specific phenotype of Wdpcp loss in skeletal progenitor populations free from the confounding effects of earlier developmental disruptions and systemic *Wdpcp* loss.

2.2 METHODS

2.2.1 Mouse strains

The *Wdpcp*$^{Cys40/Cys40}$ mouse (termed *Cys40* mutant) and *Wdpcp*$^{Flox/Flox}$ mouse have been previously described (Cui et al., 2013). The B6.Cg-Tg(Prrx1-cre)1Cjt/J mouse strain was obtained from Jackson Laboratories (Jackson Stock #005584) and is referred to as *Prx1-Cre*. The FVB-Tg(Col2a1-cre/ERT)KA3Smac/J mouse strain was obtained from Jackson Laboratories (Jackson stock #006774) and is referred to as *Col2a1-Cre*^{ERT}.

For generation of E10.5 limb buds, E11.5 limb buds, limb bud micromass cultures, and mouse embryonic fibroblasts, *Wdpcp*$^{Cys40/+}$ females were crossed with *Wdpcp*$^{Cys40/+}$ males to obtain litters containing both *Wdpcp*$^{Cys40/Cys40}$ and *Wdpcp*$^{+/+}$ embryos. *Wdpcp*$^{Cys40/+}$ and *Wdpcp*$^{+/+}$ mice had no differences in terms of skeletal morphology and were grouped and termed control. *Wdpcp*$^{Cys40/Cys40}$ embryos were termed *Cys40*.

For the generation of conditional mutants, the *Wdpcp*$^{Cys40/+}$ males were crossed to females carrying the *Wdpcp*^{Flox} allele and the specific *Cre* allele to minimize the requirement for *Cre* recombination to achieve complete deletion of *Wdpcp* (Zhulyn et al., 2014). *Prx1-Cre* mice were crossed with the *Wdpcp*$^{Flox/Flox}$ mice to induce limb bud mesenchyme specific deletion of the *Wdpcp*^{Flox} allele (Logan et al., 2002). Female *Prx1-cre;Wdpcp*$^{Flox/+}$ mice were generated by crossing male *Prx1-cre* mice to female *Wdpcp*$^{Flox/Flox}$ homozygous mice. Female *Prx1-cre;Wdpcp*$^{Flox/+}$ mice were crossed to *Wdpcp*$^{Cys40/+}$ males to obtain litters with *Prx1-cre;Wdpcp*$^{+/+}$ and *Prx1-cre;Wdpcp*$^{Cys40/Flox}$ mice.

Similarly, *Col2a1-Cre*^{ERT} mice were crossed with *Wdpcp*$^{Flox/Flox}$ mice for chondrocyte specific deletion of *Wdpcp* (Nakamura et al., 2006). Female *Col2a1-Cre*^{ERT}*;Wdpcp*$^{Flox/+}$ mice were generated by crossing male *Col2a1-Cre*^{ERT} mice to female *Wdpcp*$^{Flox/Flox}$ homozygous mice. Female *Col2a1-Cre*^{ERT}*;Wdpcp*$^{Flox/+}$ mice were crossed to *Wdpcp*$^{Cys40/+}$ males to obtain litters with *Col2a1-Cre*^{ERT}*;Wdpcp*$^{+/+}$ and *Col2a1-Cre*^{ERT}*;Wdpcp*$^{Cys40/Flox}$ mice. All reported mice are from mixed background strains. All histological specimens are shown in comparison to littermates and representative of at least 3 biological samples.

2.2.2 Genotyping and injections for *Cre* induction

For genotyping, DNA was extracted from livers of embryos and tail clips of newly weaned mice using the REDExtract-N-Amp Tissue PCR Kit (Sigma). Primers used for genotyping are included listed in Table 1. The *Wdpcp*^{Cys40} allele was genotyped using Sanger sequencing of a 150 base pair fragment to identify the relevant A>G base pair change (Figure 12A). The Wdpcp^{Flox} allele was genotyped using primers to amplify a region containing an inserted flox site (424 base pair fragment) or lacking an inserted flox site (262 base pair fragment) that could be differentiated with agarose gel electrophoresis. Presence of Cre allele was identified using primers specific to Cre that amplified 102 base pair fragment (Figure 12B). In all timed pregnancies, plug date was identified as E0.5. Temporal and spatial kinetics of Cre expression and recombination in the *Col2a1-Cre*^{ERT} mouse line with intraperitoneal 4-OH tamoxifen injection has been extensively characterized. Injection of 2 mg 4-OH tamoxifen at E11.5 is sufficient to induce strong expression of Cre in all chondrocytes in the cartilage anlagen of the limbs (Nakamura et al., 2006). For injections, 4-OH tamoxifen (Sigma) was dissolved in 100% ethanol at 100 mg/mL. This solution was further dissolved 1:10 in sterile corn oil followed by

gentle heating at 37 °C for 1 hour to ensure uniform dissolution for a final concentration of 10 mg/mL. For induction of Cre expression, 200 uL of this solution (2 mg) was injected intraperitoneally into pregnant dams at 11.5 days post plug. All animal experimentation was carried out in according to a protocol approved by the Insitutional Animal Care and Use Committee of University of Pittsburgh.

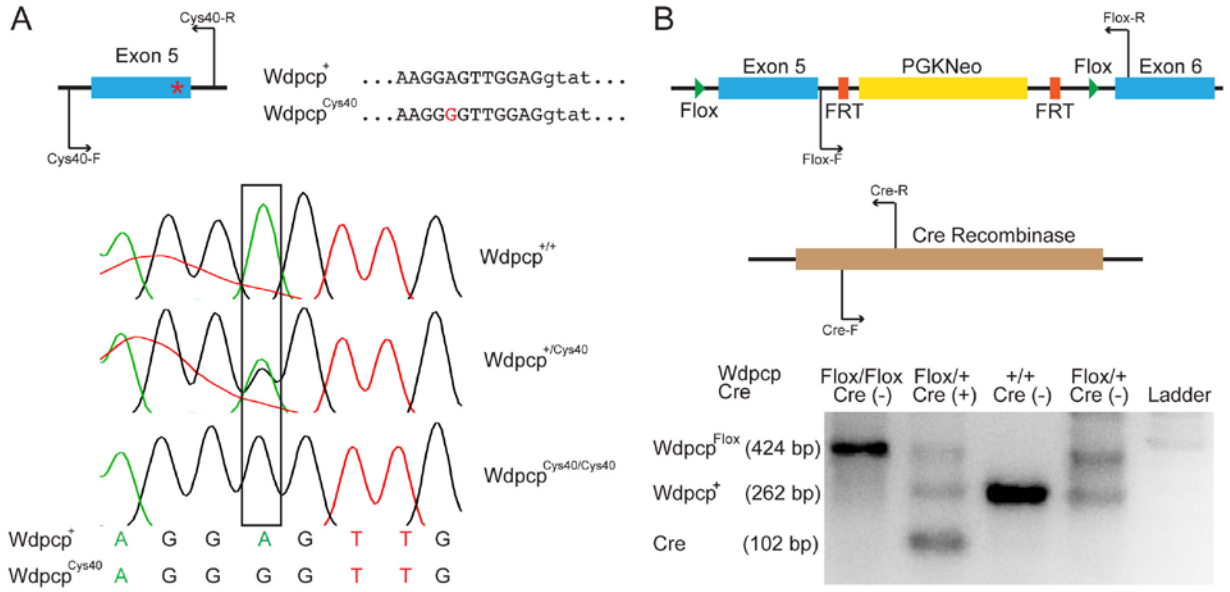

Figure 12. Genotyping of mouse strains.
The Wdpcp^{Cys40} allele is a single base pair change from A to G at the 3' end of exon 5. Wdpcp^{Cys40} allele was differentiated from Wdpcp^{+} by direct Sanger sequencing of a 150 base pair PCR fragment centered on the base pair of interest (A). The Wdpcp^{Flox} allele was differentiated from the Wdpcp^{+} allele by amplifying a fragment containing (Flox) or lacking (+) a 162 basepair inserted Flox site (B). These fragments were separated with agaorse gel electrophoresis. Presence or absence of a Cre allele was determined with presence or absence of a PCR amplification product 102 base pairs in length amplified from any inserted Cre.

Table 1. Genotyping PCR primer sequences (5'-3')

Primer Name	Sequence	Target
Cys40-F	GATCGATCGCTCAA	*Wdpcp^{Cys40}*
Cys40-R	AGAGCTGACTGATCGA	*Wdpcp^{Cys40}*
Flox-F	GCGGAGCTCTACG	*Wdpcp^{Flox}*
Flox-R	ATCGATCGATCGC	*Wdpcp^{Flox}*
Cre-F	GATCGCTAGCGAAGCGGC	*Col2a1Cre^{ERT}; Prx1-Cre*
Cre-R	GATCGCGATTAGCGCA	*Col2a1Cre^{ERT}; Prx1-Cre*

2.2.3 Timed matings

Matings were monitored for copulation plugs each morning. Plugged mice were weighed and separated from males with E0.5 considered 1 PM day of plug. Plugged females were re-weighed at E10.5 and checked for weight increase of at least 2.5 g to indicate pregnancy. Embryos displaying generalized developmental deficiency as evidenced by decreased crown to rump length were excluded from analyses.

2.2.4 Alizarin red and Alcian blue whole mount staining

Skeletal preparations were made by co-staining embryos with alizarin red S for ossified, calcium rich tissue and Alcian blue for cartilage as described previously (Mis et al., 2014). Briefly, embryos were scalded in hot tap water, skinned, and their abdominal and thoracic organs removed. Livers were saved for genotyping. Embryos were transferred into alcohol before staining 24 hours with 40% glacial acetic acid, 60% ethanol, 0.0001% Alcian Blue solution at room temperature. Embryos were destained for 24 hours in ethanol before being transferred to a solution containing 2% KOH (Sigma) in distilled water with 0.0015% Alizarin Red S (Sigma) for 5 hours. Embryos were subsequently destained in 2%KOH in distilled water overnight, followed by 1% KOH in 50% glycerol/50% distilled water. Embryos were transferred to 50% glycerol/50% distilled water for imaging. All images are representative of 2-6 specimens. For limb length quantification, the longest vector along each cartilage element was used. Six limbs from six separate animals were used for both mutants and controls.

2.2.5 Histology

Embryos were delivered by caesarean section at determined time point. Internal organs were removed and saved for genotyping as described in Section 2.2.2. Skeletons were fixed in 4% paraformaldehyde overnight before being dehydrated through an ethanol series. Following clearing in xylenes, limbs were transferred to paraffin, embedded, and sectioned at 7 microns. Sections were stained with 1% silver nitrate (Sigma) and exposed to 260 nM UVC light for 30 minutes at room temperature before destaining with 5% sodium thiosulfate (Sigma) for 5 minutes at room temperature and counter staining with nuclear fast red (Sigma).

2.2.6 RNA isolation and quantitative real-time polymerase chain reaction (qPCR)

Total RNA was extracted using TRIzol (Invitrogen) with RNeasy columns (Qiagen) for purification and removal of genomic DNA. RNA was quantified spectrophotometrically, and cDNA was synthesized from 200 ng of total RNA using Superscript III (Invitrogen) with the Oligo(dT) primers per the manufacturer's protocol. Quantitative real-time PCR was performed on Applied BioSystems StepOnePlus with Applied Biosystems SYBR Green PCR mastermix in 96-well plates. Primers were all used at a concentration of 200 nM. Cycling variables were as follows: 95 °C for 10 min, then 40 cycles of 15 second denaturation at 95 °C and 1 minute at 60 °C. Primer sequences are listed in Table 2. Expression was reported normalized to housekeeping gene *HPRT* due to reported stability of expression of this gene during skeletal development (de Kok et al., 2005; Zhai et al., 2013). For the whole limb studies, the mean and standard deviation was determined from 3 biological replicates. For micromass culture studies, mean and standard

deviation represent 3-4 biological replicates each composed of RNA isolated from 2 experimental replicates.

2.2.7 Western Blotting

Forelimb buds from E10.5 embryos were isolated by dissection. *Cys40* embryos could be differentiated from heterozygous and wild type embryos by concomitant defective ocular development in the *Cys40* embryos. This association and full penetrance of the *Cys40* phenotype was confirmed by individually genotyping embryos after forelimb buds had been combined for protein isolation. Two to three forelimb buds from separate animals were isolated with a Total Protein Extraction Kit (Millipore) supplemented with 5 mM EDTA and 1X Halt Protease and Phosphatase Inhibitor Cocktail (Thermo Scientific). Samples were sonicated to homogenized lysate, and protein concentration was quantified using BCA assay kit (Pierce) and standardized to same concentration using isolation buffer dilution. Western blots were performed as previously described (Lozito and Tuan, 2011). Protein samples were subjected to reducing SDS-PAGE and transferred to low-fluorescence background polyvinyl fluoride (PVDF) membranes (Millipore). Membranes were blocked in 3% dried milk in 0.25% Tween-20 in TBS (TBS-T) for 1 hour at room temperature and probed overnight at 4° C with primary antibody in 1% milk/TBS-T. Primary antibodies used are listed in Table 2. After washing with TBS-T, membranes were incubated for 1 hour at room temperature with HRP conjugated anti-rabbit (Abcam) (1:1000) or poly-HRP conjugated anti-goat antibody (Pierce) (1:2000) in 1% milk/TBS-T. Immunoreactive bands were visualized with SuperSignal West Dura Extended

Duration Substrate (Thermo Scientific) on a Fotodyne imaging system. Each blot was repeated at least in duplicate, and representative blots are presented.

Table 2. Antibodies

Antibody Target	Antibody Information	Antibody concentration	Application	Species
Gli3	R&D (AF3690)	1:1000	Western	Goat
pSmad1/5/9	Cell Signaling Technology (D5B10)	1:1000	Western	Rabbit
Smad1/5/9	Abcam (ab80255)	1:500	Western	Rabbit
β-actin	Santa Cruz (sc-47778)	1:1000	Western	Mouse

2.2.8 Statistical analysis

Two-tailed Student's T-test with assumption of heteroscedastic populations with significantly different variance was used to determine significance for limb lengths and for relative expression of qRT-PCR. Results are expressed as mean +/- standard deviation. All histological specimens are representative of at least 3 biological replicates.

2.3 RESULTS

2.3.1 The *Cys40* mutant mouse displays gross skeletal defects

The E17.5 *Cys40* mutant displays drastic skeletal defects including shortened and dysmorphic forelimbs and hindlimbs, severe polydactyly (8-9 digits), vertebral ossification and midline defects, and facial clefting (Figure 13). The severe polydactyly observed in the *Cys40* mutant has been observed in mice bearing mutations that affect limb bud patterning. These include

mutations in Gli3 and those that affect levels of the effector form of Gli3, the truncated Gli3 repressor (Osterwalder et al., 2014). *Gli2*$^{-/-}$*;Gli3*$^{-/-}$ mutants have an almost identical phenotype to the *Cys40* mutant . Midline defects of the vertebral bodies have been described in mutants of genes that affect the formation of the primary cilium (Yuan et al., 2015). The fusion of vertebral bodies C2-C3 is characteristic of Klippel-Feil Syndrome and has been associated with vertebral segmentation defects linked to FGF signaling dysfunction, commonly correlated with disruption of primary cilia (Tracy et al., 2004). Because of its relatively more studied development, the appendicular skeleton was chosen as an area of focus. In this regard, the investigation was broken down to examine specific components of appendicular skeletal development.

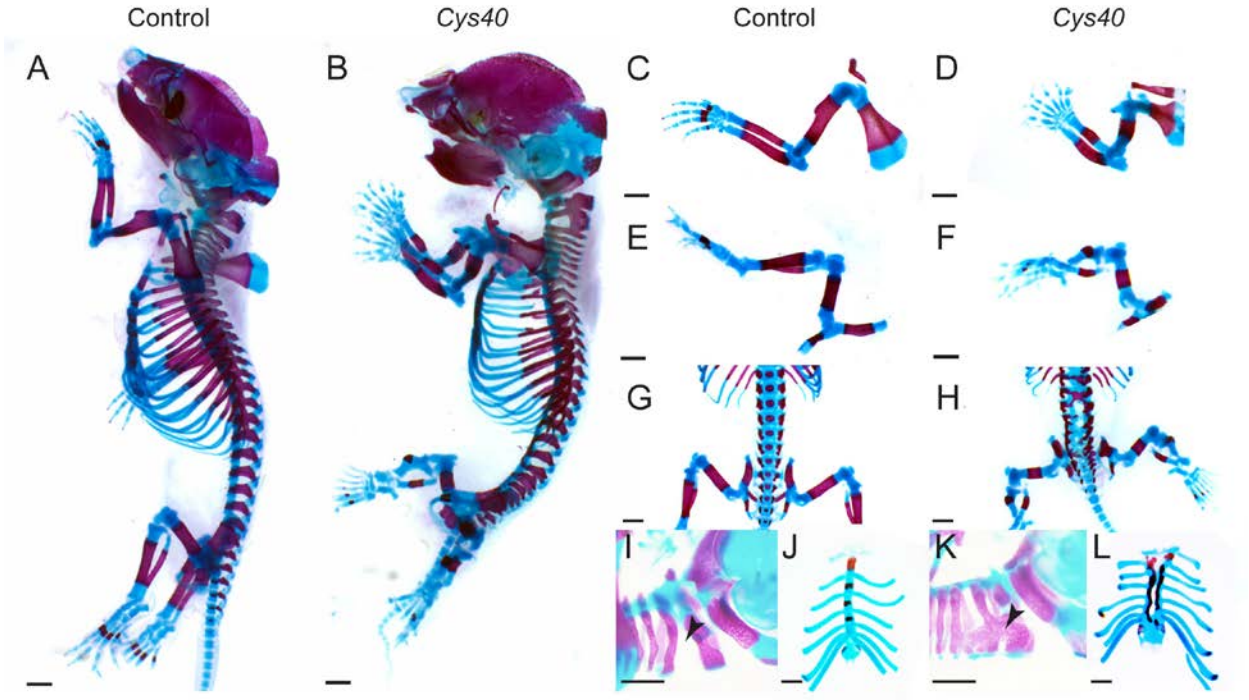

Figure 13. *Wdpcp* null mice display gross skeletal defects
Alizarin red (bone) and Alcian blue (cartilage) whole mount staining of E17.5 *Wdpcp*$^{Cys40/+}$ (control) (A) and *Wdpcp*$^{Cys40/Cys40}$ (*Cys40*) (B) embryos reveals gross skeletal defects in *Cys40* embryos. Appendicular skeletal defects include shortened, dysmorphic long bones of forelimb (C, D) and hindlimb (E, F) as well as polydactyly. Axial skeletal defects include lumbar vertebral segmentation and ossification defects in *Cys40* embryos (H) versus controls (G), cervical segmentation defects including fusion of C2-C3 vertebrae in *Cys40* embryos (K) versus controls (I), and midline sternal defects in *Cys40* embryos (L) versus control (J). Black scale bars represent 2 mm in all panels.

Having made gross characterizations of the specific defects present in E17.5 *Cys40* embryos, examination of different time points in development was undertaken to determine the critical period of *Wdpcp* function for these skeletal defects. At E14.5 *Cys40* embryos display delayed ossification of the forelimbs (Figure 14) along with significantly shortened cartilage anlagen of the long bones of both the forelimbs and hindlimbs (Figure 16) consistent with an outgrowth defect in the limb bud.

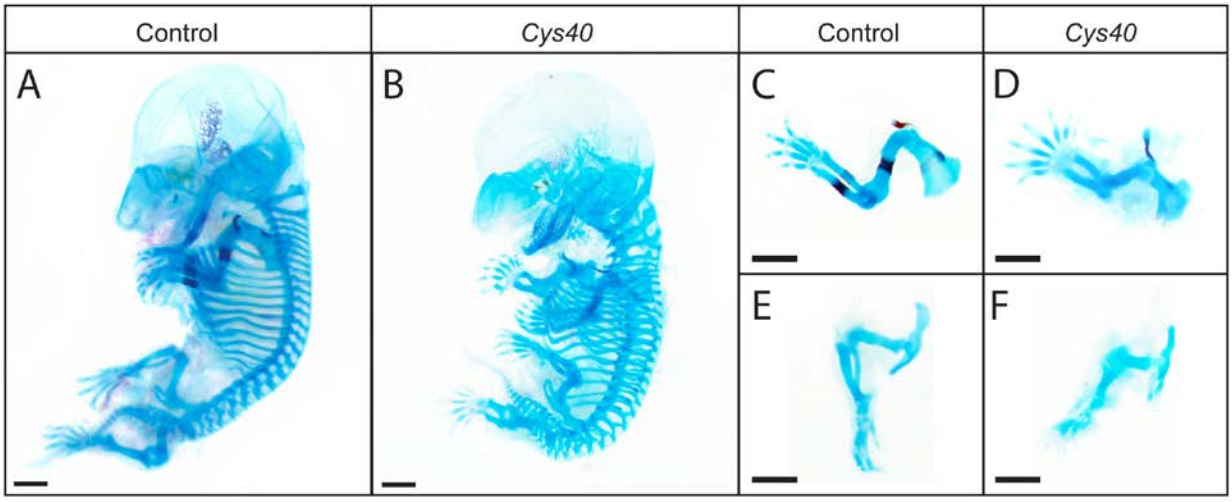

Figure 14. Skeletal phenotype of E14.5 *Cys40* mutant
Alizarin red and Alcian blue staining of homozygous *Cys40* E14.5 embryos reveals delayed ossification, polydactyly, shortened appendicular cartilage anlagen, and vertebral defects.

2.3.2 *Prx1-Cre;Wdpcp*$^{Cys40/Flox}$ recapitulates appendicular skeletal phenotype of *Cys40* mutant

Having determined that the skeletal phenotype of *Cys40* mutant mice is present at E14.5, the conditional allele of *Wdpcp* was used to generate a limb mesenchyme specific deletion with the *Prx1-Cre* line. *Prx1-Cre* expresses *Cre* recombinase in the forelimb bud mesenchyme at E9.5 and the hindlimb bud mesenchyme at E10.0. There is also some expression within mesenchymal tissues that give rise to the axial and craniofacial skeleton (Logan et al., 2002). *Prx1-*

Cre;Wdpcp$^{Cys40/Flox}$ mice were generated to ensure that minimal Cre activity would required for complete loss of Wdpcp from Cre expressing cells.

Alizarin red/Alcian blue staining of E17.5 *Prx1-Cre;Wdpcp*$^{Cys0/Flox}$ embryos (Figure 15) reveals that limb mesenchyme specific deletion of *Wdpcp* recapitulates the appendicular phenotype of the *Cys40* mutant nearly identically. E17.5 *Prx1-Cre;Wdpcp*$^{Cys0/Flox}$ embryos display shortened and dysmorphic forelimbs and hindlimbs with severe polydactyly similar to *Cys40* mutants. As expected due to the spatial and temporal expression pattern of *Prx1-Cre*, E17.5 *Prx1-Cre;Wdpcp*$^{Cys0/Flox}$ embryos fail to recapitulate aspects of distal axial skeletal phenotype including lumbar vertebral ossification and sternal midline defects. However, fusion of the C2-C3 vertebra is recapitulated in E17.5 *Prx1-Cre;Wdpcp*$^{Cys0/Flox}$ embryos.

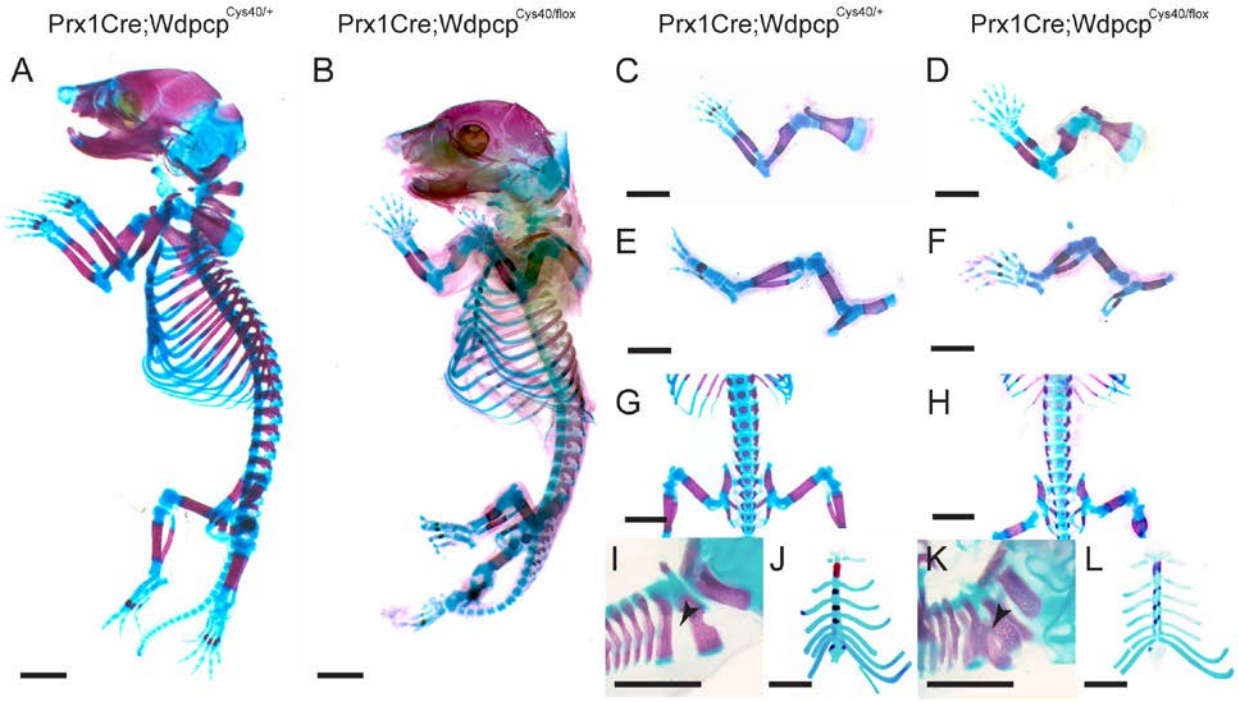

Figure 15. *Wdpcp* functions in the limb bud mesenchyme
Alizarin red and alcian blue whole mount staining of E17.5 Prx1-Cre;Wdpcp$^{Cys/+}$ (A) and Prx1Cre$^{Cys40/flox}$ (B) embryos reveals limb mesenchyme specific deletion of *Wdpcp* results in gross skeletal defects of the appendicular skeleton that recapitulate those seen the in *Cys40* mutant including forelimb and hindlimb polydactyly with shortened and dysmorphic long bones (C-F). Lumbar vertebrae (G, H) and sternae (J, L) display no segmental defects or ossification defects observed in *Cys40* embryos consistent with spatial expression pattern of *Prx1*. Cervical vertebrae display fusion of C2-C3 as seen in *Cys40* embryos consistent with expression of *Prx1* in cephalic mesoderm (I, K). Black scale bars represent 2 mm in all panels.

2.3.3 Disruption of limb bud exit to chondrogenesis with Wdpcp deficiency

Onset of chondrogenesis is delayed in the *Cys40* embryos as evidenced by expression of chondrogenic marker genes (Figure 17) at E11.5. Chondrogenesis initiates in the limb bud at ~E11.0 and is associated with upregulation of expression of genes that make up the characteristic matrix of chondrocytes. Lower expression in the *Cys40* mutants of these is consistent with the observed phenotype at E14.5 and E17.5 of the *Cys40* mutant. The E17.5 at E14.5 mutants both display formation of bone and cartilage indicating that *Wdpcp* is not absolutely required for chondrogenesis or osteogenesis. However, the decreased expression of chondrogenic markers at E11.5 indicates that *Wdpcp* does play significant role in the initiation of chondrogenesis.

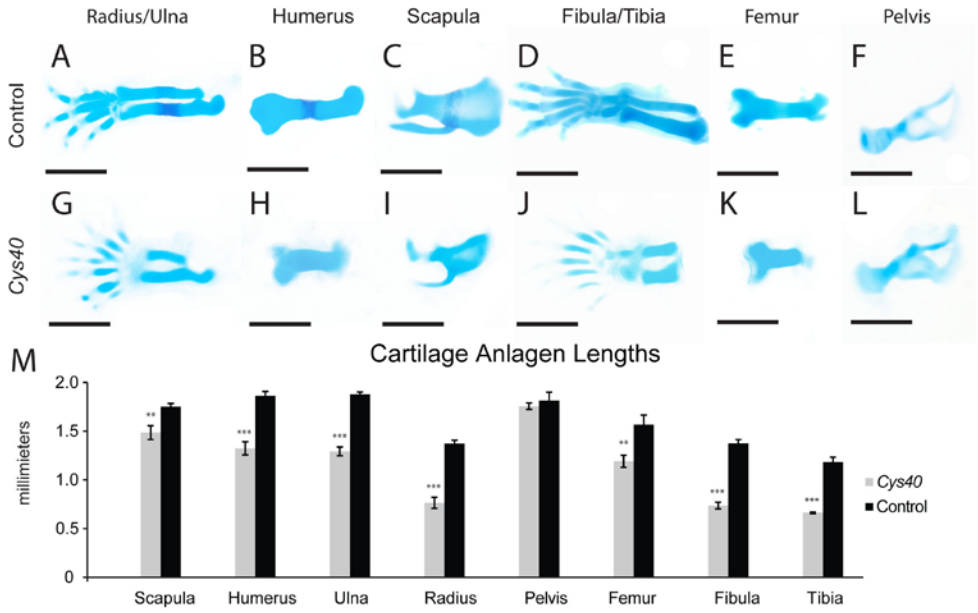

Figure 16. Cys40 embryos have smaller appendicular cartilage anlagen
Alcian blue and alizarin red staining of E14.5 embryos reveals that cartilage anlagen of the forelimb skeletal elements, including the radius, ulna (A, G), humerus (B, H), and scapula (C, I), are significantly shorter in the *Cys40* embryos compared to controls (M). Cartilage anlagen of the hindlimb skeletal elements including the fibula, tibia (D, J), and femur (E, K) are significantly shortened in *Cys40* embryos compared to controls (M). No significant difference was observed in the size of the pelvis skeletal elements (F, L) of *Cys40* embryos compared to controls (M). All scale bars are 2 mm. Error bars represent one standard deviation. *Cys40* is compared to matched control with * for $p<0.05$, ** for $p<0.01$, *** for $p<0.001$.

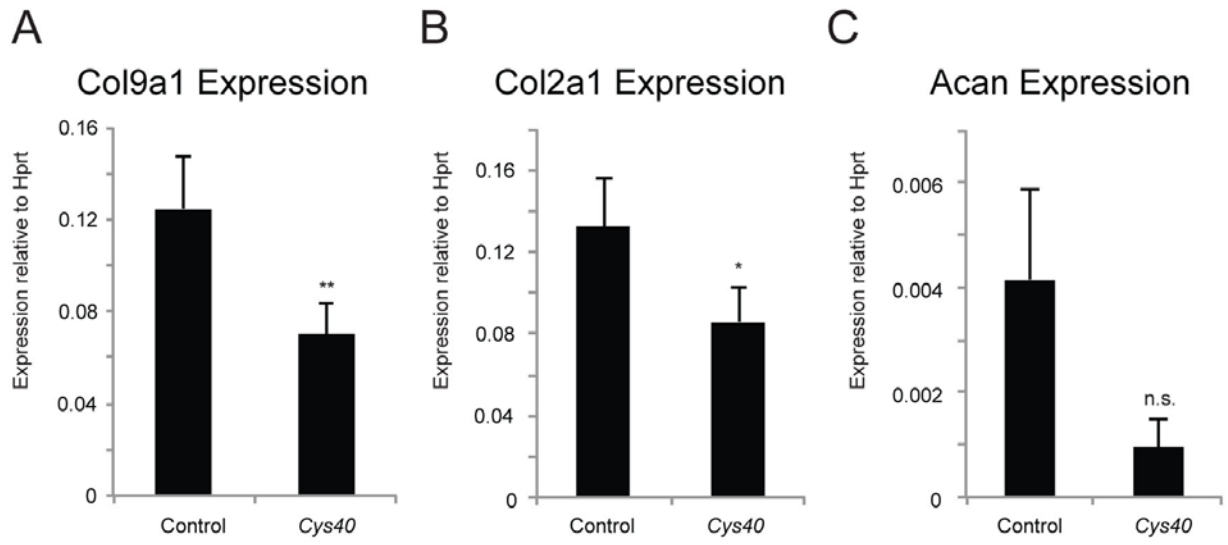

Figure 17. Loss of *Wdpcp* results in delayed chondrogenesis in the limb bud
Expression of chondrogenic marker genes *Col9a1* (A) and *Col2a1* (B) is significantly decreased in *Cys40* E11.5 forelimb buds versus controls. Expression of chondrogenic marker gene *Acan* (C) is at a lower level than *Col2a1* and *Col9a1* and is not significantly different in *Cys40* E11.5 forelimb buds versus controls. Error bars represent one standard deviation. *Cys40* is compared to matched control with * for $p<0.05$, ** for $p<0.01$, *** for $p<0.001$.

2.3.4 Disruption of limb bud signaling with Wdpcp deficiency

Having observed that *Wdpcp* deficiency affects the onset of chondrogenesis, a mechanism for the role of *Wdpcp* in chondrogenesis was sought. Previous studies have shown that BMP signaling is a key regulator of chondrogenesis. Treatment of limb bud mesenchyme with Bmp2 results in accelerated chondrogenesis (Denker et al., 1999). Limb mesenchyme specific knockout of *Bmpr1a* results in failure of chondrogenesis (Ovchinnikov et al., 2006). Disruption of the intracellular signal transducers of BMP signaling *Smad1/5/9* also results in complete disruption of chondrogenesis (Pignatti et al., 2014). Similarly, overexpression of BMP inhibitor *Grem1* in limb mesenchyme results in delayed chondrogenesis and polydactyly similar to the phenotype observed in the *Cys40* mutant (Norrie et al., 2014). Deletion of *Bmp4* in limb mesenchyme also disrupts chondrogenesis and results in polydactyly (Selever et al., 2004). BMP signaling levels in

the limb bud rise at E10.5 to initiate chondrogenesis (Pignatti et al., 2014). Limb buds isolated from E10.5 *Cys40* embryos displayed decreased activation of the BMP signaling pathway. Phosphorylation of Smad1/5/9 was reduced in *Cys40* limb buds (Figure 18D), indicating decreased transduction of BMP signal. Additionally, expression of the BMP target gene *Msx2* was significantly reduced in *Cys40* mutants ($p<0.05$) (Figure 18B). Accordingly, expression of the BMP inhibitor *Grem1* was significantly increased ($p<0.05$) in the *Cys40* mutants (Figure 18A). Interestingly, an increase in expression of *Bmp4* ($p<0.05$) was also observed in the *Cys40* mutants. This increase has been observed in other mutants with increased expression of *Grem1* in the limb mesenchyme and is believed to be reactionary compensation(Norrie et al., 2014).

The expression of *Grem1* in the limb bud mesenchyme is specifically regulated by the hedgehog pathway (Pignatti et al., 2014). Deletion of Shh in the limb bud results in loss of Grem1 expression (Benazet et al., 2009). Shh is secreted from the ZPA and functions primarily by regulating the levels of Gli transcription factors. The level of Gli3 and specifically the repressor form of Gli3 (Gli3R) is directly regulated by hedgehog pathway activation. Increasing activation of the pathway results in decreasing levels of Gli3R. Gli3R direct regulates the expression of *Grem1*. Gli3R has been shown to bind a cis acting *Grem1* enhancer, GRE1 (Zuniga et al., 2012). Thus, due to the observed elevation of *Grem1* expression, expression of Gli3 and, specifically, levels of Gli3R was determined. The *Cys40* mutant displayed decreased levels of Gli3R in the limb bud (Figure 18D). The decreased expression of Shh ($p<0.05$) is consistent with the observed deficit in limb outgrowth (Zhulyn et al., 2014). This is consistent with previous reports that *Wdpcp* is a key component and necessary for formation of the primary cilium (Cui et al., 2013), an organelle necessary for normal hedgehog signal transduction and formation of Gli3R (Goetz and Anderson, 2010).

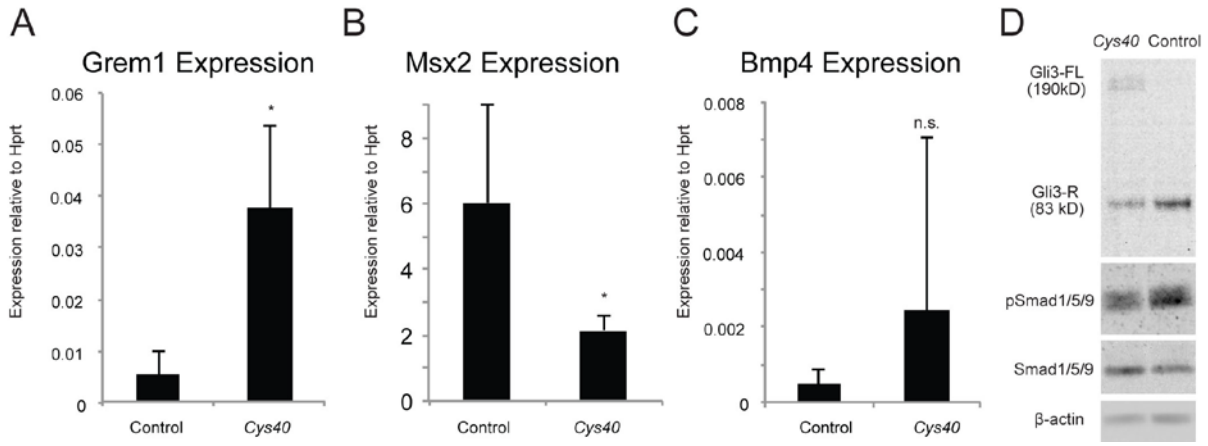

Figure 18. Loss of *Wdpcp* disrupts Gli3 repressor formation and BMP signaling in the limb bud
Expression of BMP inhibitor *Grem1* (A) is significantly increased in *Cys40* E10.5 forelimb buds versus controls. Expression of BMP pathway target *Msx2* (B) is significantly decreased in *Cys40* E10.5 forelimb buds versus controls. Expression of *Bmp4* (C) is not significantly changed in *Cys40* E10.5 forelimb buds versus controls. Western blot of E10.5 forelimb buds reveals loss of Wdpcp correlates with decreased Gli3R and increased Gli3FL as well as decreased pSMAD1/5/9 (D). Error bars represent one standard deviation. *Cys40* is compared to matched control with * for $p<0.05$, ** for $p<0.01$, *** for $p<0.001$.

2.3.5 Chondrocyte specific deletion of Wdpcp disrupts osteogenesis

Having determined a specific role for *Wdpcp* in the limb bud, further studies sought to determine whether the observed skeletal defects in the *Cys40* mice were a propagation of the deficits accumulated during limb bud signaling or whether they were compounded with deficits acquired later in skeletal development. To rule out the effects of *Wdpcp* in the limb bud and on chondrogenesis in the observed skeletal dysmorphogenesis, mice bearing a chondrocyte specific deletion of *Wdpcp* were generated by crossing mice carrying a tamoxifen-inducible, chondrocyte specific Cre recombinase allele (*Col2a1-Cre*^{ERT}). In this mouse, an inactive form of Cre recombinase is expressed from the collagen 2 (*Col2a1*) promoter, a gene whose expression is restricted to chondrocytes (Nakamura et al., 2006). Where it is expressed, the inactive Cre recombinase can be activated with administration of 4-OH tamoxifen. Thus, injection of 4-OH tamoxifen into pregnant mothers at a specific time point in development can induce activation of

Cre recombinase activity in all chondrocytes at a specific time point. Previous characterization of this mouse line demonstrated that injection of 2 mg of 4-OH tamoxifen at E11.5 was sufficient to induce Cre recombinase activity in all chondrocytes and chondrocyte descendants of the developing limbs (Nakamura et al., 2006).

The *Col2a1-Cre*^{ERT} mice were bred to mice carrying a floxed allele of *Wdpcp*. This allele has LoxP sites inserted on either side of exon 5 of *Wdpcp* (Figure 12). Loxp sites are the targets of Cre recombinase and in cells with active Cre recombinase, two single LoxP sites are recombined and the intervening short segment of DNA excised and degraded (Gu et al., 1993). In order to ensure that efficient deletion of *Wdpcp* was achieved, mice carrying the Col2aCre^{ERT} a single floxed allele along with the null *Cys40* allele were generated (*Col2a1-Cre*^{ERT}*;Wdpcp*$^{Cys40/Flox}$) to minimize the required level of Cre activity necessary for completed deletion of functional *Wdpcp*.

Mice bearing chondrocyte specific deletion of *Wdpcp* appeared grossly normal at E17.5, indicating that limb length deficits and polydactyly were due primarily to dysfunction resulting from *Wdpcp* loss in the limb bud prior to chondrogenesis. On closer examination of the growth plate structure and long bones at E14.5, there was a slight deficit in osteogenesis in the *Col2a1-Cre*^{ERT}*;Wdpcp*$^{Cys40/Flox}$ *mice* as evidenced by decreased von Kossa staining for bone at primary center of ossification in the humerus (Figure 19).

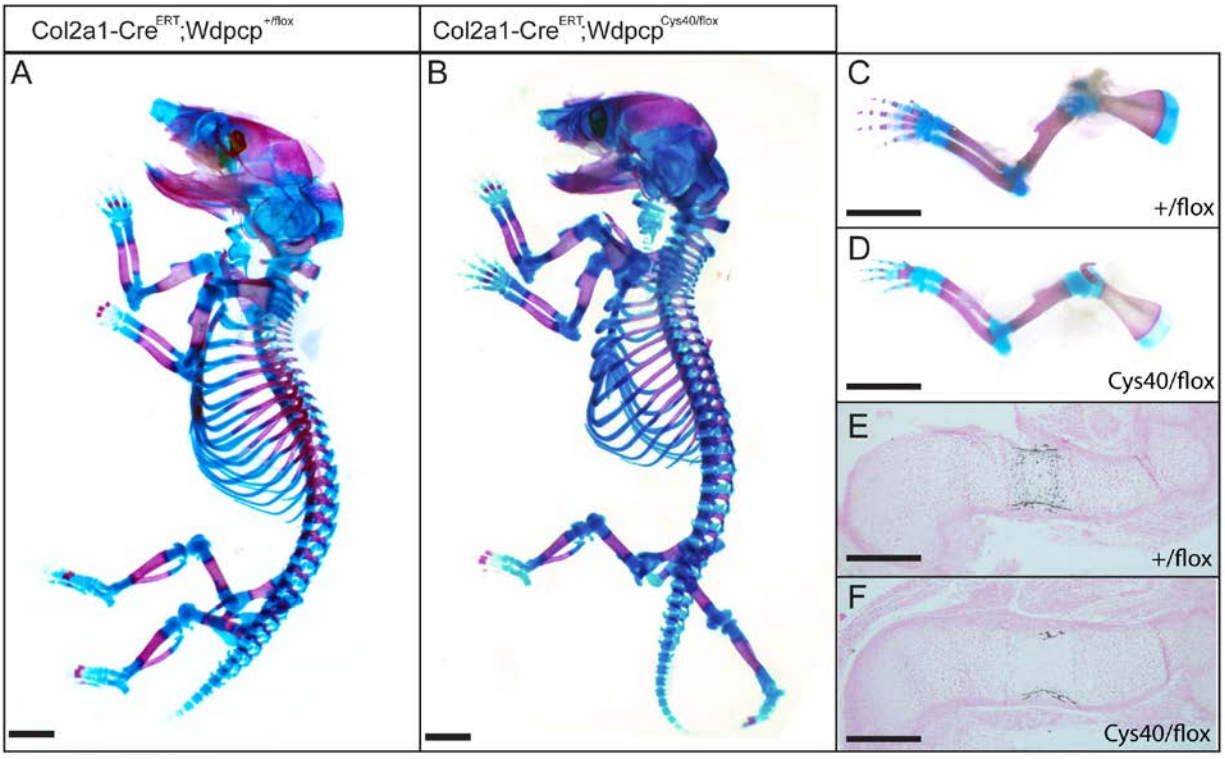

Figure 19. Skeletal phenotype of chondrocyte specific deletion of *Wdpcp*.
Alizarin red Alcian blue staining of E17.5 Col2a1-Cre^{ERT};Wdpcp$^{+/flox}$ (A,C) littermate controls and Col2a1-Cre^{ERT};Wdpcp$^{Cys40/flox}$ mice (B,D) injected with tamoxifen at E11.5 display no gross skeletal tissue differences. Sections of E14.5 humerus stained with von Kossa for bone (black) show that Col2a1-Cre^{ERT};Wdpcp$^{Cys40/flox}$ mice have decreased trabecular bone at the primary center of ossification at this time point.

2.4 DISCUSSION

The ability of *Prx1-Cre;Wdpcp*$^{Cys40/Flox}$ mice to recapitulate the appendicular skeletal phenotype of the *Wdpcp*$^{Cys40/Cys40}$ mouse indicates that *Wdpcp* functions during appendicular skeletal development in the limb mesenchyme and/or limb mesenchymal progenitors. The failure of the *Col2a1-Cre*^{ERT}*;Wdpcp*$^{Cys40/Flox}$ mice induced with tamoxifen injection at E11.5 to recapitulate the patterning and outgrowth phenotype indicates that Wdpcp exerts its influence over these processes prior to onset of chondrogenesis. The severe polydactyly observed in the

Wdpcp$^{Cys40/Cys40}$ and *Prx1-Cre;Wdpcp*$^{Cys40/Flox}$ mice is characteristic of mice carrying mutations in genes that disrupted ciliogenesis (Heydeck et al., 2009; Zeng et al., 2010). Disruption of the primary cilium alters post-translational processing of the hedgehog target transcription factors Gli2 and Gli3 to disrupt hedgehog signal transduction. In the *Cys40* mice, processing of full-length Gli3 to truncated Gli3 repressor is disrupted, resulting in a functional loss of Gli3 repressor. The increase in expression of the BMP inhibitor *Grem1* correlates with the observed decrease in activation of the BMP signaling pathway as measured by phosphorylated Smad1/5/9 in the E10.5 limb bud and decreased expression of BMP target gene *Msx2* in the E10.5 limb bud. BMP signaling is necessary to trigger exit of mesenchymal limb bud progenitors from proliferation to chondrogenic differentiation (Lopez-Rios et al., 2012). Mice lacking Wdpcp display decreased expression of chondrogenic markers *Col2a1, Acan*, and *Col9a1* and increased expression of the proliferative marker Ccnd1 at E11.5 and E12.5 in the forelimb buds..

Given that there is an observed deficit in the Gli3R that is correlated with increased *Grem1* expression and decreased BMP signaling, it would be informative to determine the effects of different double mutants on the phenotype of these mice. Mice overexpressing the truncated repressor form of Gli3 (Gli3R^{701}) have deficient limb bud outgrowth with oligodactyly (Cao et al., 2013). *Wdpcp*$^{Cys40/Cys40-}$*;Gli3R*$^{701/701}$ mice could be hypothesized to display an intermediate phenotype between the polydactyly observed in the *Cys40* mutant and the oligodactyly observed in the *Gli3R*^{701} mutant that is dependent on the dosage of Gli3R received by limb mesenchyme. An inducible model of Gli3R over expression could determine temporal specificity for this requirement.

The underlying phenotype of disrupted exit to chondrogenesis in the *Cys40* mice is associated with increased expression of BMP inhibitor Grem1 and decreased BMP signaling

pathway activation. *Prx1-Cre;Rosa*^{Grem1} mice are engineered to overexpress Grem1 in the limb bud mesenchyme, similar to the overexpression of Grem1 observed in the *Cys40* mutant. These mice display a phenotype very similar to the *Cys40* mutant mice including polydactyly and shortened and dysmorphic long bones (Norrie et al., 2014). Conversely, mice with a targeted deletion of the Grem1 display oligodactyly(Benazet et al., 2009). *Wdpcp*$^{Cys40/Cys40}$*;Grem1*$^{-/-}$ mice could be hypothesized to display a phenotype that resembles the *Grem1*$^{-/-}$ mice, confirming *Wdpcp* controls the process of chondrogenesis via modulation of hedgehog signaling input on BMP signaling.

Osteoblast specific deletion of *Wdpcp* using *Osx-Cre* or *Col1a1-Cre* could be investigated. Studies on the role of primary cilia deletion with these Cre strains demonstrate similar findings including decreased bone formation and decreased formation spongy bone(Qiu et al., 2012; Temiyasathit et al., 2012). The effects of deletion of *Wdpcp* on adult cartilage homeostasis should also be examined. Studies using the non-inducible *Col2a1-Cre* line have shown differences in cartilage mechanical properties and early development of osteoarthritis symptoms (Irianto et al., 2014). Determining the effect of induction of primary cilia loss after the developmental period may yield interesting insights into the function of primary cilia in adult cartilage homeostasis independent of developmental effects.

2.5 CONCLUSION

These studies demonstrate that *Wdpcp* acts within the limb bud mesenchyme to facilitate chondrogenesis. The ability of the *Prx1-Cre;Wdpcp*$^{Cys40/flox}$ mice to recapitulate the appendicular skeletal phenotype of the *Wdpcp*$^{Cys40/Cys40}$ mice demonstrates that the observed phenotype is due

to loss of *Wdpcp* from the limb bud mesenchyme. The observed appendicular skeletal phenotype does not depend on loss of *Wdpcp* function from any adjacent tissues such as the limb ectoderm or from tissues that may secrete or regulate circulating factors. The lack of outgrowth and patterning defects observed in the appendicular skeleton of the *Col2a1-Cre^{ERT};Wdpcp$^{Cys40/flox}$* mice demonstrate that *Wdpcp* affects these processes prior to chondrocyte differentiation at E12.0 when the injection of tamoxifen has induced Cre recombinase activity. It also suggests that disruption of cilia due to *Wdpcp* loss does not play a major role in growth plate organization. Examining the phenotype of these mice at later points for premature closure of the growth plate as was observed in *Col2a1-Cre;Kif3a$^{flox/flox}$* mice will be informative. The decreased trabecular bone staining at E14.5 in the *Col2a1-Cre^{ERT};Wdpcp$^{cys40/flox}$* mice points to disrupted bone formation and possibly osteoblast differentiation in these mice. These findings are consistent decreased hedgehog signaling responsiveness due to disrupted ciliogenesis.

3.0 WDPCP IS NECESSARY FOR NORMAL CHONDROGENESIS AND OSTEOGENESIS

3.1 INTRODUCTION

Having demonstrated a specific set of signaling deficits associated dysfunctional hedgehog signaling and associated skeletal developmental processes, in vitro approaches were utilized to further investigate the effects of alterations in cell signaling on these skeletal development processes. Utilizing cells derived from *Cys40* mutants and littermate controls, limb bud micromass culture was used to assay chondrogenesis and two-dimensional osteogenesis with mouse embryonic fibroblasts (MEFs) was utilized to assay osteogenesis.

3.2 METHODS

3.2.1 In vitro chondrogenic differentiation: limb bud micromass

Wdpcp$^{Cys40/+}$ male and female mice were crossed and pregnant females sacrificed at E11.5 to generate litters with Cys40 mutants and littermate controls. E11.5 Homozygous Cys40 mutants could be visually differentiated from embryos carrying at least one functional copy of *Wdpcp* by disrupted eye formation. However, *Wdpcp*$^{Cys40/+}$ and *Wdpcp*$^{+/+}$ mice could not be differentiated

within the time period required to pool limbs and establish cultures. Given that no phenotypic or molecular differences were observed between heterozygous and wild-type embryos, these limbs were pooled to create control cultures. Micromass cultures were prepared as previously described (Bruce et al., 2010; DeLise et al., 2000; Denker et al., 1999; Stanton et al., 2004). Dissected limbs were dissociated in 1 unit/mL dispase (Stem Cell Technologies) for 1.5 h at 37 °C. Digested limbs were pipetted up and down with 200 uL pipette to break up cells before being diluted in 10 mL 2:3 DMEM/F-12 medium containing 10% MSC qualified FBS (Invitrogen) (growth medium) to neutralize trypsin. This suspension was passed through a 40 um filter and pelleted at 1,200g. After re-suspension in 2:3 DMEM/F-12 medium, cell number was counted using hematocytometer. Cells were then divided into experimental groups, pelleted and resuspended in 2:3 DMEM/F-12 supplemented with either DMSO or appropriate pharmacological agent dissolved in DMSO. Cells were diluted to 10 million cell/mL and spotted in 10 uL droplets on Nunc 24 –well culture dishes. Cells were allowed to adhere for 1.5h in a cell incubator with humidified atmosphere containing 5% CO_2. After two hours wells were flood with growth medium containing appropriate pharmacological agent. Cultures were harvested after 3 days.

3.2.2 Generation of mouse embryonic fibroblasts (MEFs)

Wdpcp$^{Cys40/+}$ females were bred to *Wdpcp*$^{Cys40/+}$ males and pregnant females were sacrificed at E13.5. Embryos were immediately delivered by Caesarean section into pre-warmed DMEM. Livers were removed and saved for genotyping (Figure 12). Internal organs including digestive tract, kidneys, diaphragm, heart, lungs, spleen, bladder, and aorta were removed. Single embryos were decapitated and remaining skeletal and dermal elements from each embryo were placed

individually in 1 mL 0.5% Trypsin EDTA and minced with sterilized razor blades in 10 cm cell culture dish. Minced embryos were incubated in tissue culture incubator at 37 C for 5 minutes. Minced and digested embryos were diluted in 10 mL cell culture medium composed of DMEM supplemented with 10% MSC qualified FBS (Gibco) with 1X Penicillin/Streptomycin/Fungizone (Gibco) growth medium to inactivate trypsin. MEFs were pipetted up and down to break up remaining tissue before spinning at 1000g to pellet in 15 mL Vulcan tube. MEFs were resuspended in growth medium and plated on T75 at what was considered passage 0. MEFs were expanded two days with growth medium changed each day. MEFs were passaged on day 2 and split to two T150 (1:4). MEFs were grown to 90% confluence, passaged, and frozen in cryoprotective freezing medium (Lonza) for storage in liquid nitrogen. All experiments using MEFs were conducted at passage 3 or 4.

3.2.3 In vitro osteogenic differentiation

It was reported in that MEFs were capable of differentiation into adipogenic, osteogenic, and chondrogenic lineages (Saeed et al., 2012). Following expansion, MEFs were seeded at 70% confluence (100,000 cells/cm^2) in growth medium for two days before changing to standard osteogenic medium containing 1 mM β-glycerolphosphate, 100 nM ascorbic acid, and 20 ng/mL rBMP2 (Peprotech) supplemented with 10 nM smooth agonist (SAG, Calbiochem). Osteogenic medium was changed every 4 days. Alkaline phosphatase activity was measured with para-nitrophenyl phosphate assay (Sigma) at day 4 of osteogenic differentiation. Eight independent biological replicates were used for quantification. Statistics were performed as described in Section 2.2.8.

3.2.4 Histology

3.2.4.1 Alcian Blue staining

Alcian blue staining was used to assay chondrogenesis of limb bud micromass cultures. Cultures were rinsed with PBS and fixed in 4% paraformaldehyde at room temperature for 15 minutes. Following PBS rinse, cultures were stained overnight at 4C with 1% Alcian blue stain solution at pH 1.0 (EK Industries). Cultures were rinsed with PBS 3x and imaged on upright Olympus SZX16 microscope. A representative image of 3 to 4 independent biological replicates is shown for Alcian Blue staining.

3.2.4.2 Alizarin Red staining

Alizarin red staining was used to assay calcium matrix deposition of osteogenic cultures. MEFs were fixed in 70% ethanol before being stained for 15 minutes with 2% alizarin red solution at pH 4.2 (Rowley Biochemical Institute). For quantification 1 mL of cetylpyridinium chloride was used per 6 well plate well to solubilize dye. DNA was isolated from an analogous 6 well plate well with 1 mL of 0.5% Triton X-100 in distilled water and quantified using Quant-iT PicoGreen dsDNA Assay Kit (Life Technologies). Soluble alizarin red was quantified spectroscopically (A_{580}). Six independent biologic replicates were used for quantification. Statistics were performed as described in Section 2.2.8.

3.2.5 RNA isolation and qPCR

RNA isolation, reverse transcription, and qPCR assays were performed as described in section 2.2.6, with 3 experimental replicates each containing two pooled biological replicates to obtain

sufficient RNA concentration. Relative expression was determined using validated primers (Appendix A) and the $\Delta\Delta C_T$ method, with expression reported relative to endogenous control hypoxanthine-guanine phosphoribosyltransferase (*Hprt*). Statistics were performed as described in Section 2.2.8.

3.3 RESULTS

3.3.1 Micromasses lacking functional Wdpcp do not respond to Smo antagonism with enhanced chondrogenesis

To further investigate the role of *Wdpcp* in chondrogenesis, we utilized in vitro limb bud micromass cultures (Bruce et al., 2010; DeLise et al., 2000; Denker et al., 1999) from *Cys40* and control limb buds (Figure 20A-D). *Cys40* cultures displayed decreased Alcian Blue staining (Figure 20A,C) and *Col2a1* expression (Figure 20G) compared to wild type controls. *Ptch1* and *Gli1* are direct transcriptional targets of Gli3 and increased expression is associated with activation of the hedgehog pathway (Briscoe and Therond, 2013; Goodrich et al., 1996; Hui and Angers, 2011). As expected with decreased formation of the truncated repressor form of Gli3, expression of *Ptch1* and *Gli1* was significantly increased in *Cys40* cultures (Figure 20E,F). As in the *Cys40* limb buds, the observed decrease in chondrogenesis was correlated with an increase in the expression of *Grem1* (Figure 20H).

Having observed that the deficient formation of hedgehog pathway transcription factor Gli3 repressor in the *Cys40* limb buds was associated with increased *Grem1* expression and concomitant decrease in chondrogenic differentiation, we hypothesized that silencing of the

hedgehog pathway could decrease *Grem1* expression and rescue chondrogenesis. Cyclopamine is a hedgehog pathway antagonist that functions by inhibiting the activity of Smo (Chen et al., 2002). Alcian Blue staining (Figure 20B,D) and *Col2a1* expression levels (Figure 20E) revealed that treatment of both control and *Cys40* cultures with cyclopamine had no effect on chondrogenesis. While we did observe a significant decrease in the expression of *Gli1* (Figure 20E) with cyclopamine treatment as expected (Chen et al., 2002), *Ptch1* and *Grem1* expression were not significantly affected in either *Cys40* or control cultures (Figure 20F,H). Previous studies have noted that cyclopamine has minimal effect on chondrogenesis of wild type limb bud cultures (Bruce et al., 2010). The lack of response to cyclopamine observed in the *Cys40* cultures is consistent with the disruption of hedgehog signaling below the level of Smo at the primary cilium (Huangfu and Anderson, 2005).

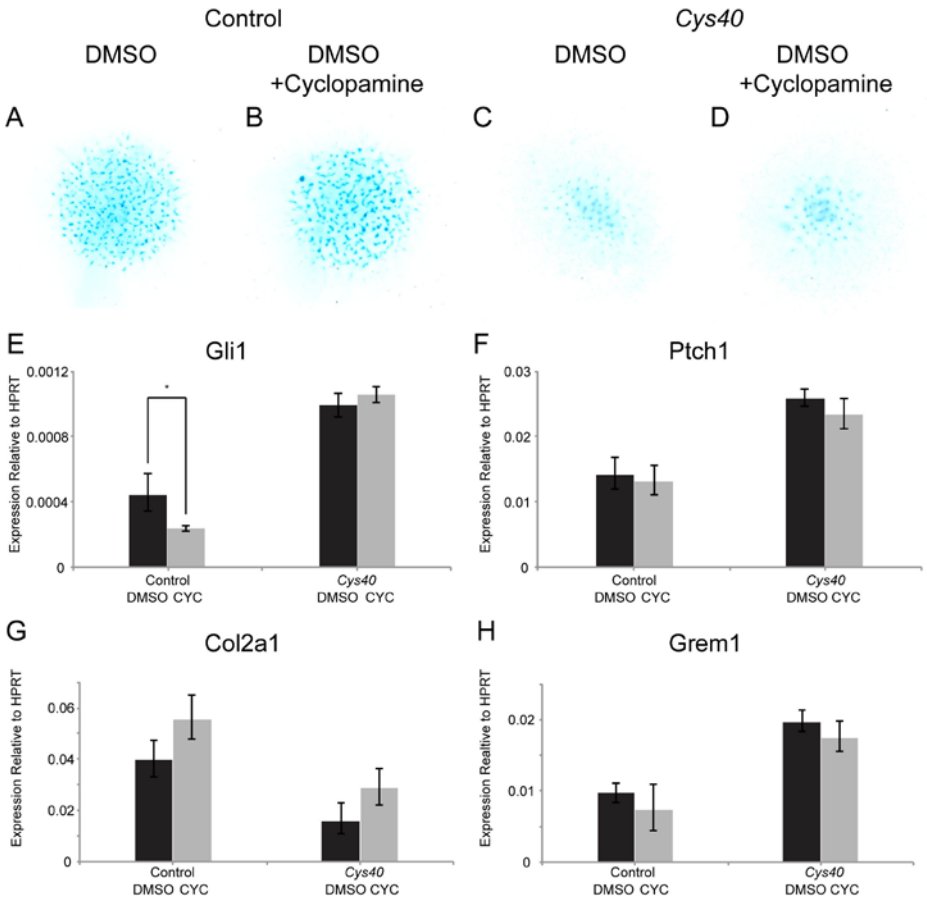

Figure 20. In vitro chondrogenesis of micromass culture of *Wdpcp* null limb bud cells cannot be rescued with Smo antagonism

Alcian Blue staining of control (A, B) and *Cys40* (C, D) E11.5 limb bud micromass cultures treated with carrier control DMSO or 5 μM cyclopamine (CYC). Expression of hedgehog pathway reporter *Gli1* (E) and *Ptch1* (F) in *Cys40* cultures is not significantly affected by treatment with 5 μM cyclopamine. Expression of chondrogenic marker gene *Col2a1* (G) in *Cys40* cultures is not significantly affected by treatment with 5 μM cyclopamine. Expression of BMP antagonist *Grem1* (H) is not significantly affected in *Cys40* cultures treated with 5 μM cyclopamine. Error bars represent one standard deviation. Effect of drug treatment within a genotype is calculated using Student's t-test with * for $p<0.05$, ** for $p<0.01$, *** for $p<0.001$.

3.3.2 Direct Gli antagonism rescues chondrogenic deficit in Wdpcp deficient micromasses

Having observed that inhibition of hedgehog at the level of *Smo* was unable to affect chondrogenesis or associated signaling, we used a direct inhibitor of the downstream transcription factor Gli known as GANT61 (Lauth et al., 2007). It was observed that chondrogenesis could be rescued in *Cys40* MEFs by inhibition of hedgehog pathway at the level

of the Gli transcription factors with direct inhibition of Gli-DNA interactions with Gli antagonist GANT 61. Treatment of *Cys40* limb bud micromass cultures with 50 uM GANT61 results in increased Alcian blue staining of *Cys40* and control cultures (Figure 21A-D) as well as significantly decreased expression ($p<0.05$) of hedgehog pathway reporter *Ptch1*. These findings coincide with significantly decreased expression of BMP antagonist *Grem1* (Figure 21H) and significantly increased expression of chondrogenic marker gene *Col2a1* (Figure 21G).

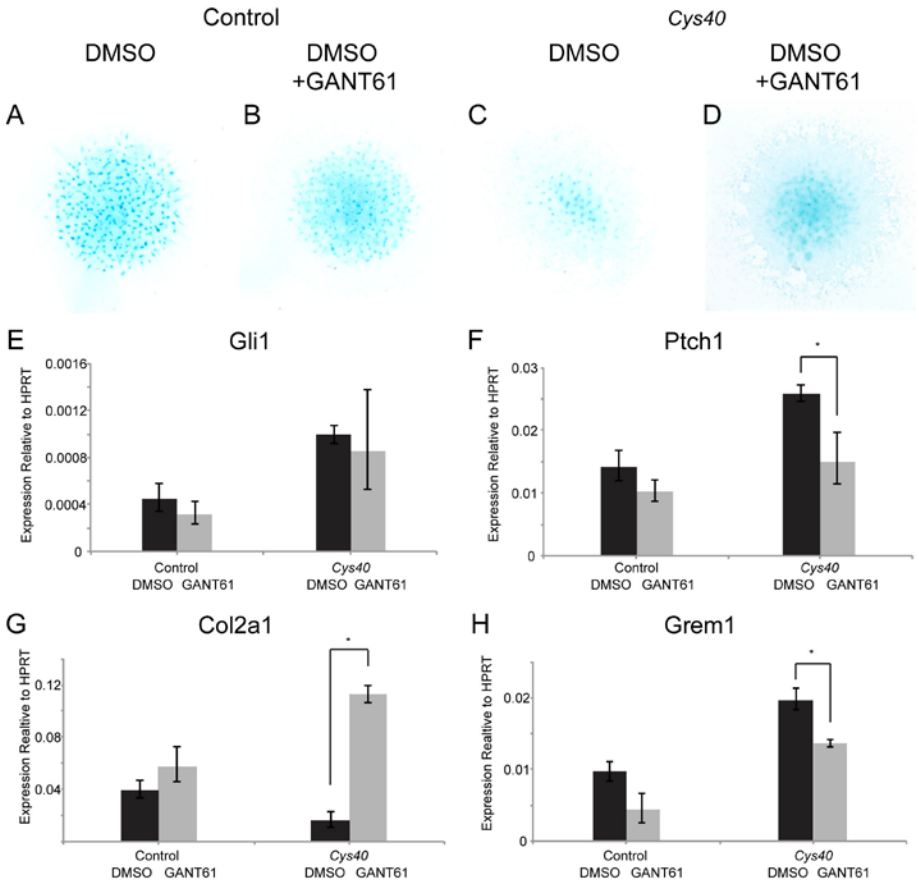

Figure 21. In vitro chondrogenesis in micromass cultures of *Wdpcp* null limb buds can be rescued with Gli antagonist treatment

Alcian blue staining of limb bud micromass cultures derived from control embryos (A-B) and *Cys40* embryos (C-D) shows treatment with Gli inhibitor GANT61 increases Alcian blue staining of *Cys40* cultures (D) versus DMSO treated control cultures (C). No significant change is observed in expression of hedgehog pathway target *Gli1* with GANT61 treatment in either control of *Cys40* cultures (E). Increase in Alcian blue staining of GANT61 treated *Cys40* cultures corresponds with decrease in expression of hedgehog pathway target *Ptch1* (F), increase in expression of chondrogenic marker *Col2a1* (G), and decrease in expression of BMP inhibitor *Grem1* (H). Error bars represent one standard deviation. Effect of drug treatment within a genotype is calculated using Student's t-test with * for $p<0.05$, ** for $p<0.01$, *** for $p<0.001$.

3.3.3 *Cys40* mutant MEFs display deficient in vitro hedgehog stimulated osteogenesis

Cys40 mutant MEFs display decreased osteogenic differentiation compared to control. Deposition of calcified matrix as assayed by alizarin red staining at 20 days of osteogenic medium culture is significantly reduced in *Cys40* MEFs versus controls (Figure 22A-C). Alkaline phosphatase activity at 4 days of osteogenic medium culture, necessary for generating the phosphate component of hydroxyapatite, is significantly decreased in *Cys40* MEFs versus controls (Figure 22C). Analysis of gene expression after 20 days of culture in osteogenic medium reveals decreased expression of hedgehog pathway reporter genes *Gli1* and *Ptch1* in *Cys40* MEFs versus controls (Figure 22D). Expression of early osteogenic marker *Runx2* is not significantly different between *Cys40* MEFs and controls, while expression of late osteogenic markers *Osx, Col1a1,* and *Ocn* is significantly decreased in *Cys40* MEFs versus controls (Figure 22E).

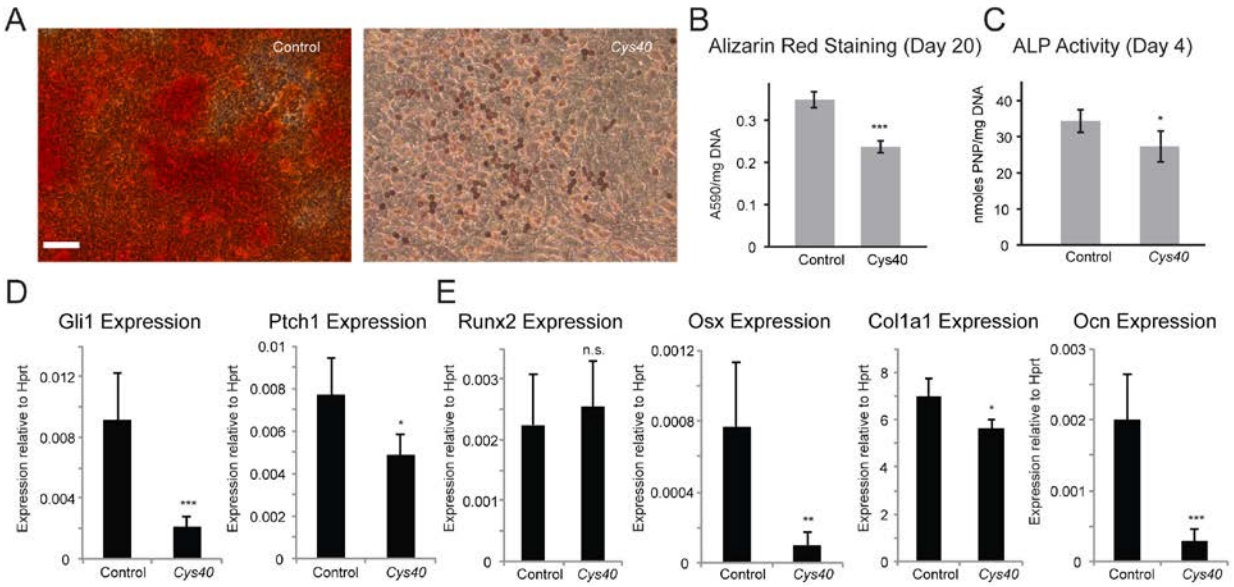

Figure 22. *Cys40* MEFs display decreased osteogenesis

Alizarin red staining for calcified matrix is significantly decreased in *Cys40* MEFs at day 20 compared to control MEFs (A, B). Alkaline phosphatase activity at day 4 is significantly decreased in *Cys40* MEFs at day 4 compared to control MEFs (C). Hedgehog pathway activity as assayed by expression of hedgehog reporter genes *Gli1* and *Ptch1* is significantly decreased in *Cys40* MEFs compared to controls at day 20 of osteogenic medium culture (D). Expression of early osteogenic differentiation marker *Runx2* is not significantly different between *Cys40* MEFs and control MEFs at day 20 of osteogenic medium culture. Expression of mature osteogenic markers *Osx, Col1a1,* and *Ocn* is significantly decreased in *Cys40* MEFs compared to controls at day 20 of osteogenic medium culture. Error bars represent one standard deviation. Effect of drug treatment within a genotype is calculated using Student's t-test with * for $p<0.05$, ** for $p<0.01$, *** for $p<0.001$.

3.4 DISCUSSION

Cys40 cultures display increased activation of the hedgehog reporter genes *Gli1* and *Ptch1* in agreement with the observed loss of Gli3R in the limb buds. *Cys40* cultures also display decreased chondrogenesis versus control as assayed by Alcian blue stained nodule formation and expression of chondrogenic marker *Col2a1* in agreement with observed chondrogenic delay in E10.5 *Cys40* limb buds. The upregulation of early chondrogenic marker *Cdh2* in both *Cys40* and cyclopamine treated MEFs maybe due to off target effects of high doses of cyclopamine used

(Meyers-Needham et al., 2012) or could signal that upregulation of *Cdh2* is independent of hedgehog signaling in this culture system. GANT61 is able to suppress hedgehog signaling and mimic the effect of Gli3R in the *Cys40* MEFs due to its function as a direct Gli-DNA interaction inhibitor (Lauth et al., 2007). By inhibiting all Gli-DNA interactions, the balance of Gli activator to repressor becomes irrelevant, and GANT61 serves as a potent inhibitor of hedgehog signaling. The inhibition of hedgehog signaling by complete disruption of all activating Gli-DNA interactions with GANT61 treatment allows *Grem1* expression levels to decrease, facilitating the activation of BMP signaling to rescue of chondrogenesis as measured by Alcian blue staining and expression of chondrogenic marker gene *Col2a1*.

Other studies utilizing the limb bud micromass model have noted that activation of the hedgehog pathway via Smo agonist purmorphamine treatment suppresses chondrogenic differentiation (Lewandowski et al., 2014). They have similarly noted increased expression hedgehog activated genes *Gli1* and *Ptch1* coincides with increased expression of *Grem1* as well as suppression of the BMP target gene *Msx2* (Lewandowski et al., 2014). Limb micromass cultures from *Prx1-Cre;Ptch1*$^{flox/flox}$ mice with constitutively activated hedgehog signaling in limb mesenchyme display increased expression of *Gli1* and *Ptch1* but also show increased expression of chondrogenic transcription factors *Sox5*, *Sox6,* and *Sox9*. However, expression of *Col2a1* is decreased in *Prx1-Cre;Ptch1*$^{flox/flox}$ hindlimb cultures and Alcian blue staining is significantly reduced in all *Prx1-Cre;Ptch1*$^{flox/flox}$ cultures. It is also noted that exogenous Shh application has no significant detrimental effect on Alcian blue staining or *Col2a1* expression (Bruce et al., 2010). This observed difference between the two studies may be due to the increased levels of *Ptch1* that effectively inhibit Shh, but cannot inhibit *Smo* activation caused by purmorphamine.

The significantly decreased deposition of alizarin red staining calcified matrix, decreased alkaline phosphatase activity, and reduced expression of late osteogenic marker genes *Ocn, Col1a1*, and *Osx* all indicate that osteogenesis in the *Cys40* MEFs is impaired (Figure 22). The failure to see a significant difference expression of *Runx2* is likely due to the fact that this is an early marker of osteogenic differentiation. The decreased osteogenesis observed in response of *Cys40* MEFs to hedgehog activity correlates with the decreased hedgehog responsiveness that is reported in chapter 4. Hedgehog pathway activation is essential to osteogenesis and the formation of bone as documented in numerous studies. $Ihh^{-/-}$ mice and mice with constitutive inactivation of hedgehog signaling due to $Smo^{-/-}$ display defective bone formation (Long, 2012; St-Jacques et al., 1999). Additionally, the osteogenesis deficit in *Cys40* MEFs and decreased bone formation observed in E14.5 $Col2a1\text{-}Cre^{ERT};Wdpcp^{flox/Cys40}$ mice versus controls agree with reports of other mutants that affect the formation of primary cilia (Qiu et al., 2012; Song et al., 2007; Temiyasathit et al., 2012).

3.5 CONCLUSION

The ability of direct Gli inhibitor GANT61, but not Smo inhibitor, cyclopamine to rescue the deficit in chondrogenesis observed in *Cys40* forelimb bud micromasses demonstrates that hedgehog signaling is disrupted in *Cys40* mice below the level of *Smo*. Furthermore, the ability of direct Gli inhibition to decrease the expression of *Grem1* concomitant with the increase in chondrogenesis as assayed by Alcian blue staining confirms that the observed increased levels of *Grem1* in the E10.5 *Cys40* forelimbs is responsive to hedgehog signaling. Loss of Gli3 repressor and suppressive hedgehog effects on transcription *Grem1* disrupts chondrogenesis early in limb

skeletogenesis (Figure 20). Conversely, failure to fully activate hedgehog pathway targets disrupts osteogenesis later in limb skeletogenesis as evidenced by decreased expression of hedgehog target genes and decreased osteogenic differentiation as measured by expression of mature osteoblast markers, calcified matrix deposition and alkaline phosphatase activity in *Cys40* MEFs (Figure 22). These findings underlie the importance utilizing stage specific models and assays to dissect the specific disruption of signaling pathways. The phenotype of *Cys40* mutant results not from complete silencing or complete hyperactivation of a signaling pathway, but from loss of responsiveness.

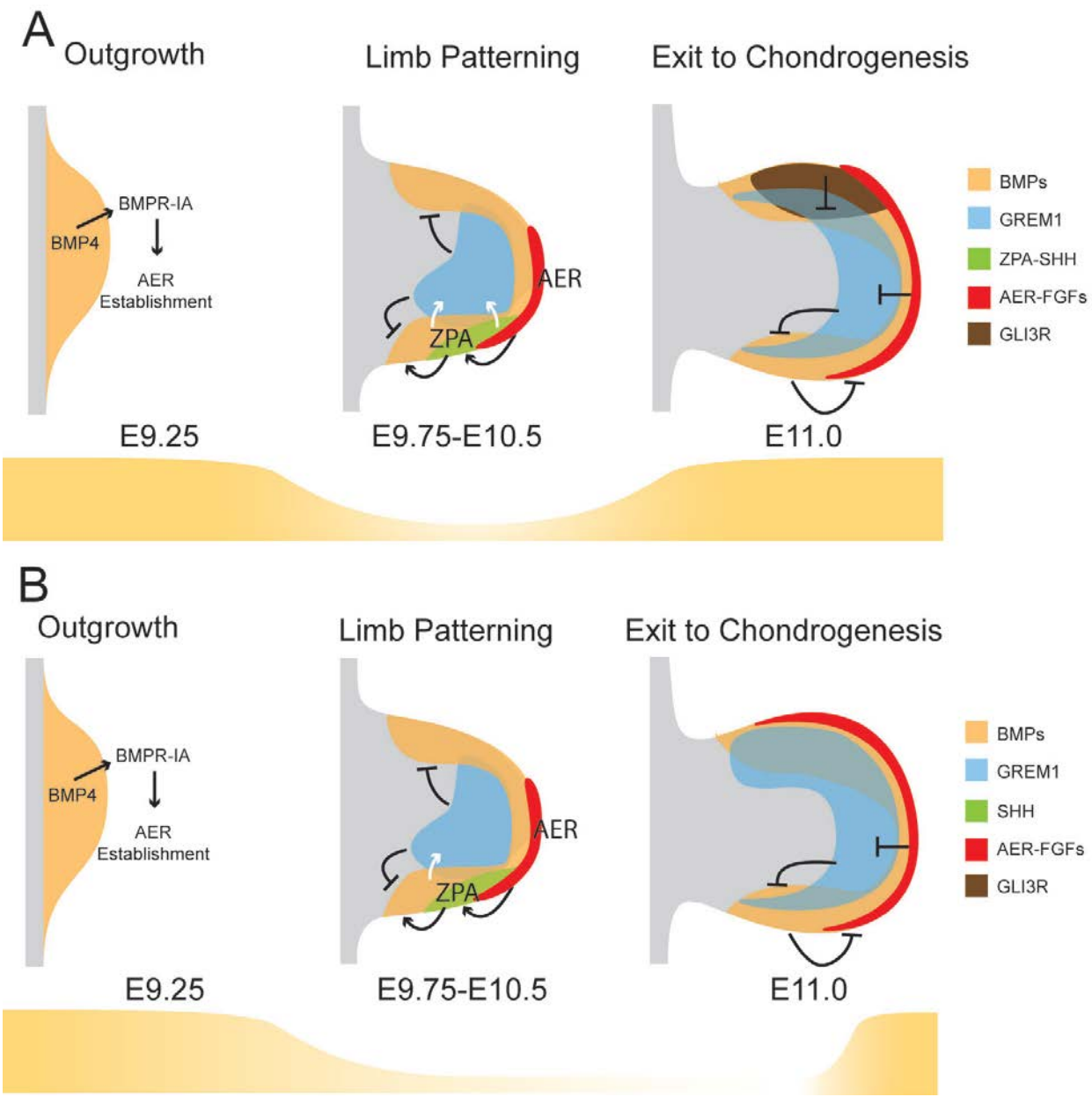

Figure 23. Effects of *Wdpcp* loss on chondrogenesis are mediated by hedgehog control of BMP signaling. In the normal limb bud (A), limb bud outgrowth is initiated by formation of the apical ectodermal ride (AER). The AER secretes FGFs (red) that support the expression of Shh (green) from the zone of polarizing activity (ZPA) at the posterior aspect of the limb bud. Shh from the ZPA drives expression of both BMPs (yellow) and BMP inhibitor, Grem1 (blue), in the limb mesenchyme. Grem1 limits the activity of BMPs to suppress the BMP signaling pathway and delay chondrogenesis to allow proliferation and limb bud outgrowth. When the limb bud reaches a critical size, Shh (green) signal from the ZPA no longer reaches the anterior aspect of the limb bud mesenchyme, allowing accumulation of the repressive form of the hedgehog transcription factor Gli3R (brown). Gli3R serves to inhibit the expression of Grem1 in the limb bud mesenchyme, allowing BMP pathway activity to rise and trigger chondrogenesis. In the *Cys40* mutants (B), Gli3R levels are decreased, leading to increased Grem1 expression, decreased BMP activity, and inhibited chondrogenesis. (Adapted from Pignatti et al., 2014 with permission)

4.0 WDPCP AFFECTS HEDGEHOG SIGNALING AT THE PRIMARY CILIUM BY ALTERING GLI PHOSPHORYLATION

4.1 INTRODUCTION

The previous two sections characterized the effects of the hedgehog defect in the *Cys40* mutant on the process of skeletal development. The experiments in this section sought to uncover the specific mechanism by which hedgehog signaling was disrupted with loss of Wdpcp. Pharmacologic and genetic rescue of hedgehog pathway responsive genes and proliferative response was used as a read out to show that loss of Wdpcp disrupts hedgehog signaling by altering phosphorylation of Gli transcription factors that determines their further post-translational processing.

4.2 METHODS

4.2.1 Generation and culture of MEFs

MEFs used in these experiments were isolated and expanded from embryos derived from $Wdpcp^{Cys40/+}$ matings as described in 3.2.2. For all drug treatment experiments, MEFs were grown to confluence, trypsinized, and re-plated at full confluence (150,000 cells/cm^2) in

appropriate size culture well in growth medium for 1 day before changing to starvation medium (DMEM supplemented with 0.25% MSC qualified FBS). Previous studies had demonstrated that cell cycle arrest as induced by serum starvation and confluence are necessary to induce optimal ciliation and hedgehog responsiveness of MEFs (Rohatgi et al., 2007). Following 2 days of culture with starvation medium, medium was changed to starvation medium supplemented with pharmacological agent dissolved in DMSO (Sigma) for 24 hours. MEFs were fixed for imaging or harvested for RNA or protein at this time point.

All drugs were diluted in DMSO to be added 1:1000. DMSO was added 1:1000 for carrier control. Smoothened agonist (SAG) (Calbiochem) was used at 100 nM. Cyclopamine (LKT laboratories) was used at 10 uM. GANT61 (Sigma) was used at 50 uM. 3-isobutyl-1-methylxanthine (IBMX) (Sigma) was used at 2.5 uM. Protein kinase A inhibitor fragment 14-22, myristylated trifuloroacetate salt (PKAi) (Sigma) was used at 60 uM.

For lentiviral infection, MEFs were plated at 100,000 cells/cm^2 in growth medium for 1 day. Medium was changed to lentiviral infection medium consisting of 1:1 lentiviral medium isolated from HEK293 lentiviral packaging cultures to DMEM without antibiotics. Polybrene was added to transfection medium 1:1000 for a final concentration of 10 ug/mL (Santa Cruz Biotech). Infection was allowed to take place for 48 hours. Following infection, medium was changed to starvation medium for 3 days. MEFs were fixed for imaging or harvested for RNA or protein at this time point.

4.2.2 Immunofluorescence of primary cilia

MEFs were cultured in 12 well plates on circular cover slips as described for drug treatments in section 4.2.1 to induce ciliogenesis. At end of culture period, MEFs were washed in PBS and

fixed with 4% paraformaldehyde for 15 min at room temperature. MEFs were washed in PBS before incubation in PBS with 0.1% Triton X-100 (PBST) for 30 minutes at room temperature following by blocking with 5% chicken serum (Gibco) in PBST for 1 hour at room temperature. Primary antibodies were diluted in PBS with 5% chicken serum and incubated overnight at 4C. Mouse monoclonal antibody against acetylated alpha tubulin (Sigma Clone 6-11-B) is an established marker of primary cilia axoneme and was used at 1:500. Rabbit polyclonal antibody to centrosomal gamma tubulin (Abcam) is an established marker of basal body of primary cilia and was used at 1:200. Following overnight incubation, coverslips were allowed to equilibrate at room temperature before washing with PBST followed by incubation with PBST with 5% chicken serum with diluted secondaries for 2 hours at room temperature. Chicken secondary antibodies labeled with Alexafluor dyes 647 against mouse and 488 against rabbit (Invitrogen) were both used at 1:200. Negative controls included omission of primary antibodies and primary isotype (Igg) controls. Specific information regarding primary and secondary antibodies is included in Appendix A. Nuclei were stained using 4',6'-Diamidino-2-Phenylindole (DAPI; Invitrogen) at 1 ug/mL for 3 minutes following secondaries. Images were acquired on Zeiss inverted epifluorescent microscope with 60X objective.

4.2.3 Generation of Gli mutant lentiviral constructs

To study the effects of overexpression of truncated Gli3 repressor (Gli3R) and constitutively activated Gli2 (Gli2PcgE) on proliferation and hedgehog signaling in Wdpcp deficient MEFs, these complementary DNA (cDNA) for these constructs were cloned in the pLenti6 overexpression vector. A lentivirus containing enhanced green fluorescent protein (EGFP) was used as a control. The pLenti6 construct contains HIV 5' LTR (long terminal repeat) and HIV 3'

LTR for stable integration into the genome of the intervening DNA segment. Expression of the inserted cDNA is driven by a constitutively active cytomegalovirus (CMV) promoter. Additionally, this vector contains an ampicillin selection gene for bacterial cloning, and a blasticidin selection gene for eukaryotic selection.

Dr. Bing Wang provided the p6 lentivirus construct. The *Gli2pcgE* cDNA was obtained from Addgene courtesy of Dr. Rajat Rohatgi. The Gli3R cDNA was generated from the cDNA clone for full-length mouse *Gli3* (GeneCopoeia). For construction of the pLenti6-Gli2PcgE-TRIP lentivirus, DNA primers were designed that included two unique restriction sites for cloning in the 5' end and a 20-24 basepair segment that hybridized to either end of the Gli2PcgE cDNA in the 3' end. The forward primer included restriction enzyme recognition sites for the SpeI and SbfI enzymes, while the reverse primer included restriction enzyme recognition sites for the BstBI and SalI enzymes. This allowed for insertion of Gli2PcgE in the correct 5' to 3' orientation.

These cloning primers were used to carry out PCR amplification of Gli2PcgE from the template plasmid obtained from Dr. Rajat Rohatgi with Phusion high fidelity PCR kit (New England Biolabs). PCR product size was verified with gel electrophoresis and PCR products were digested with DpnI to eliminate residual template plasmid. Following purification with PCR clean up kit (Qiagen), PCR products were digested with SpeI followed by SacII. The p6lentiEGFP was digested with SpeI and SacII and the digested pLenti6 backbone (~7.4 kbp) was gel purified from the EGFP fragment and uncut vector with an agaorse gel purification kit (Qiagen). The digested and purified PCR product was added to the digested and purified pLenti6 backbone at molar concentration of 10:1 and used with a ligation reaction kit (New England Biolabs) overnight at room 4C. Ligation product was transformed into OneShot Stbl3 competent

cells (Lifetechnologies) with heat shock and transformed colonies selected for on an ampicillin agarose plate. Purified mini-prepped plasmids (Qiagen) were digested with SpeI and SacII to verify insert and vector size. Vectors were sequence verified with Sanger sequencing to screen for unintended mutagenesis. For Gli3R, steps were analogous but SpeI and BstBI enzymes were used. Lentiviral construct maps are provided in Appendix A.

4.2.4 Infection and cell culture of MEFs

Growth medium containing Dulbecco's modified E Medium (DMEM) supplemented with 10% fetal bovine serum (FBS) and 100 ug/mL (1X) penicillin/Strep/fungizone. Cyclopamine, smoothened agonist, GANT61 were dissolved in dimethyl sulfoxide (DMSO) and stored at -20C. All drugs diluted in DMSO before being added to cell culture medium in 1:1000 ratio.

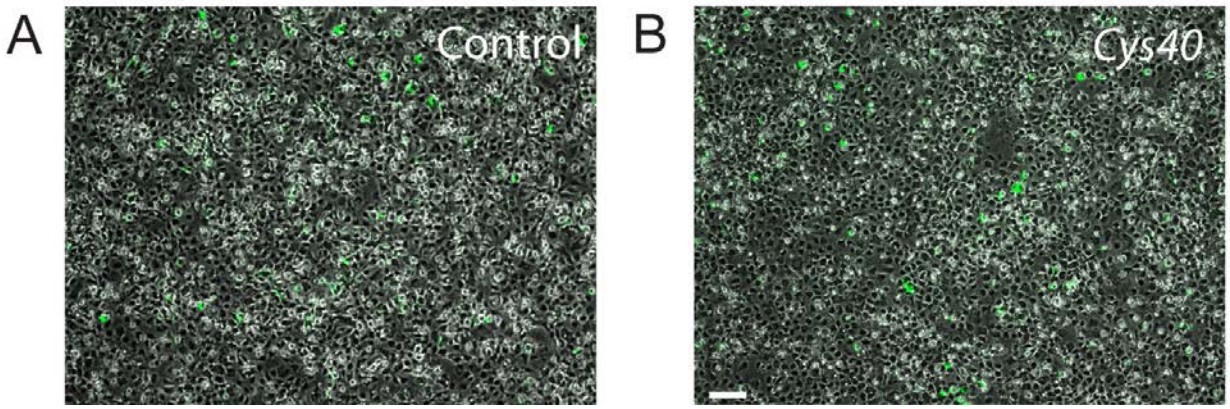

Figure 24. Verification of lentiviral tropism in MEFs.
Control (A) and *Cys40* (B) MEFs both exhibited expression of EGFP after infection with pLenti6-EGFP-TRIP lentivirus. Efficiency of infection was similar between control and *Cys40* MEFs.

4.2.5 Edu proliferation assay

The Click-iT Plus Edu 594 assay was used to quantify cell proliferation over final 24 hours of cell culture as described in section 4.2.1. Following serum starvation period, 10 mM EdU

dissolved in PBS was added to culture medium at 1:1000 for a final concentration of 10 uM. Following fixation with 4% paraformaldehyde for 15 min at room temperature, EdU staining was performed per the manufacturer's protocol (Lifetechnologies). Hoechst staining was performed to identify all nuclei. Images were acquired on Zeiss inverted epifluorescent microscope with 10X objective. Three fields were captured for each treatment condition and presented images are representative.

4.2.6 Western Blotting

Protein was isolated from a well of a 6 well plate using a Total Protein Isolation Kit (Millipore) supplemented with Halt protease and phosphatase inhibitor cocktail and 5 mM EDTA. Sample preparation and Western blot for Gli3 was carried out as described in section 2.2.6. Three independent biological replicates were completed for each condition and each blot was done in duplicate. Images presented are representative.

4.2.7 RNA isolation and qPCR

RNA isolation, reverse transcription, and qPCR assays were performed as described in section 2.2.6, with 3 experimental replicates each containing two pooled biological replicates to obtain sufficient RNA concentration. Ccnd1 was used as a marker of cell proliferation. Activity of the hedgehog pathway was measured with Gli1 and Hhip activity. Relative expression was determined using validated primers (Appendix A) and the $\Delta\Delta C_T$ method, with expression reported relative to endogenous control hypoxanthine-guanine phosphoribosyltransferase (*Hprt*). Statistics were performed as described in Section 2.2.8.

4.3 RESULTS

4.3.1 MEFs lacking *Wdpcp* are not responsive to Smo agonists

Control MEFs respond to SAG stimulation with increased expression of Gli1 ($p<0.05$) and increased cell proliferation as assayed by EdU staining (Figure 25). Cys40 MEFs fail to increase Gli1 expression, Ccnd1 expression, or proliferation as assayed by EdU staining in response to SAG stimulation.

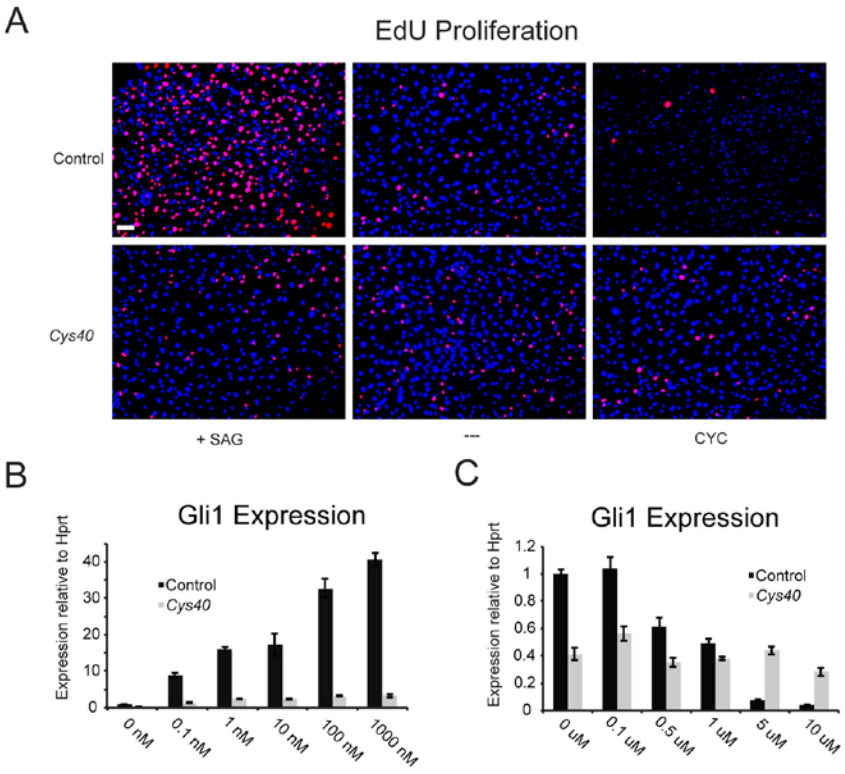

Figure 25. *Cys40* MEFs display decreased responsiveness to modulation of Smo activity.
Treatment of control MEFs with Smoothened agonist (SAG) results in increased proliferation while treatment of *Cys40* MEFs with SAG has no effect on proliferation as assayed by EdU incorporation. Treatment of control MEFs with Smoothened antagonist cyclopamine (CYC) results in decreased proliferation while treatment of *Cys40* MEFs with cyclopamine has no effect on proliferation as assayed by EdU incorporation (A). Increasing doses of SAG treatment result in increasing expression of hedgehog reporter gene *Gli1* in controls MEFs versus no significant change in *Cys40* MEFs (B). Increasing doses of cyclopamine treatment result in decreasing expression of hedgehog reporter gene *Gli1* in control MEFs versus no significant change in *Cys40* MEFs (C). Error bars represent one standard deviation. Effect of drug treatment within a genotype is calculated using Student's t-test with * for $p<0.05$, ** for $p<0.01$, *** for $p<0.001$.

4.3.2 Direct inhibition of Gli silence ectopic activation of hedgehog pathway due to *Wdpcp* loss

Treatment with direct Gli inhibitor GANT61 resulted in reduction of proliferation of both *Cys40* MEFs as well as control MEFs as assayed by EdU positive MEFs after 24 hours of treatment (Figure 26A). Additionally, there is a significant reduction in the expression of both hedgehog reporter gene *Gli1* and proliferation reporter gene *Ccnd1* for both *Cys40* and control MEFs (Figure 26B,C).

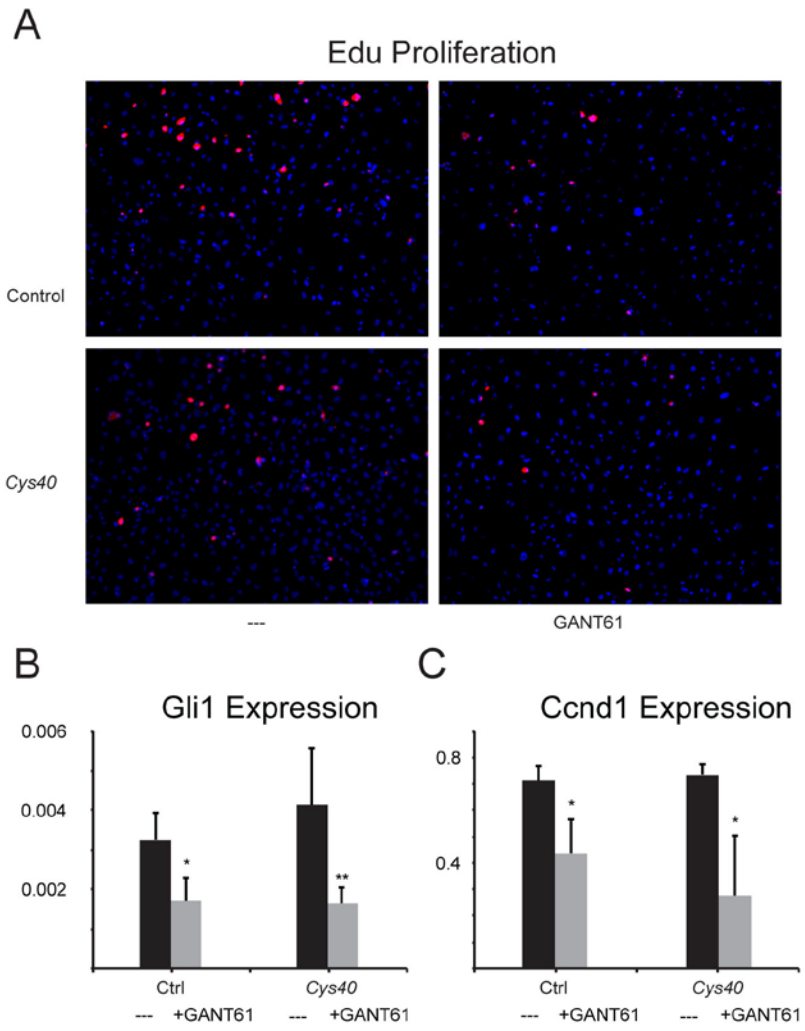

Figure 26. Direct Gli inhibition suppresses hedgehog pathway and proliferation.
Treatment of *Cys40* and control MEFs with direct Gli inhibitor GANT61 (50 uM) suppresses proliferation as assayed by EdU incorporation after 24 hours of cell culture treatment (A). Decreased proliferation correlates with decreased expression of hedgehog responsive gene *Gli1* (B) and of proliferation marker *Ccnd1* (C). All panels are at same scale and scale bar is 10 um. Expression is expressed relative to *Hrpt*. Error bars represent one standard deviation. Effect of drug treatment within a genotype is calculated using Student's t-test with * for $p<0.05$, ** for $p<0.01$, *** for $p<0.001$.

4.3.3 Lentiviral overexpression of Gli3R silences ectopic activation of hedgehog pathway due to *Wdpcp* loss

Having determined that direct inhibition of all Gli-DNA interactions was capable of inhibited hedgehog pathway activity and proliferation, it was hypothesized that overexpression of the Gli3

repressor form could have a similar silencing effect on hedgehog pathway activity and proliferation in *Cys40* MEFs. Over expression of the repressor form of Gli3 would essentially be a rescue of the Gli3 processing defect present in *Cys40* MEFs. Transfection with lentivirus that overexpresses the repressor form of Gli3 would correct the decreased Gli3 repressor:activator ratio that results from deficient Gli3 processing in *Cys40* mutants. As hypothesized, lentiviral overexpression of the truncated repressor of Gli3 silenced both hedgehog pathway activity in *Cys40* MEFs as assayed by *Gli1* mRNA levels ($p<0.05$) and proliferation as assayed by EdU staining (Figure 27). Reduction of *Ccnd1* mRNA levels was not significantly reduced but may be with blasticidin selection to ensure higher enrichment of transfected MEFs.

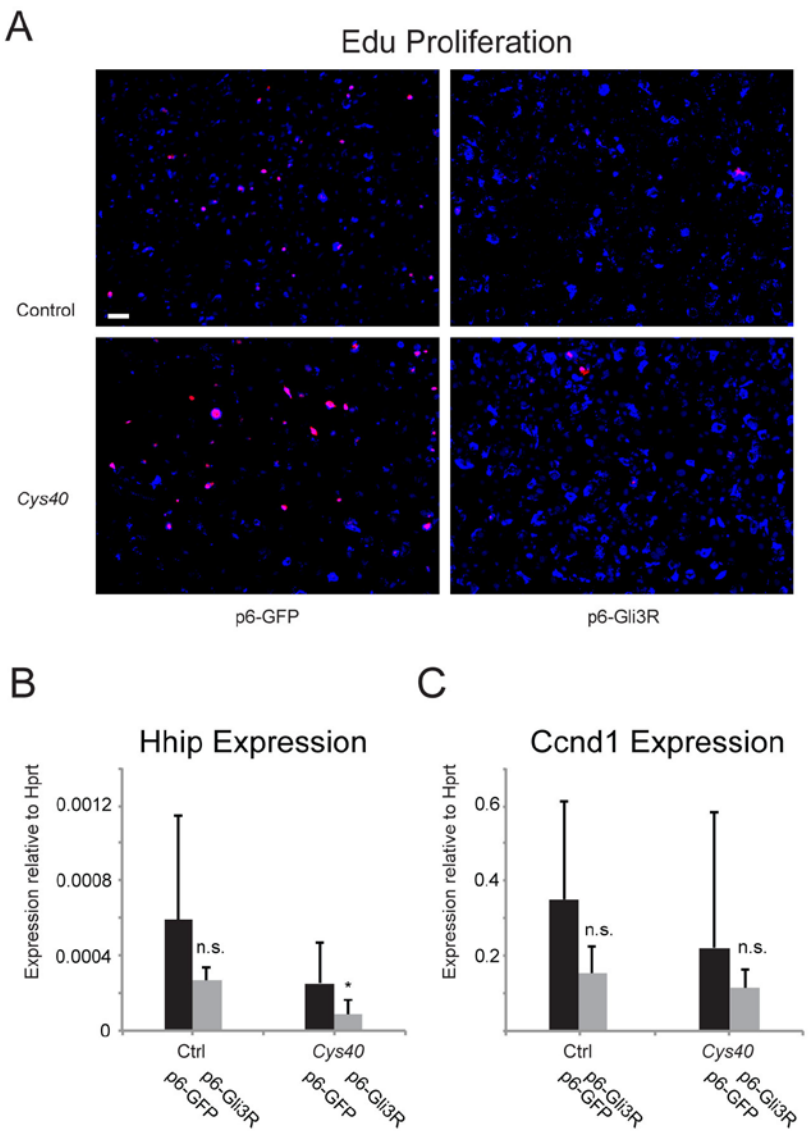

Figure 27. Lentiviral overexpression of Gli3R suppresses hedgehog pathway and proliferation in *Cys40* MEFs.

Infection of *Cys40* and control MEFs pLenti6-Gli3R-TRIP lentivirus for overexpression of Gli3R suppresses proliferation as assayed by EdU incorporation after 24 hours of cell culture treatment (A). Decreased proliferation correlates with decreased expression of hedgehog responsive gene *Hhip* (B) and of proliferation marker *Ccnd1* (C). All panels are at same scale and scale bar is 10 um. Error bars represent one standard deviation. Effect of drug treatment within a genotype is calculated using Student's t-test with * for $p<0.05$, ** for $p<0.01$, *** for $p<0.001$.

4.3.4 MEFs lacking Wdpcp have impaired ciliogenesis

Immunofluorescence staining with acetylated alpha tubulin for the ciliary axoneme and gamma tubulin for the ciliary basal body reveals *Cys40* MEFs fail to form functional primary cilia (Figure 28). This is consistent with the impaired responsiveness to Smo activation and inhibition and disrupted Gli3 processing observed in *Cys40* forelimb buds.

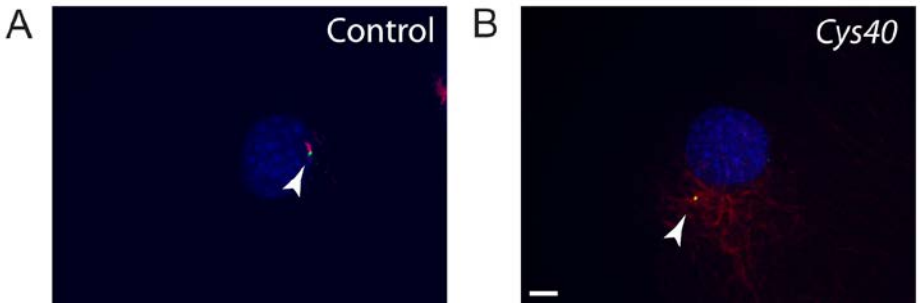

Figure 28. *Cys40* MEFs display defective ciliogenesis.
Immunofluorescence staining of MEFs for cilia axoneme marker, acetylated alpha tubulin (red) and ciliary basal body/centrosome marker gamma tubulin (green) reveals deficient ciliogenesis in *Cys40* MEFs. White scale bar represents 2 uM. Scale is same in both images.

4.3.5 Hedgehog signaling and Gli3 processing are responsive to PKA modulation in MEFs lacking Wdpcp

Because PKA is a known negative regulator of the hedgehog signaling pathway, we hypothesized that Gli3 processing could be rescued in *Cys40* MEFs with PKA stimulation with the phosphodiesterase inhibitor IBMX. Treatment of both *Cys40* and control MEFs with IBMX resulted in complete depletion of full length Gli3 and accumulation of Gli3R as well as suppressed expression of hedgehog reporter gene *Gli1* ($p<0.05$). Conversely, inactivation of

PKA with treatment with PKAi resulted in increased accumulation of full length Gli3. Expression of hedgehog reporter gene *Gli1* did not increase significantly with PKAi treatment, likely do to the fact that Gli2FL and not Gli3FL is the primary activating transcription factor (Figure 29).

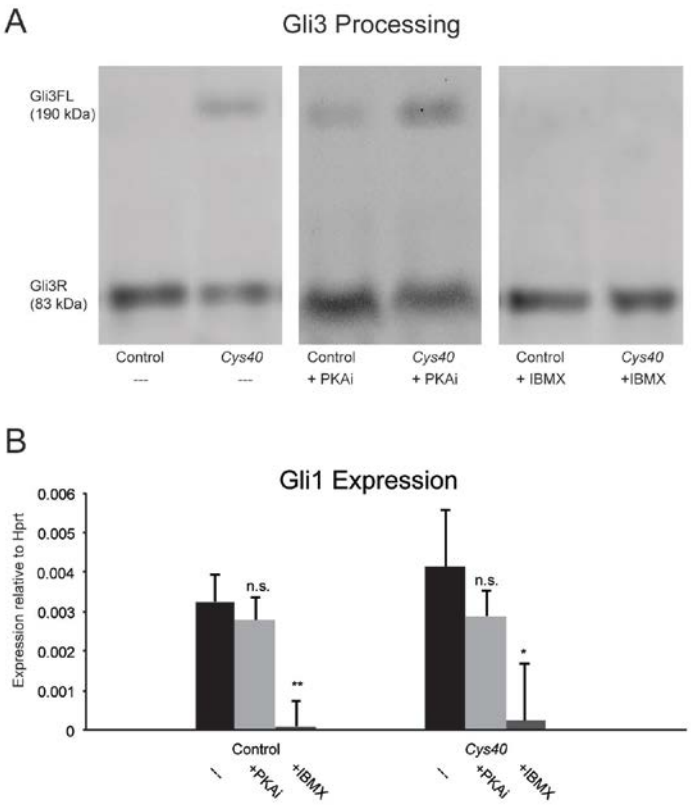

Figure 29. PKA signaling affects Gli processing independent of *Wdpcp*.
Gli3 processing is deficient in untreated *Cys40* MEFs compared to control MEFs. Treatment of MEFs with PKAi inhibits Gli3 processing in both *Cys40* and control MEFs. Treatment of MEFs with IBMX facilitates Gli3 processing in both *Cys40* and control MEFs (A). Expression of hedgehog reporter *Gli1* follows Gli3 processing and Gli3R levels, with significant reductions in *Gli1* expression in MEFs treated with IBMX. Error bars represent one standard deviation. Effect of drug treatment within a genotype is calculated using Student's t-test with * for $p<0.05$, ** for $p<0.01$, *** for $p<0.001$.

4.3.6 MEFs lacking Wdpcp respond to PKA signaling

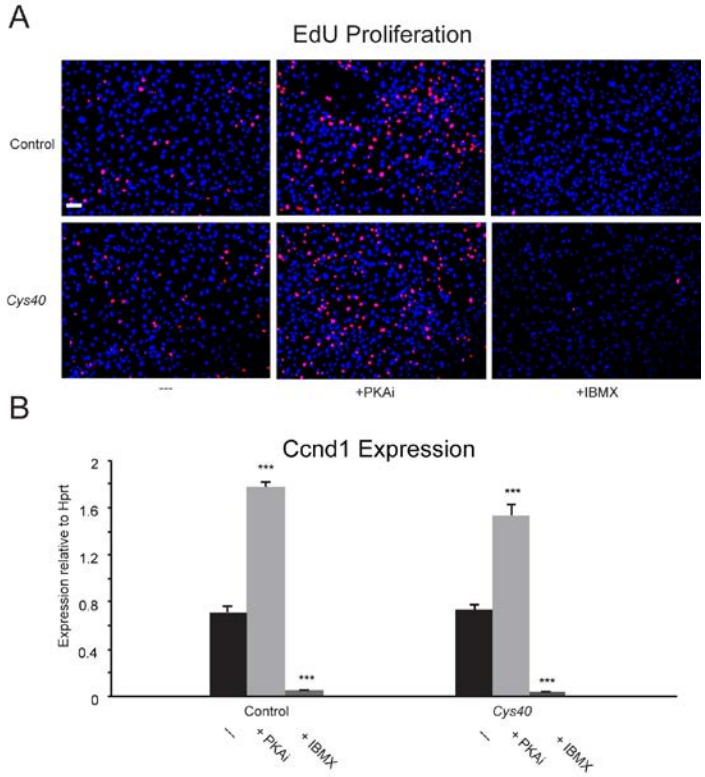

Figure 30. PKA signaling affects proliferation independent of *Wdpcp*.
Treatment of both control and *Cys40* MEFs with PKAi results in increased proliferation as assayed by EdU incorporation. Treatment of both control and *Cys40* MEFs with IBMX results in decreased proliferation as assayed by EdU incorporation (A). Expression of proliferation marker *Ccnd1* correlates with observed changes in proliferation observe with EdU staining, with PKAi treatment increasing *Ccnd1* expression, and IBMX treatment suppressing *Ccnd1* expression. All panels are at same scale and scale bar is 10 um. Error bars represent one standard deviation. Effect of drug treatment within a genotype is calculated using Student's t-test with * for $p<0.05$, ** for $p<0.01$, *** for $p<0.001$.

Control MEFs and *Cys40* MEFs both respond to stimulation of PKA via IBMX treatment with increased proliferation as assayed by EdU staining and increased expression of proliferation marker gene *Ccnd1* (Figure 30). This indicates that PKA modulation is able to affect hedgehog target proliferation regardless of presence of *Wdpcp* or primary cilia.

4.3.7 Gli2 mutants mimicking Gli Pc-g phosphorylation rescue loss of hedgehog activation due to Wdpcp loss

Having demonstrated that PKA can effect Gli3 processing and hedgehog signaling, we hypothesized that mimicking the amino terminal phosphorylation shown previously to be necessary for activation of Gli transcription factors (Niewiadomski et al., 2014) might be able to rescue the deficiency in hedgehog activation present in MEFs lacking *Wdpcp*. Using site directed mutagenesis, we generated the pLenti6-Gli2pcgE-TRIP with the relevant amino terminal serine and threonine residues (Pcg) mutated to negatively charged aspartic acid residues to mimic phosphorylation (Figure 3). *Cys40* MEFs infected with pLenti6-Gli2pcgE-TRIP for overexpression of constitutively phosphorylated Gli2 displayed increased *Hhip* expression (Figure 31), indicating that loss of *Wdpcp* may disrupt the ability of PKA to provide phosphorylation of the amino terminal residues in Gli2 necessary for hedgehog activation.

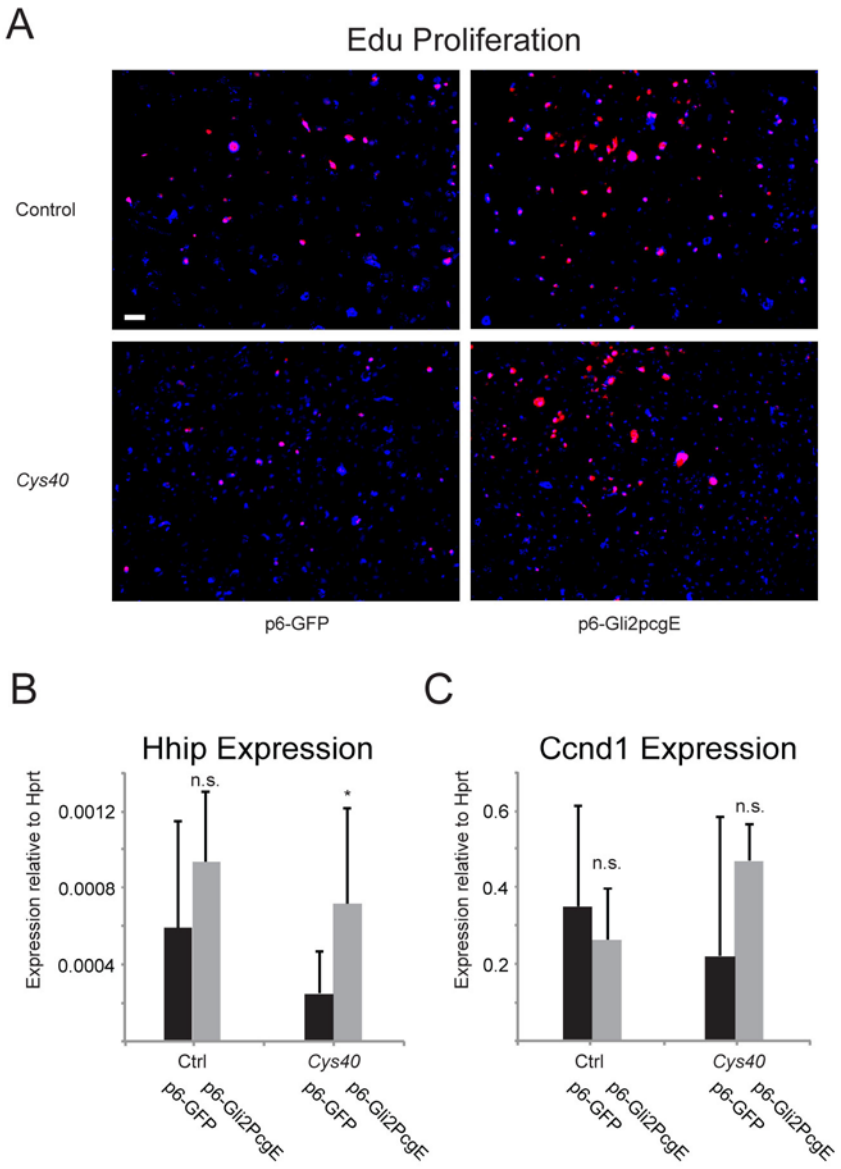

Figure 31. Lentiviral overexpression of activated Gli2 increases proliferation and hedgehog activity in *Cys40* MEFs.

Infection of *Cys40* and control MEFs pLenti6-Gli2PcgE-TRIP lentivirus for overexpression of activated Gli2 increases proliferation as assayed by EdU incorporation after 24 hours of cell culture treatment (A). Increased proliferation correlates with increased expression of hedgehog responsive gene *Hhip* (B) and of proliferation marker *Ccnd1* (C). All panels are at same scale and scale bar is 10 um. Error bars represent one standard deviation. Effect of drug treatment within a genotype is calculated using Student's t-test with * for $p<0.05$, ** for $p<0.01$, *** for $p<0.001$.

4.4 DISCUSSION

These findings also demonstrate that PKA can rescue the *Wdpcp* loss of function and potentially other primary cilia mutants, suggesting a role for primary cilia in Gli phosphorylation. Our finding that stimulation of PKA is able to suppress expression of hedgehog target gene *Gli1* (Figure 29B) and restore formation of truncated Gli3 repressor (Figure 29A) in MEFs lacking *Wdpcp* is in accordance with previous findings that PKA functions as a negative regulator of hedgehog signaling in cells with disrupted ciliogenesis (Wen et al., 2010). More recently, a number of PKA has also been implicated in hedgehog activation through phosphorylation of amino terminal residues (Figure 3) (Niewiadomski et al., 2013). Our findings that the pLenti6-Gli2PcgE-TRIP lentivirus is able to increase expression of hedgehog pathway target gene *Hhip* MEFs lacking functional *Wdpcp* (Figure 31) suggests that primary cilia and *Wdpcp* may facilitate the PKA mediated phosphorylation of Gli2 necessary for hedgehog activation. Recent studies have suggested that the primary cilium may regulate hedgehog signaling by serving as a center where the action of PKA on Gli2 and Gli3 is tightly regulated. PKA is localized to the base of the primary cilium (Tuson et al., 2011), and recent studies have identified G-protein coupled receptors that activate the PKA pathway, are localized to the primary cilium, and modulate hedgehog pathway activation (Mukhopadhyay and Rohatgi, 2014; Mukhopadhyay et al., 2013). The role of *Wdpcp* in constraining these receptors to the primary cilium and regulating their activity bears future investigation in light of our findings.

These findings suggest that post-translational modification occurring subsequent to phosphorylation may not require cilia. Sumoylation, ubiquitinylation, phosphorylation and many other post-translational modifications are known to play important roles in the turnover, processing, and activation of Gli transcription factors (Cox et al., 2010; Kent et al., 2006;

Mukhopadhyay and Rohatgi, 2014). Future studies with mutant forms of Gli will be essential to dissecting the role of different cilia associated and hedgehog associated proteins in this pathway. Observing the effects of these mutants on processing, subcellular localization, and expression of target genes will yield new insights to mechanics of this critical signaling pathway.

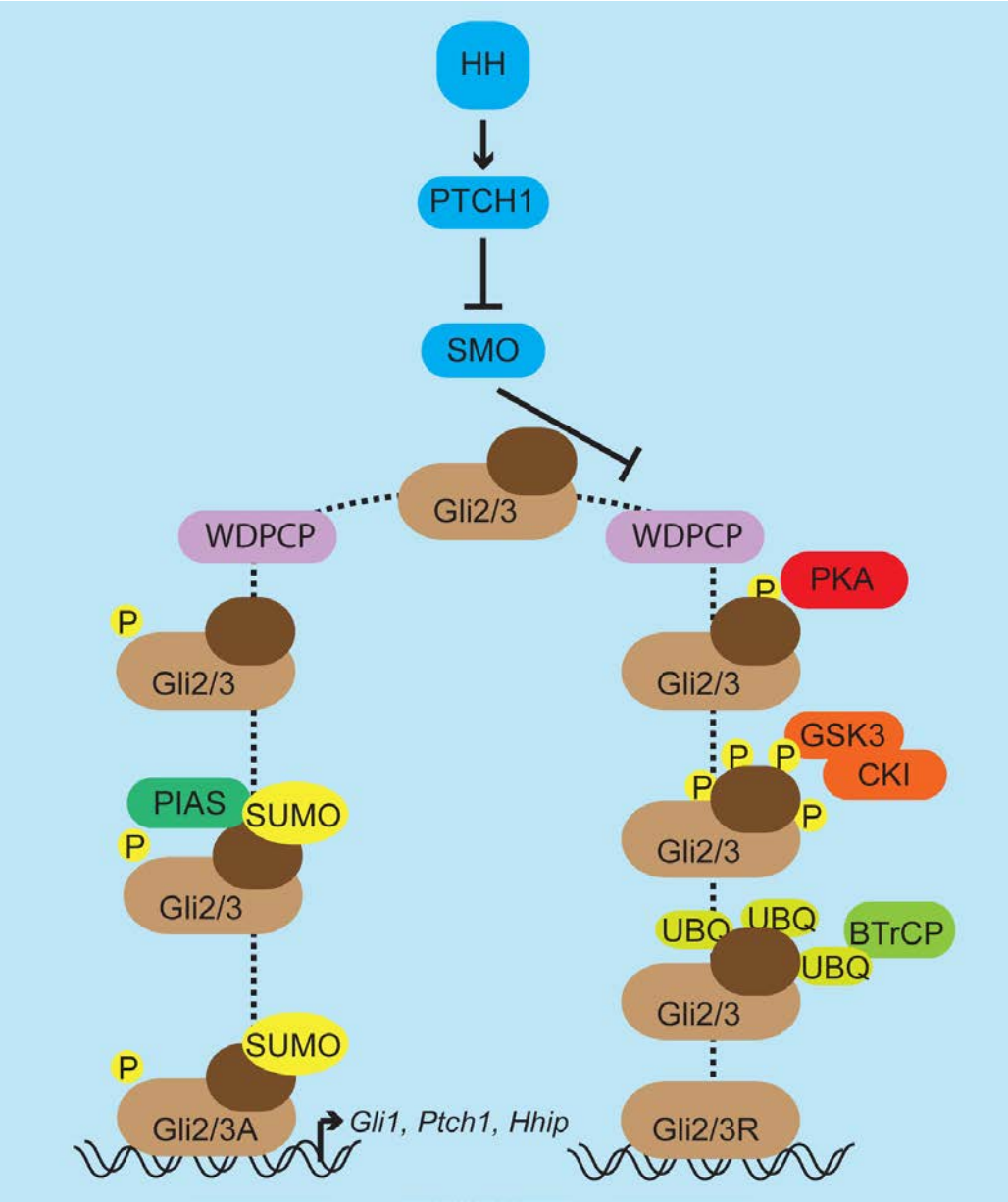

Figure 32. Wdpcp functions at or above PKA in the hedgehog pathway.
The diminished response of cells lacking Wdpcp to both Smo (blue) agonism and antagonism indicates that Wdpcp functions downstream of Smo in the hedgehog pathway. The ability of PKA modulation to effect hedgehog signaling output and Gli3 processing independently of Wdpcp (purple) indicates that Wdpcp acts at or above PKA (red) in the processing of Gli transcription factors (brown) in the hedgehog pathway.

4.5 CONCLUSION

Loss of Wdpcp in *Cys40* MEFs affects hedgehog signaling via disruption of formation of the primary cilium. Disruption of the primary cilium results in deficient Gli3 processing to the repressor form as well as deficient activation of Gli2/3 to the activator form as evidenced by the decreased responsiveness of *Cys40* MEFs to both *Smo* agonists and antagonist. Furthermore, this data suggest that *Wdpcp* and the primary cilium function somewhere downstream of *Smo* in the hedgehog signaling pathway (Figure 32). *Gli3* processing in the *Cys40* MEFs can be rescued with application of the phosphodiesterase inhibitor and PKA activator IBMX. As expected, increased processing of Gli3 to the repressor form as stimulated by PKA suppresses activation of the hedgehog pathway due to the increased levels of repressor. Conversely, PKAi application inhibits Gli3 processing in both *Cys40* and control MEFs (Figure 29A). However, no significant increase in expression of hedgehog pathway target gene *Gli1* is observed with PKAi treatment (Figure 29B), suggesting that PKA functions primarily as a positive regulator of Gli3 repressor processing to repressor and not as a negative regulator of Gli activator formation. While no significant effects on hedgehog pathway activity were observed with PKAi treatment, it should be noted that PKAi treatment did result in significant increase in proliferation (Figure 30). Proliferation is a multifactorial readout and PKA is a promiscuous kinase, making it difficult to draw specific conclusions about the effects PKAi treatment and the role of PKA from these findings. However, combined with the findings of alteration of Gli3 processing and changes in *Gli1* expression (Figure 29). The ability of PKA treatment to affect proliferation of both *Cys40* and control MEFs can be interpreted to indicate that PKA acts at the same level as or downstream of *Wdpcp* in control of proliferation. The final experiments in this series examine the effect of lentiviral overexpression of a constitutively activated form of Gli2 with sites Pc-g

modified to mimic phosphorylation. The increased expression of hedgehog pathway target gene *Hhip* (Figure 31B) suggests providing phosphorylation of Gli2 on residues Pc-g is able to rescue the activation lost with loss of *Wdpcp* and disruption of the primary cilium. This result suggests that *Wdpcp* acts upstream of Gli2Pc-gE phosphorylation in the formation of the activator form of Gli.

5.0 IMPACT AND FUTURE DIRECTIONS

5.1 IMPACT

5.1.1 Skeletal Development and Tissue Engineering

These findings support previous findings that repression of hedgehog signaling is necessary for initiation of cartilage condensation and chondrogenesis. These findings also support a role for primary cilia in transducing the hedgehog signal necessary for osteogenesis. The findings of this study suggest that repression of hedgehog signaling will enhance chondrogenesis and suppress hypertrophic differentiation. While temporal activation of hedgehog signaling will suppress chondrogenesis, it will eventually promote hypertrophic chondrocyte differentiation and osteogenesis in established chondrocytes.

5.1.2 Osteoarthritis

Hedgehog signaling is known to play an important role in adult homeostasis of cartilage. Dysfunctional activation of hedgehog signaling is associated with the accelerated development of osteoarthritis (Lin et al., 2009). The primary cilium is also believed to be an important mediator of mechanosensation in cartilage and bone (Yuan et al., 2015). This work demonstrates that *Wdpcp* is necessary for normal cartilage homeostasis in mice. Additionally, it was shown

that dysfunction resulting from loss of *Wdpcp* is associated with increased hedgehog signaling. This suggests that therapeutic strategies that prevent loss of primary cilia and/or repress hedgehog signaling may be able to restore cartilage homeostasis.

5.1.3 Cancer

Dysfunctional hedgehog signaling is a hallmark of many malignancies including basal cell carcinoma, medulloblastoma, pancreatic cancer, chondrosarcoma, colorectal, and ovarian cancers (Amakye et al., 2013). 98% of basal cell carcinomas result from a mutation in the hedgehog receptor Ptch (Iwasaki et al., 2012). While the majority of these tumors are cured by resection, in the cases where this has been delayed or is technically difficult (e.g. on a sensitive area of the face) medical therapies would be useful. Indeed, the first hedgehog pathway therapeutic, vismodegib, passed clinical trials and received FDA approval for this indication in late 2011. While some tumors such as basal cell carcinoma have shown significant responses to Vismodegib, clinical trials investigating the therapeutic potential of *Smo* antagonists for other tumor types such as pancreatic cancers and chondrosarcoma have been discontinued due to disappointing results (Amakye et al., 2013).

With mutations in over 500 of an estimated 20,000 human genes or homologs identified as disrupting ciliogenesis, low activation of hedgehog signaling that results from disruption of primary cilia may play a larger role in malignancy than is currently appreciated. Deciphering the role of the primary cilium and associated components in regulating hedgehog signaling via Gli modification will open the door for the design of targeted therapeutics that modulate hedgehog signaling downstream of *Smo*. This work demonstrates a role for *Wdpcp* in PKA mediated phosphorylation of Gli2 and Gli3 for both the activation and repression of hedgehog signaling,

suggesting that Gli phosphorylation is a key regulatory step downstream of or at the same level as the primary cilium in the hedgehog pathway. Our findings suggest that targeting Gli phosphorylation could be a significantly more effective strategy for repression of hedgehog signaling than *Smo* inhibition. However, PKA is a promiscuous kinase and further work to clarify the binding partners that mediate site-specific phosphorylation of Gli is necessary to uncover hedgehog pathway specific targets.

5.2 FUTURE DIRECTIONS

The effect of postnatal deletion of *Wdpcp* on the homeostasis of adult chondrocytes is an area of current investigation. *Col2a1-Cre^{ERT}:Wdpcp$^{flow/flox}$* mice with chondrocyte-specific deletion of *Wdpcp* induced with tamoxifen injection at 6 weeks of age display drastic changes in gait and osteoarthritic symptoms versus *Col2a1-Cre^{ERT};Wdpcp$^{+/+}$* mice injected at the same time at 6 months post injection. Further characterization of this phenotype is underway.

Having observed the delay in ossification in the *Col2a1-Cre^{ERT};Wdpcp$^{Cys40/Flox}$* mice, current investigations are examining the effect of non-skeletal tissues on the process of osteogenesis. Vascular invasion of the hypertrophic zone at the primary site of ossification is necessary for normal osteogenesis. Endothelial specific deletion of Wdpcp utilizing the *Tie2-Cre* mouse line crossed to the Wdpcp^{Flox} mice will be used to investigate the role of Wdpcp in the vascularization of bone.

Having investigated and described the appendicular skeletal defect of the *Cys40* mutant, the craniofacial and axial skeletal defects remain areas for future investigation. We note that E13.5 *Cys40* embryos display facial clefting (Figure 33). Our initial characterization of the

disruption of the hedgehog pathway in *Cys40* mice will facilitate investigations into the mechanism of these phenotypes. For example, the craniofacial skeleton is derived primarily from neural crest cells, a population has been demonstrated to be specifically labeled in lineage tracing studies by *Wnt1-Cre* (Firulli et al., 2014). To determine whether the craniofacial defects observed are due to cell autonomous function of *Wdpcp* in these cells or due to the function of *Wdpcp* in cells outside this population, *Wnt1-cre* mice may be crossed to $Wdpcp^{flox}$ mice to generate mice with a conditional deletion of *Wdpcp* in neural crest cells. These studies would provide insights into the mechanisms of craniofacial skeleton morphogenesis and facial clefting and may suggest potential therapies and/or risk factors associated with facial clefting.

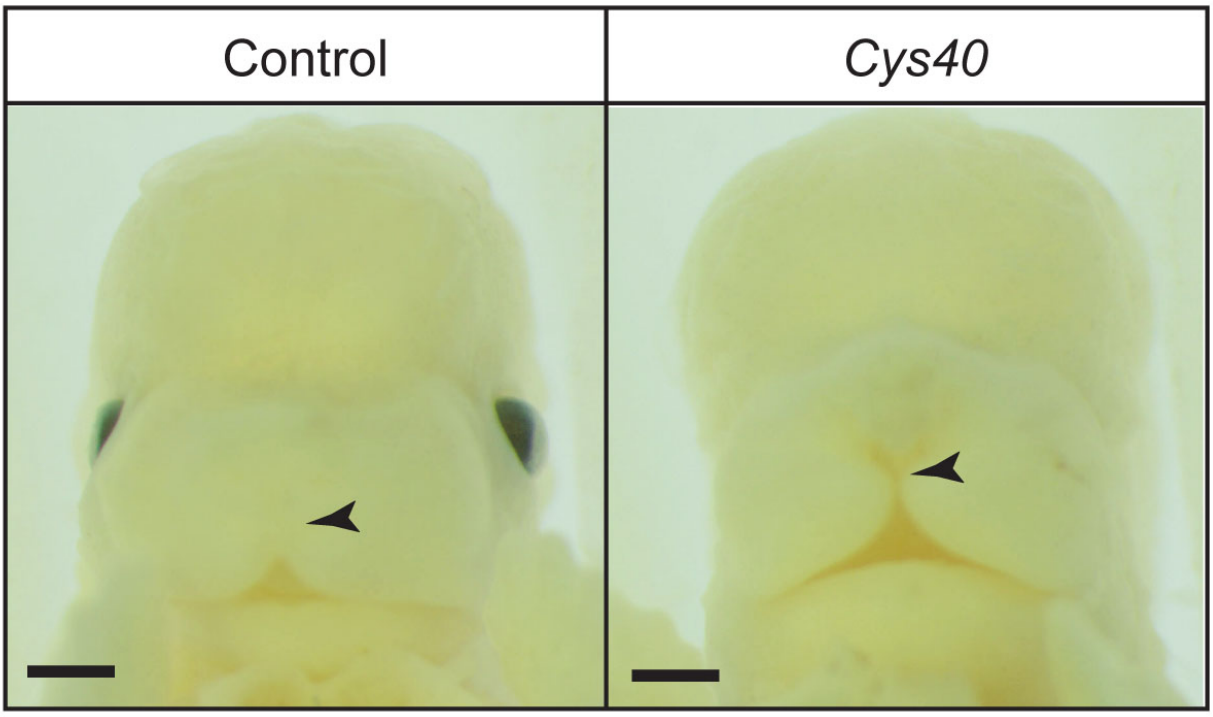

Figure 33. Craniofacial skeletal defects in *Cys40* mutant mice.
E13.5 *Cys40* mutant mice display facial clefting versus matched littermate controls. Recapitulation of cleft phenotype is variable in *Prx1-Cre;*$Wdpcp^{Cys40/Flox}$ mice.

In the axial skeleton, the effects of *Wdpcp* deletion on degeneration of the intervertebral disc beg investigation. Recent investigations have demonstrated important roles for hedgehog

signaling in both the development and maintenance of adult homeostasis of the intervertebral disc (Dahia et al., 2012). The *Noto-Cre*^{ERT} mouse line expresses an inducible Cre recombinase specifically in the notochord, and later in adults, specifically in the nucleus pulposus of the intervertebral discs (Ukita et al., 2009). Breeding this Cre line to *Wdpcp*^{flox} mice would generate mice with an inducible nucleus pulposus specific deletion of *Wdpcp*. It would be informative to determine the effects of *Wdpcp* los and primary cilium disruption in these tissues because it has not been studied.

Our studies highlight the central importance of Gli phosphorylation in regulation of hedgehog signaling output, and demonstrate that further studies into the specific role of *Wdpcp* and the primary cilium in regulating the process of Gli phosphorylation are warranted. Residue specific mutants of Gli3 both with mutations of phosphorylatable serine and threonine to unphosphorylatable alanine and mutations of serine and threonine to glutamic acid to mimic phosphorylation should be generated and studied for their ability to be processed to shortened repressor form in absence of primary cilia. The subcellular and ciliary localization of GFP tagged versions of these mutant Gli forms would yield insights into the interactions that govern the site-specific phosphorylation of Gli. Immunoprecipitation studies utilizing these mutated forms of Gli would provide insights into downstream interactions and how site-specific phosphorylation of Gli leads to formation of activator versus repressor. These studies will provide essential information for the design of therapeutics that modulate Gli phosphorylation and alter hedgehog pathway output.

APPENDIX A

A.1 RT-PCR PRIMERS

Gene		Reference	Sequence	Accession
Gli1	5’	MGH PrimerBank	CCAAGCCAACTTTATGTCAGGG	NM_010296
Gli1	3’	MGH PrimerBank	AGCCCGCTTCTTTGTTAATTTGA	NM_010296
Ptch1	5’	MGH PrimerBank	GCCTTCGCTGTGGGATTAAAG	NM_008957
Ptch1	3’	MGH PrimerBank	CTTCTCCTATCTTCTGACGGGT	NM_008957
Wdpcp	5’	MGH PrimerBank	GCTTGACTGAACTACACCTGTG	NM_145425
Wdpcp	3’	MGH PrimerBank	TGAGTGTCCAAGGATAATCTCGT	NM_145425
Col2a1	5’	MGH PrimerBank	GGGAATGTCCTCTGCGATGAC	NM_031163
Col2a1	3’	MGH PrimerBank	GAAGGGGATCTCGGGGTTG	NM_031163
Grem1	5’	Benazet et al 2009	CCCACGGAAGTGACAGAATGA	NM_011824
Grem1	3’	Benazet et al 2009	AAGCAACGCTCCCACAGTGTA	NM_011824
Sdc3	5’	MGH PrimerBank	AGAGGCCGGTGGATCTTGA	NM_011520
Sdc3	3’	MGH PrimerBank	CTCCTGCTCGAAGTAGCCAGA	NM_011520
Cdh2	5’	MGH PrimerBank	AGCGCAGTCTTACCGAAGG	NM_007664
Cdh2	3’	MGH PrimerBank	TCGCTGCTTTCATACTGAACTTT	NM_007664
Sox9	5’	MGH PrimerBank	AGTACCCGCATCTGCACAAC	NM_011448
Sox9	3’	MGH PrimerBank	ACGAAGGGTCTCTTCTCGCT	NM_011448
Bmp4	5’	Benazet et al 2009	AGCCGAGCCAACACTGTGA	NM_007554
Bmp4	3’	Benazet et al 2009	GTTCTCCAGATGTTCTTCGTGATG	NM_007554
Ccnd1	5’	Lopez-Rios 2012	CAGACGTTCAGAACCAGATTC	NM_007631
Ccnd1	3’	Lopez-Rios 2012	CCCTCCAATAGCAGCGAAAAC	NM_007631
Shh	5’	MGH PrimerBank	AAAGCTGACCCCTTTAGCCTA	NM_009170
Shh	3’	MGH PrimerBank	TTCGGAGTTTCTTGTGATCTTCC	NM_009170
Msx2	5’	MGH PrimerBank	TTCACCACATCCCAGCTTCTA	NM_013601
Msx2	3’	MGH PrimerBank	TTGCAGTCTTTTCGCCTTAGC	NM_013601
Hhip	5’	MGH PrimerBank	CCACCACACAGGATCTCTCC	NM_020259
Hhip	3’	MGH PrimerBank	TGAAGATGCTCTCGTTTAAGCTG	NM_020259
Hprt	5’	MGH PrimerBank	TCAGTCAACGGGGGACATAAA	NM_013556
Hprt	3’	MGH PrimerBank	GGGGCTGTACTGCTTAACCAG	NM_013556
Acan	5’	MGH PrimerBank	CCTGCTACTTCATCGACCCC	NM_007424
Acan	3’	MGH PrimerBank	AGATGCTGTTGACTCGAACCT	NM_007424
Col9a1	5’	MGH PrimerBank	CGACCGACCAGCACATCAA	NM_007740
Col9a1	3’	MGH PrimerBank	AGGGGGACCCTTAATGCCT	NM_007740
Ocn	5’	MGH PrimerBank	CTGACCTCACAGATCCCAAGC	NM_007541
Ocn	3’	MGH PrimerBank	TGGTCTGATAGCTCGTCACAAG	NM_007541
Col1a1	5’	MGH PrimerBank	TAAGGGTCCCCAATGGTGAGA	NM_007742
Col1a1	3’	MGH PrimerBank	GGGTCCCTCGACTCCTACAT	NM_007742
Runx2	5’	MGH PrimerBank	GGTGGTCCGCGATGATCTC	NM_009820
Runx2	3’	MGH PrimerBank	GAGGGCACAAGTTCTATCTGGA	NM_009820
Osx	5’	MGH PrimerBank	ATGGCGTCCTCTCTGCTTG	NM_130458
Osx	3’	MGH PrimerBank	TGAAAGGTCAGCGTATGGCTT	NM_130458

A.2 LENTIVIRAL CONSTRUCTS

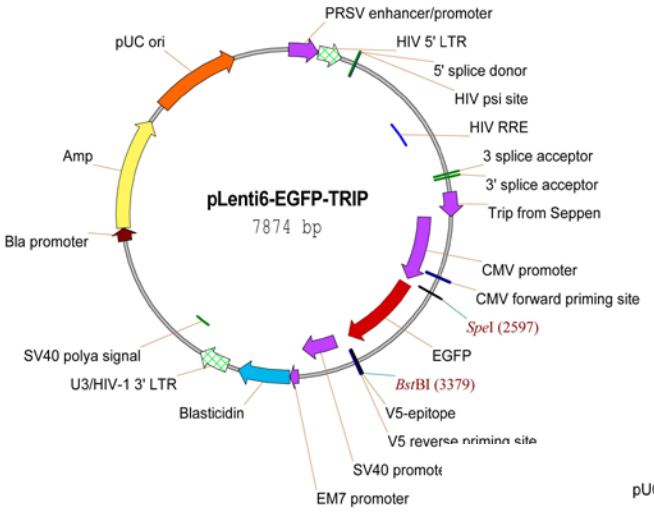

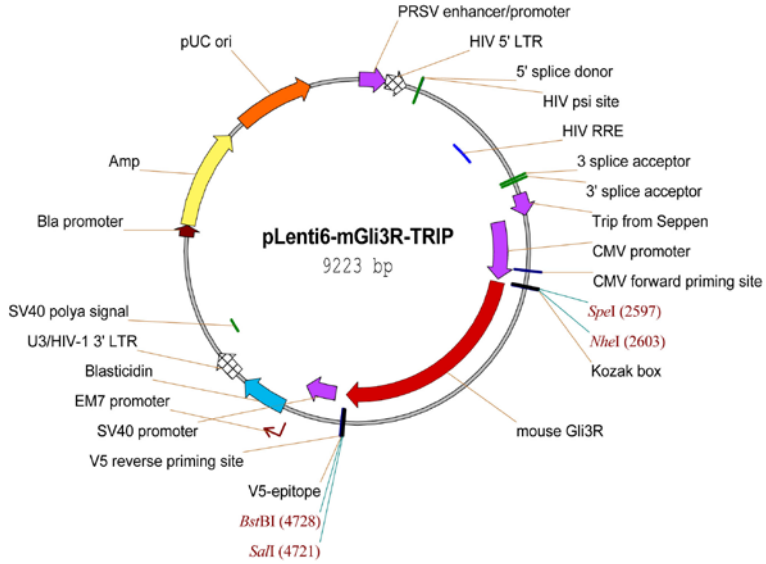

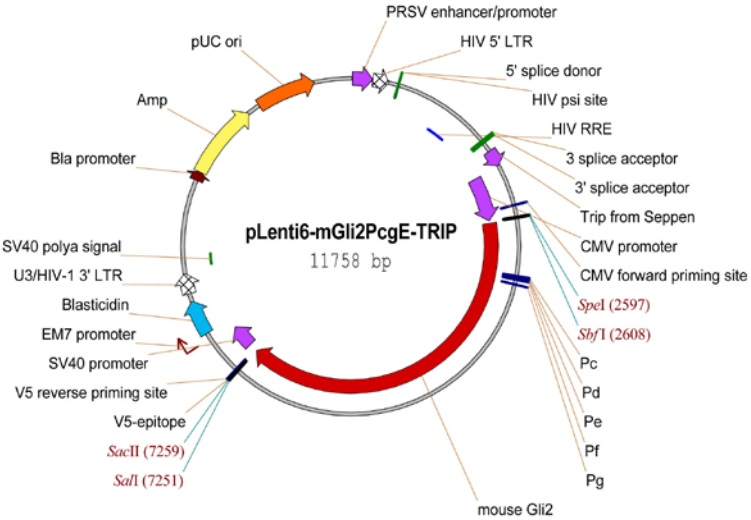

BIBLIOGRAPHY

Abramson, S.B., Attur, M., 2009. Developments in the scientific understanding of osteoarthritis. Arthritis research & therapy 11, 227.

Abzhanov, A., Rodda, S.J., McMahon, A.P., Tabin, C.J., 2007. Regulation of skeletogenic differentiation in cranial dermal bone. Development 134, 3133-3144.

Acloque, H., Ocana, O.H., Matheu, A., Rizzoti, K., Wise, C., Lovell-Badge, R., Nieto, M.A., 2011. Reciprocal repression between Sox3 and snail transcription factors defines embryonic territories at gastrulation. Developmental cell 21, 546-558.

Akiyama, H., Kim, J.E., Nakashima, K., Balmes, G., Iwai, N., Deng, J.M., Zhang, Z., Martin, J.F., Behringer, R.R., Nakamura, T., de Crombrugghe, B., 2005. Osteo-chondroprogenitor cells are derived from Sox9 expressing precursors. Proceedings of the National Academy of Sciences of the United States of America 102, 14665-14670.

Aliferis, K., Helle, S., Gyapay, G., Duchatelet, S., Stoetzel, C., Mandel, J.L., Dollfus, H., 2012. Differentiating Alstrom from Bardet-Biedl syndrome (BBS) using systematic ciliopathy genes sequencing. Ophthalmic genetics 33, 18-22.

Amakye, D., Jagani, Z., Dorsch, M., 2013. Unraveling the therapeutic potential of the Hedgehog pathway in cancer. Nature medicine 19, 1410-1422.

Anz, A.W., Hackel, J.G., Nilssen, E.C., Andrews, J.R., 2014. Application of biologics in the treatment of the rotator cuff, meniscus, cartilage, and osteoarthritis. The Journal of the American Academy of Orthopaedic Surgeons 22, 68-79.

Asagiri, M., Takayanagi, H., 2007. The molecular understanding of osteoclast differentiation. Bone 40, 251-264.

Bade, M.J., Kohrt, W.M., Stevens-Lapsley, J.E., 2010. Outcomes before and after total knee arthroplasty compared to healthy adults. The Journal of orthopaedic and sports physical therapy 40, 559-567.

Bangs, F., Antonio, N., Thongnuek, P., Welten, M., Davey, M.G., Briscoe, J., Tickle, C., 2011. Generation of mice with functional inactivation of talpid3, a gene first identified in chicken. Development 138, 3261-3272.

Bastida, M.F., Sheth, R., Ros, M.A., 2009. A BMP-Shh negative-feedback loop restricts Shh expression during limb development. Development 136, 3779-3789.

Benazet, J.D., Bischofberger, M., Tiecke, E., Goncalves, A., Martin, J.F., Zuniga, A., Naef, F., Zeller, R., 2009. A self-regulatory system of interlinked signaling feedback loops controls mouse limb patterning. Science 323, 1050-1053.

Benazet, J.D., Pignatti, E., Nugent, A., Unal, E., Laurent, F., Zeller, R., 2012. Smad4 is required to induce digit ray primordia and to initiate the aggregation and differentiation of chondrogenic progenitors in mouse limb buds. Development 139, 4250-4260.

Benazet, J.D., Zeller, R., 2009. Vertebrate limb development: moving from classical morphogen gradients to an integrated 4-dimensional patterning system. Cold Spring Harbor perspectives in biology 1, a001339.

Bimonte, S., De Angelis, A., Quagliata, L., Giusti, F., Tammaro, R., Dallai, R., Ascenzi, M.G., Diez-Roux, G., Franco, B., 2011. Ofd1 is required in limb bud patterning and endochondral bone development. Developmental biology 349, 179-191.

Bonewald, L.F., 2011. The Amazing Osteocyte. Journal of Bone and Mineral Research 26, 229-238.

Briscoe, J., Therond, P.P., 2013. The mechanisms of Hedgehog signalling and its roles in development and disease. Nature reviews. Molecular cell biology 14, 416-429.

Brooks, E.R., Wallingford, J.B., 2012. Control of vertebrate intraflagellar transport by the planar cell polarity effector Fuz. The Journal of cell biology 198, 37-45.

Bruce, S.J., Butterfield, N.C., Metzis, V., Town, L., McGlinn, E., Wicking, C., 2010. Inactivation of Patched1 in the mouse limb has novel inhibitory effects on the chondrogenic program. The Journal of biological chemistry 285, 27967-27981.

Burge, R., Dawson-Hughes, B., Solomon, D.H., Wong, J.B., King, A., Tosteson, A., 2007. Incidence and economic burden of osteoporosis-related fractures in the United States, 2005-2025. Journal of bone and mineral research : the official journal of the American Society for Bone and Mineral Research 22, 465-475.

Buscher, D., Bosse, B., Heymer, J., Ruther, U., 1997. Evidence for genetic control of Sonic hedgehog by Gli3 in mouse limb development. Mechanisms of development 62, 175-182.

Butterfield, N.C., Metzis, V., McGlinn, E., Bruce, S.J., Wainwright, B.J., Wicking, C., 2009. Patched 1 is a crucial determinant of asymmetry and digit number in the vertebrate limb. Development 136, 3515-3524.

Cao, T., Wang, C., Yang, M., Wu, C., Wang, B., 2013. Mouse limbs expressing only the Gli3 repressor resemble those of Sonic hedgehog mutants. Developmental biology 379, 221-228.

Carpenter, D., Stone, D.M., Brush, J., Ryan, A., Armanini, M., Frantz, G., Rosenthal, A., de Sauvage, F.J., 1998. Characterization of two patched receptors for the vertebrate hedgehog protein family. Proceedings of the National Academy of Sciences of the United States of America 95, 13630-13634.

Chang, C.F., Serra, R., 2013. Ift88 regulates Hedgehog signaling, Sfrp5 expression, and beta-catenin activity in post-natal growth plate. Journal of orthopaedic research : official publication of the Orthopaedic Research Society 31, 350-356.

Chang, D.T., Lopez, A., von Kessler, D.P., Chiang, C., Simandl, B.K., Zhao, R., Seldin, M.F., Fallon, J.F., Beachy, P.A., 1994. Products, genetic linkage and limb patterning activity of a murine hedgehog gene. Development 120, 3339-3353.

Chen, J., Smaoui, N., Hammer, M.B., Jiao, X., Riazuddin, S.A., Harper, S., Katsanis, N., Riazuddin, S., Chaabouni, H., Berson, E.L., Hejtmancik, J.F., 2011. Molecular analysis of Bardet-Biedl syndrome families: report of 21 novel mutations in 10 genes. Investigative ophthalmology & visual science 52, 5317-5324.

Chen, J.K., Taipale, J., Cooper, M.K., Beachy, P.A., 2002. Inhibition of Hedgehog signaling by direct binding of cyclopamine to Smoothened. Genes & development 16, 2743-2748.

Chen, Y., Knezevic, V., Ervin, V., Hutson, R., Ward, Y., Mackem, S., 2004. Direct interaction with Hoxd proteins reverses Gli3-repressor function to promote digit formation downstream of Shh. Development 131, 2339-2347.

Chuang, P.T., McMahon, A.P., 1999. Vertebrate Hedgehog signalling modulated by induction of a Hedgehog-binding protein. Nature 397, 617-621.

Cohn, M.J., Tickle, C., 1996. Limbs: a model for pattern formation within the vertebrate body plan. Trends in genetics : TIG 12, 253-257.

Collier, S., Lee, H., Burgess, R., Adler, P., 2005. The WD40 repeat protein fritz links cytoskeletal planar polarity to frizzled subcellular localization in the Drosophila epidermis. Genetics 169, 2035-2045.

Corbit, K.C., Aanstad, P., Singla, V., Norman, A.R., Stainier, D.Y., Reiter, J.F., 2005. Vertebrate Smoothened functions at the primary cilium. Nature 437, 1018-1021.

Cox, B., Briscoe, J., Ulloa, F., 2010. SUMOylation by Pias1 regulates the activity of the Hedgehog dependent Gli transcription factors. PloS one 5, e11996.

Cui, C., Chatterjee, B., Francis, D., Yu, Q., SanAgustin, J.T., Francis, R., Tansey, T., Henry, C., Wang, B., Lemley, B., Pazour, G.J., Lo, C.W., 2011. Disruption of Mks1 localization to the mother centriole causes cilia defects and developmental malformations in Meckel-Gruber syndrome. Disease models & mechanisms 4, 43-56.

Cui, C., Chatterjee, B., Lozito, T.P., Zhang, Z., Francis, R.J., Yagi, H., Swanhart, L.M., Sanker, S., Francis, D., Yu, Q., San Agustin, J.T., Puligilla, C., Chatterjee, T., Tansey, T., Liu, X., Kelley, M.W., Spiliotis, E.T., Kwiatkowski, A.V., Tuan, R., Pazour, G.J., Hukriede, N.A., Lo, C.W., 2013. Wdpcp, a PCP protein required for ciliogenesis, regulates directional cell migration and cell polarity by direct modulation of the actin cytoskeleton. PLoS biology 11, e1001720.

Dahia, C.L., Mahoney, E., Wylie, C., 2012. Shh signaling from the nucleus pulposus is required for the postnatal growth and differentiation of the mouse intervertebral disc. PloS one 7, e35944.

Dai, P., Akimaru, H., Tanaka, Y., Maekawa, T., Nakafuku, M., Ishii, S., 1999. Sonic Hedgehog-induced activation of the Gli1 promoter is mediated by GLI3. The Journal of biological chemistry 274, 8143-8152.

de Kok, J.B., Roelofs, R.W., Giesendorf, B.A., Pennings, J.L., Waas, E.T., Feuth, T., Swinkels, D.W., Span, P.N., 2005. Normalization of gene expression measurements in tumor tissues: comparison of 13 endogenous control genes. Laboratory investigation; a journal of technical methods and pathology 85, 154-159.

DeLise, A.M., Stringa, E., Woodward, W.A., Mello, M.A., Tuan, R.S., 2000. Embryonic limb mesenchyme micromass culture as an in vitro model for chondrogenesis and cartilage maturation. Methods in molecular biology 137, 359-375.

Denker, A.E., Haas, A.R., Nicoll, S.B., Tuan, R.S., 1999. Chondrogenic differentiation of murine C3H10T1/2 multipotential mesenchymal cells: I. Stimulation by bone morphogenetic protein-2 in high-density micromass cultures. Differentiation; research in biological diversity 64, 67-76.

Dougall, W.C., Glaccum, M., Charrier, K., Rohrbach, K., Brasel, K., De Smedt, T., Daro, E., Smith, J., Tometsko, M.E., Maliszewski, C.R., Armstrong, A., Shen, V., Bain, S., Cosman, D., Anderson, D., Morrissey, P.J., Peschon, J.J., Schuh, J., 1999. RANK is essential for osteoclast and lymph node development. Genes & development 13, 2412-2424.

Echelard, Y., Epstein, D.J., St-Jacques, B., Shen, L., Mohler, J., McMahon, J.A., McMahon, A.P., 1993. Sonic hedgehog, a member of a family of putative signaling molecules, is implicated in the regulation of CNS polarity. Cell 75, 1417-1430.

Firulli, B.A., Fuchs, R.K., Vincentz, J.W., Clouthier, D.E., Firulli, A.B., 2014. Hand1 phosphoregulation within the distal arch neural crest is essential for craniofacial morphogenesis. Development 141, 3050-3061.

Francis-West, P.H., Abdelfattah, A., Chen, P., Allen, C., Parish, J., Ladher, R., Allen, S., MacPherson, S., Luyten, F.P., Archer, C.W., 1999. Mechanisms of GDF-5 action during skeletal development. Development 126, 1305-1315.

Garcia-Gonzalo, F.R., Reiter, J.F., 2012. Scoring a backstage pass: mechanisms of ciliogenesis and ciliary access. The Journal of cell biology 197, 697-709.

Goetz, S.C., Anderson, K.V., 2010. The primary cilium: a signalling centre during vertebrate development. Nature reviews. Genetics 11, 331-344.

Goodrich, L.V., Johnson, R.L., Milenkovic, L., McMahon, J.A., Scott, M.P., 1996. Conservation of the hedgehog/patched signaling pathway from flies to mice: induction of a mouse patched gene by Hedgehog. Genes & development 10, 301-312.

Gu, H., Zou, Y.R., Rajewsky, K., 1993. Independent control of immunoglobulin switch recombination at individual switch regions evidenced through Cre-loxP-mediated gene targeting. Cell 73, 1155-1164.

Haycraft, C.J., Banizs, B., Aydin-Son, Y., Zhang, Q., Michaud, E.J., Yoder, B.K., 2005. Gli2 and Gli3 localize to cilia and require the intraflagellar transport protein polaris for processing and function. PLoS genetics 1, e53.

Haycraft, C.J., Zhang, Q., Song, B., Jackson, W.S., Detloff, P.J., Serra, R., Yoder, B.K., 2007. Intraflagellar transport is essential for endochondral bone formation. Development 134, 307-316.

Heydeck, W., Zeng, H., Liu, A., 2009. Planar cell polarity effector gene Fuzzy regulates cilia formation and Hedgehog signal transduction in mouse. Developmental dynamics : an official publication of the American Association of Anatomists 238, 3035-3042.

Hinck, A.P., 2012. Structural studies of the TGF-betas and their receptors - insights into evolution of the TGF-beta superfamily. FEBS letters 586, 1860-1870.

Hojo, H., Ohba, S., Yano, F., Saito, T., Ikeda, T., Nakajima, K., Komiyama, Y., Nakagata, N., Suzuki, K., Takato, T., Kawaguchi, H., Chung, U.I., 2012. Gli1 protein participates in Hedgehog-mediated specification of osteoblast lineage during endochondral ossification. The Journal of biological chemistry 287, 17860-17869.

Hootman, J.M., Helmick, C.G., 2006. Projections of US prevalence of arthritis and associated activity limitations. Arthritis and rheumatism 54, 226-229.

Huangfu, D., Anderson, K.V., 2005. Cilia and Hedgehog responsiveness in the mouse. Proceedings of the National Academy of Sciences of the United States of America 102, 11325-11330.

Huangfu, D., Liu, A., Rakeman, A.S., Murcia, N.S., Niswander, L., Anderson, K.V., 2003. Hedgehog signalling in the mouse requires intraflagellar transport proteins. Nature 426, 83-87.

Hui, C.C., Angers, S., 2011. Gli proteins in development and disease. Annual review of cell and developmental biology 27, 513-537.

Irianto, J., Ramaswamy, G., Serra, R., Knight, M.M., 2014. Depletion of chondrocyte primary cilia reduces the compressive modulus of articular cartilage. Journal of biomechanics 47, 579-582.

Ishikawa, H., Thompson, J., Yates, J.R., 3rd, Marshall, W.F., 2012. Proteomic analysis of mammalian primary cilia. Current biology : CB 22, 414-419.

Iwasaki, J.K., Srivastava, D., Moy, R.L., Lin, H.J., Kouba, D.J., 2012. The molecular genetics underlying basal cell carcinoma pathogenesis and links to targeted therapeutics. Journal of the American Academy of Dermatology 66, e167-178.

Jessell, T.M., 2000. Neuronal specification in the spinal cord: inductive signals and transcriptional codes. Nature reviews. Genetics 1, 20-29.

Jia, J., Amanai, K., Wang, G., Tang, J., Wang, B., Jiang, J., 2002. Shaggy/GSK3 antagonizes Hedgehog signalling by regulating Cubitus interruptus. Nature 416, 548-552.

Jiang, J., Struhl, G., 1996. Complementary and mutually exclusive activities of decapentaplegic and wingless organize axial patterning during Drosophila leg development. Cell 86, 401-409.

Jiang, J., Struhl, G., 1998. Regulation of the Hedgehog and Wingless signalling pathways by the F-box/WD40-repeat protein Slimb. Nature 391, 493-496.

Jiang, Y., Tuan, R.S., 2014. Origin and function of cartilage stem/progenitor cells in osteoarthritis. Nature reviews. Rheumatology.

Johnson, D.R., 1967. Extra-toes: anew mutant gene causing multiple abnormalities in the mouse. Journal of embryology and experimental morphology 17, 543-581.

Kent, D., Bush, E.W., Hooper, J.E., 2006. Roadkill attenuates Hedgehog responses through degradation of Cubitus interruptus. Development 133, 2001-2010.

Khosla, S., 2009. Increasing options for the treatment of osteoporosis. The New England journal of medicine 361, 818-820.

Kim, S.K., Shindo, A., Park, T.J., Oh, E.C., Ghosh, S., Gray, R.S., Lewis, R.A., Johnson, C.A., Attie-Bittach, T., Katsanis, N., Wallingford, J.B., 2010. Planar cell polarity acts through septins to control collective cell movement and ciliogenesis. Science 329, 1337-1340.

Kotlarz, H., Gunnarsson, C.L., Fang, H., Rizzo, J.A., 2009. Insurer and out-of-pocket costs of osteoarthritis in the US: evidence from national survey data. Arthritis and rheumatism 60, 3546-3553.

Kragl, M., Knapp, D., Nacu, E., Khattak, S., Maden, M., Epperlein, H.H., Tanaka, E.M., 2009. Cells keep a memory of their tissue origin during axolotl limb regeneration. Nature 460, 60-65.

Krauss, S., Concordet, J.P., Ingham, P.W., 1993. A functionally conserved homolog of the Drosophila segment polarity gene hh is expressed in tissues with polarizing activity in zebrafish embryos. Cell 75, 1431-1444.

Kronenberg, H.M., 2003. Developmental regulation of the growth plate. Nature 423, 332-336.

Kurtz, S., Ong, K., Lau, E., Mowat, F., Halpern, M., 2007. Projections of primary and revision hip and knee arthroplasty in the United States from 2005 to 2030. The Journal of bone and joint surgery. American volume 89, 780-785.

Kuss, P., Kraft, K., Stumm, J., Ibrahim, D., Vallecillo-Garcia, P., Mundlos, S., Stricker, S., 2014. Regulation of cell polarity in the cartilage growth plate and perichondrium of metacarpal elements by HOXD13 and WNT5A. Developmental biology 385, 83-93.

Langhans, M.T., Alexander, P.G., Tuan, R.S., 2014. Skeletal Development, in: Moody, S.A. (Ed.), Principles of Developmental Genetics, 2nd ed. Elsevier, Washington, D.C., pp. 505-530.

Lauth, M., Bergstrom, A., Shimokawa, T., Toftgard, R., 2007. Inhibition of GLI-mediated transcription and tumor cell growth by small-molecule antagonists. Proceedings of the National Academy of Sciences of the United States of America 104, 8455-8460.

Lawrence, R.C., Felson, D.T., Helmick, C.G., Arnold, L.M., Choi, H., Deyo, R.A., Gabriel, S., Hirsch, R., Hochberg, M.C., Hunder, G.G., Jordan, J.M., Katz, J.N., Kremers, H.M., Wolfe, F., National Arthritis Data, W., 2008. Estimates of the prevalence of arthritis and other rheumatic conditions in the United States. Part II. Arthritis and rheumatism 58, 26-35.

Lee, J.J., von Kessler, D.P., Parks, S., Beachy, P.A., 1992. Secretion and localized transcription suggest a role in positional signaling for products of the segmentation gene hedgehog. Cell 71, 33-50.

Lewandowski, J.P., Pursell, T.A., Rabinowitz, A.H., Vokes, S.A., 2014. Manipulating gene expression and signaling activity in cultured mouse limb bud cells. Developmental dynamics : an official publication of the American Association of Anatomists 243, 928-936.

Lin, A.C., Seeto, B.L., Bartoszko, J.M., Khoury, M.A., Whetstone, H., Ho, L., Hsu, C., Ali, S.A., Alman, B.A., 2009. Modulating hedgehog signaling can attenuate the severity of osteoarthritis. Nature medicine 15, 1421-1425.

Liu, A., Wang, B., Niswander, L.A., 2005. Mouse intraflagellar transport proteins regulate both the activator and repressor functions of Gli transcription factors. Development 132, 3103-3111.

Logan, M., Martin, J.F., Nagy, A., Lobe, C., Olson, E.N., Tabin, C.J., 2002. Expression of Cre Recombinase in the developing mouse limb bud driven by a Prxl enhancer. Genesis 33, 77-80.

Long, F., Chung, U.I., Ohba, S., McMahon, J., Kronenberg, H.M., McMahon, A.P., 2004. Ihh signaling is directly required for the osteoblast lineage in the endochondral skeleton. Development 131, 1309-1318.

Long, F.X., 2012. Building strong bones: molecular regulation of the osteoblast lineage. Nat Rev Mol Cell Bio 13, 27-38.

Lopez-Rios, J., Speziale, D., Robay, D., Scotti, M., Osterwalder, M., Nusspaumer, G., Galli, A., Hollander, G.A., Kmita, M., Zeller, R., 2012. GLI3 constrains digit number by controlling both progenitor proliferation and BMP-dependent exit to chondrogenesis. Developmental cell 22, 837-848.

Lozito, T.P., Tuan, R.S., 2011. Mesenchymal Stem Cells Inhibit Both Endogenous and Exogenous MMPs via Secreted TIMPs. Journal of cellular physiology 226, 385-396.

Lozito, T.P., Tuan, R.S., 2015. Lizard tail regeneration: regulation of two distinct cartilage regions by Indian hedgehog. Developmental biology 399, 249-262.

Malashichev, Y., Christ, B., Prols, F., 2008. Avian pelvis originates from lateral plate mesoderm and its development requires signals from both ectoderm and paraxial mesoderm. Cell and tissue research 331, 595-604.

McGlashan, S.R., Haycraft, C.J., Jensen, C.G., Yoder, B.K., Poole, C.A., 2007. Articular cartilage and growth plate defects are associated with chondrocyte cytoskeletal abnormalities in Tg737orpk mice lacking the primary cilia protein polaris. Matrix biology : journal of the International Society for Matrix Biology 26, 234-246.

Meyers-Needham, M., Lewis, J.A., Gencer, S., Sentelle, R.D., Saddoughi, S.A., Clarke, C.J., Hannun, Y.A., Norell, H., da Palma, T.M., Nishimura, M., Kraveka, J.M., Khavandgar, Z., Murshed, M., Cevik, M.O., Ogretmen, B., 2012. Off-target function of the Sonic hedgehog inhibitor cyclopamine in mediating apoptosis via nitric oxide-dependent neutral sphingomyelinase 2/ceramide induction. Molecular cancer therapeutics 11, 1092-1102.

Mis, E.K., Liem, K.F., Jr., Kong, Y., Schwartz, N.B., Domowicz, M., Weatherbee, S.D., 2014. Forward genetics defines Xylt1 as a key, conserved regulator of early chondrocyte maturation and skeletal length. Developmental biology 385, 67-82.

Miyazono, K., Kamiya, Y., Morikawa, M., 2010. Bone morphogenetic protein receptors and signal transduction. Journal of biochemistry 147, 35-51.

Mo, R., Freer, A.M., Zinyk, D.L., Crackower, M.A., Michaud, J., Heng, H.H., Chik, K.W., Shi, X.M., Tsui, L.C., Cheng, S.H., Joyner, A.L., Hui, C., 1997. Specific and redundant functions of Gli2 and Gli3 zinc finger genes in skeletal patterning and development. Development 124, 113-123.

Mohler, J., Vani, K., 1992. Molecular organization and embryonic expression of the hedgehog gene involved in cell-cell communication in segmental patterning of Drosophila. Development 115, 957-971.

Mostowy, S., Cossart, P., 2012. Septins: the fourth component of the cytoskeleton. Nature reviews. Molecular cell biology 13, 183-194.

Mukhopadhyay, S., Rohatgi, R., 2014. G-protein-coupled receptors, Hedgehog signaling and primary cilia. Seminars in cell & developmental biology 33, 63-72.

Mukhopadhyay, S., Wen, X., Ratti, N., Loktev, A., Rangell, L., Scales, S.J., Jackson, P.K., 2013. The ciliary G-protein-coupled receptor Gpr161 negatively regulates the Sonic hedgehog pathway via cAMP signaling. Cell 152, 210-223.

Nakamura, E., Nguyen, M.T., Mackem, S., 2006. Kinetics of tamoxifen-regulated Cre activity in mice using a cartilage-specific CreER(T) to assay temporal activity windows along the proximodistal limb skeleton. Developmental dynamics : an official publication of the American Association of Anatomists 235, 2603-2612.

Niewiadomski, P., Kong, J.H., Ahrends, R., Ma, Y., Humke, E.W., Khan, S., Teruel, M.N., Novitch, B.G., Rohatgi, R., 2014. Gli protein activity is controlled by multisite phosphorylation in vertebrate Hedgehog signaling. Cell reports 6, 168-181.

Niewiadomski, P., Zhujiang, A., Youssef, M., Waschek, J.A., 2013. Interaction of PACAP with Sonic hedgehog reveals complex regulation of the hedgehog pathway by PKA. Cellular signalling 25, 2222-2230.

Norrie, J.L., Lewandowski, J.P., Bouldin, C.M., Amarnath, S., Li, Q., Vokes, M.S., Ehrlich, L.I., Harfe, B.D., Vokes, S.A., 2014. Dynamics of BMP signaling in limb bud mesenchyme and polydactyly. Developmental biology 393, 270-281.

Nusslein-Volhard, C., Wieschaus, E., 1980. Mutations affecting segment number and polarity in Drosophila. Nature 287, 795-801.

Ohlmeyer, J.T., Kalderon, D., 1998. Hedgehog stimulates maturation of Cubitus interruptus into a labile transcriptional activator. Nature 396, 749-753.

Osterwalder, M., Speziale, D., Shoukry, M., Mohan, R., Ivanek, R., Kohler, M., Beisel, C., Wen, X., Scales, S.J., Christoffels, V.M., Visel, A., Lopez-Rios, J., Zeller, R., 2014. HAND2 targets define a network of transcriptional regulators that compartmentalize the early limb bud mesenchyme. Developmental cell 31, 345-357.

Ovchinnikov, D.A., Selever, J., Wang, Y., Chen, Y.T., Mishina, Y., Martin, J.F., Behringer, R.R., 2006. BMP receptor type IA in limb bud mesenchyme regulates distal outgrowth and patterning. Developmental biology 295, 103-115.

Pan, Y., Bai, C.B., Joyner, A.L., Wang, B., 2006. Sonic hedgehog signaling regulates Gli2 transcriptional activity by suppressing its processing and degradation. Molecular and cellular biology 26, 3365-3377.

Park, H.L., Bai, C., Platt, K.A., Matise, M.P., Beeghly, A., Hui, C.C., Nakashima, M., Joyner, A.L., 2000. Mouse Gli1 mutants are viable but have defects in SHH signaling in combination with a Gli2 mutation. Development 127, 1593-1605.

Pignatti, E., Zeller, R., Zuniga, A., 2014. To BMP or not to BMP during vertebrate limb bud development. Seminars in cell & developmental biology 32, 119-127.

Pizette, S., Abate-Shen, C., Niswander, L., 2001. BMP controls proximodistal outgrowth, via induction of the apical ectodermal ridge, and dorsoventral patterning in the vertebrate limb. Development 128, 4463-4474.

Qiu, N., Xiao, Z., Cao, L., Buechel, M.M., David, V., Roan, E., Quarles, L.D., 2012. Disruption of Kif3a in osteoblasts results in defective bone formation and osteopenia. Journal of cell science 125, 1945-1957.

Rachner, T.D., Khosla, S., Hofbauer, L.C., 2011. Osteoporosis: now and the future. Lancet 377, 1276-1287.

Riddle, R.D., Johnson, R.L., Laufer, E., Tabin, C., 1993. Sonic hedgehog mediates the polarizing activity of the ZPA. Cell 75, 1401-1416.

Rodriguez-Merchan, E.C., 2013. Regeneration of articular cartilage of the knee. Rheumatology international 33, 837-845.

Roelink, H., Augsburger, A., Heemskerk, J., Korzh, V., Norlin, S., Ruiz i Altaba, A., Tanabe, Y., Placzek, M., Edlund, T., Jessell, T.M., et al., 1994. Floor plate and motor neuron induction by vhh-1, a vertebrate homolog of hedgehog expressed by the notochord. Cell 76, 761-775.

Rohatgi, R., Milenkovic, L., Scott, M.P., 2007. Patched1 regulates hedgehog signaling at the primary cilium. Science 317, 372-376.

Saeed, H., Taipaleenmaki, H., Aldahmash, A.M., Abdallah, B.M., Kassem, M., 2012. Mouse embryonic fibroblasts (MEF) exhibit a similar but not identical phenotype to bone marrow stromal stem cells (BMSC). Stem cell reviews 8, 318-328.

Sandell, L.J., 2012. Etiology of osteoarthritis: genetics and synovial joint development. Nature reviews. Rheumatology 8, 77-89.

Sasaki, H., Nishizaki, Y., Hui, C., Nakafuku, M., Kondoh, H., 1999. Regulation of Gli2 and Gli3 activities by an amino-terminal repression domain: implication of Gli2 and Gli3 as primary mediators of Shh signaling. Development 126, 3915-3924.

Selever, J., Liu, W., Lu, M.F., Behringer, R.R., Martin, J.F., 2004. Bmp4 in limb bud mesoderm regulates digit pattern by controlling AER development. Developmental biology 276, 268-279.

Smith, L.J., Nerurkar, N.L., Choi, K.S., Harfe, B.D., Elliott, D.M., 2011. Degeneration and regeneration of the intervertebral disc: lessons from development. Disease models & mechanisms 4, 31-41.

Song, B., Haycraft, C.J., Seo, H.S., Yoder, B.K., Serra, R., 2007. Development of the post-natal growth plate requires intraflagellar transport proteins. Developmental biology 305, 202-216.

St-Jacques, B., Hammerschmidt, M., McMahon, A.P., 1999. Indian hedgehog signaling regulates proliferation and differentiation of chondrocytes and is essential for bone formation (vol 13, pg 2072, 1999). Genes & development 13, 2617-2617.

Stanton, L.A., Sabari, S., Sampaio, A.V., Underhill, T.M., Beier, F., 2004. p38 MAP kinase signalling is required for hypertrophic chondrocyte differentiation. The Biochemical journal 378, 53-62.

Tabata, T., Eaton, S., Kornberg, T.B., 1992. The Drosophila hedgehog gene is expressed specifically in posterior compartment cells and is a target of engrailed regulation. Genes & development 6, 2635-2645.

te Welscher, P., Fernandez-Teran, M., Ros, M.A., Zeller, R., 2002. Mutual genetic antagonism involving GLI3 and dHAND prepatterns the vertebrate limb bud mesenchyme prior to SHH signaling. Genes & development 16, 421-426.

Temiyasathit, S., Tang, W.J., Leucht, P., Anderson, C.T., Monica, S.D., Castillo, A.B., Helms, J.A., Stearns, T., Jacobs, C.R., 2012. Mechanosensing by the primary cilium: deletion of Kif3A reduces bone formation due to loading. PloS one 7, e33368.

Tracy, M.R., Dormans, J.P., Kusumi, K., 2004. Klippel-Feil syndrome: clinical features and current understanding of etiology. Clinical orthopaedics and related research, 183-190.

Tsanev, R., Tiigimagi, P., Michelson, P., Metsis, M., Osterlund, T., Kogerman, P., 2009. Identification of the gene transcription repressor domain of Gli3. FEBS letters 583, 224-228.

Tuson, M., He, M., Anderson, K.V., 2011. Protein kinase A acts at the basal body of the primary cilium to prevent Gli2 activation and ventralization of the mouse neural tube. Development 138, 4921-4930.

Ukita, K., Hirahara, S., Oshima, N., Imuta, Y., Yoshimoto, A., Jang, C.W., Oginuma, M., Saga, Y., Behringer, R.R., Kondoh, H., Sasaki, H., 2009. Wnt signaling maintains the notochord fate for progenitor cells and supports the posterior extension of the notochord. Mechanisms of development 126, 791-803.

Urist, M.R., 1965. Bone: formation by autoinduction. Science 150, 893-899.

Vortkamp, A., 2001. Interaction of growth factors regulating chondrocyte differentiation in the developing embryo. Osteoarthritis and cartilage / OARS, Osteoarthritis Research Society 9 Suppl A, S109-117.

Wallingford, J.B., 2012. Planar cell polarity and the developmental control of cell behavior in vertebrate embryos. Annual review of cell and developmental biology 28, 627-653.

Walsh, D.W., Godson, C., Brazil, D.P., Martin, F., 2010. Extracellular BMP-antagonist regulation in development and disease: tied up in knots. Trends in cell biology 20, 244-256.

Wei, Q., Zhang, Y., Li, Y., Zhang, Q., Ling, K., Hu, J., 2012. The BBSome controls IFT assembly and turnaround in cilia. Nature cell biology 14, 950-957.

Wen, X., Lai, C.K., Evangelista, M., Hongo, J.A., de Sauvage, F.J., Scales, S.J., 2010. Kinetics of hedgehog-dependent full-length Gli3 accumulation in primary cilia and subsequent degradation. Molecular and cellular biology 30, 1910-1922.

Wong, Y.L., Behringer, R.R., Kwan, K.M., 2012. Smad1/Smad5 signaling in limb ectoderm functions redundantly and is required for interdigital programmed cell death. Developmental biology 363, 247-257.

Woolf, A.D., Pfleger, B., 2003. Burden of major musculoskeletal conditions. Bulletin of the World Health Organization 81, 646-656.

Yeung Tsang, K., Wa Tsang, S., Chan, D., Cheah, K.S., 2014. The chondrocytic journey in endochondral bone growth and skeletal dysplasia. Birth defects research. Part C, Embryo today : reviews 102, 52-73.

Yuan, X., Serra, R.A., Yang, S., 2015. Function and regulation of primary cilia and intraflagellar transport proteins in the skeleton. Annals of the New York Academy of Sciences 1335, 78-99.

Zeller, R., Lopez-Rios, J., Zuniga, A., 2009. Vertebrate limb bud development: moving towards integrative analysis of organogenesis. Nature reviews. Genetics 10, 845-858.

Zeng, H., Hoover, A.N., Liu, A., 2010. PCP effector gene Inturned is an important regulator of cilia formation and embryonic development in mammals. Developmental biology 339, 418-428.

Zhai, Z., Yao, Y., Wang, Y., 2013. Importance of suitable reference gene selection for quantitative RT-PCR during ATDC5 cells chondrocyte differentiation. PloS one 8, e64786.

Zhang, W., Moskowitz, R.W., Nuki, G., Abramson, S., Altman, R.D., Arden, N., Bierma-Zeinstra, S., Brandt, K.D., Croft, P., Doherty, M., Dougados, M., Hochberg, M., Hunter, D.J., Kwoh, K., Lohmander, L.S., Tugwell, P., 2008. OARSI recommendations for the management of hip and knee osteoarthritis, Part II: OARSI evidence-based, expert consensus guidelines. Osteoarthritis and cartilage / OARS, Osteoarthritis Research Society 16, 137-162.

Zhang, Z., Lv, X., Yin, W.C., Zhang, X., Feng, J., Wu, W., Hui, C.C., Zhang, L., Zhao, Y., 2013. Ter94 ATPase complex targets k11-linked ubiquitinated ci to proteasomes for partial degradation. Developmental cell 25, 636-644.

Zhu, J., Nakamura, E., Nguyen, M.T., Bao, X., Akiyama, H., Mackem, S., 2008. Uncoupling Sonic hedgehog control of pattern and expansion of the developing limb bud. Developmental cell 14, 624-632.

Zhulyn, O., Li, D., Deimling, S., Vakili, N.A., Mo, R., Puviindran, V., Chen, M.H., Chuang, P.T., Hopyan, S., Hui, C.C., 2014. A switch from low to high Shh activity regulates establishment of limb progenitors and signaling centers. Developmental cell 29, 241-249.

Zuniga, A., Laurent, F., Lopez-Rios, J., Klasen, C., Matt, N., Zeller, R., 2012. Conserved cis-regulatory regions in a large genomic landscape control SHH and BMP-regulated Gremlin1 expression in mouse limb buds. BMC developmental biology 12, 23.